Engineering Probiotic Bacteria for Use as Antibiotic Alternatives

A DISSERTATION

SUBMITTED TO THE FACULTY OF THE

UNIVERSITY OF MINNESOTA

BY

Brittany Anne Forkus

IN PARTIAL FULLFILLMENT OF THE REQUIREMENTS
FOR THE DEGREE OF DOCTOR OF PHILOSOPHY

Wei-Shou Hu

February 2018

Acknowledgements

This dissertation would not have been completed without the critical help and support I have received along the way from my advisors, peers, and family.

Firstly, I must thank Professor Wei-Shou Hu for helping me finish strongly with a dissertation I am proud of. The way you advise students and care about their personal and professional development really embodies what the University of Minnesota stands for and I am so happy I got the opportunity to work closely with you.

I would also like to thank my committee members, Professor Hackel, Professor Zhang, and Professor Johnson, for their continued support and investment in my education. Professor Hackel is not listed on my transcript as an official advisor, however, your technical and professional support has largely shaped my development as a researcher. Professor James Johnson, collaborating with you has been a highlight of my graduate school experience and has challenged me in areas outside of classical chemical engineering, I thank you for the opportunity.

I must also extend my gratitude to Professor Paul Dauenhauer who has pushed me academically since teaching me Kinetics at UMASS Amherst. Thanks to you and your continued investment in me, I have found a career I am passionate about and have a strong foundation to continue to grow from. I will always remember how you said that once you study engineering you see the world differently and now, in this position, I couldn't agree more.

I thank the Kaznessis and Hu group members for their critiques and support throughout my studies. I especially thank Seth Ritter, who has been my co-pilot in this

journey, you have continued to challenge me, offer comic relief, and broaden my skillset, and it has been a privilege to work with you.

I thank my peers, Sadie Johnson, Jeff Ting, Larry Stern, Panagiota Kryiakou, and Koustav Ganguly for making my graduate school experience a memorable and positive journey. Scott White, I thank you for carrying me through some of the darker times of grad school and celebrating the highs with me.

Lastly I thank my family. They have supported me throughout my entire academic career and I know they will continue to support me after. I am lucky to have such great role models in my life and whose company make my life so rich. Shannon and Paul, your support and friendship are two of the most valuable assets of my life. Sophia and Corin, I look forward to seeing what great things you two will accomplish. Renee, thank you for ignoring the job description of a stepmom and being there for me whenever I need it. Mom, thank you for being a working female who has inspired me to build my own career. Dad, thank you for always believing I would make it to this point even when I doubted it.

Dedication

To my family

'The beautiful thing about learning is that no one can take it away from you' –B.B. King

Abstract

Decades of overuse of antibiotics has led to the emergence of resistant infections across the globe. Healthcare professionals are running out of viable options, as clinical isolates have begun resisting treatment to even last resort therapies. The emergence of these 'superbugs', coupled with the lack of new drugs in the discovery pipeline, has led to the possibility of a 'post-antibiotic' era.

With the primary driving force for resistance development being the overuse of antibiotics, technologies are being sought to limit their injudicious application within the clinical and agricultural sectors. An attractive contender in the fight against microbial resistance are antimicrobial peptides (AMPs). AMPs are small peptides that are produced natively from organisms across all domains of life as a first line of defense against microbial challenge. However, despite decades of research on their therapeutic potential, AMPs have widely failed in translational success due to delivery and synthesis challenges.

Many AMPs are unable to survive passage to the gastrointestinal (GI) tract, the residence of many bacterial pathogens, limiting their utility to topical applications. In this work, we propose engineering probiotic bacteria as AMP-delivery vehicles to overcome their inherent transport barriers and localize their production at the site of infection. We focus on modifying the probiotic, *E. coli* Nissle 1917 (EcN), which has shown promise in both human and animal health.

This work takes a synthetic biology approach to iteratively improve and redesign AMP biosynthetic gene clusters. Through strong collaborations with the Veterans'

Affairs Medical Center and Department of Veterinary Sciences, the work within takes a highly translational approach incorporating professional veterinary and clinical oversight at the design stages to develop systems with meaningful downstream applications.

We describe our development of an engineered EcN derivative, EcN(J25), that has antagonistic activity against foodborne *Salmonella*. With EcN(J25), we demonstrated the first *in vivo* success of AMP-producing probiotics. EcN(J25) was capable of reducing *Salmonella* carriage in poultry by 97% after a two-week period with no detectable impact on the native microbiome. This proof-of-concept opens an alternative method to reduce pathogen counts in livestock without incorporating medically important antibiotics in the feed supply.

We then developed an alternative EcN derivative, EcN(C7), which targets the rising multi-drug resistant *E. coli* strain, sequence Type ST131. The goal was to develop an engineered probiotic that could be used as a decolonization measure for ST131 in the clinic. We further explored mechanisms of resistance of ST131 to aid in the development of future combination therapies.

We also describe our development of two new synthetic biology tools, ProTeOn+ and pMPES. ProTeOn+ is a synthetic-hybrid promoter that enables robust protein expression without exogenous induction. ProTeOn+ has demonstrated functional utility in many of the described engineered AMP networks. pMPES serves as a modular peptide expression system that allows heterologous secretion of a variety of AMPs from EcN.

This work take a synthetic biology perspective to describe many of the challenges and potential of engineered probiotics, laying a foundation for future work in this field.

Table of Contents

Table of Figures

List of Tables

Chapter 1 Introduction

1.1 The Rise of Antibiotic Resistant Bacteria

The discovery of antibiotics in the 1920s revolutionized modern medicine, providing cures for some of the most widespread diseases of the time. Between 1940 and 1960, the 'Golden Age' of antibiotics took place, where many hallmark drugs were developed such as the penicillins, cephalosporins, and aminoglycosides. Antibiotics have since saved millions of lives each year and have contributed to increasing the average life expectancy in the United States from 47yrs in 1900 to approximately 80yrs today[1].

However, concern is rising as bacteria are developing resistance mechanisms to traditional antibiotics. Resistant infections lead to prolonged illnesses, increased medical costs, and more treatment failures. Each year in the U.S. alone, two million people are infected with antibiotic resistant bacteria which result in 23,000 fatalities[2]. Estimates predict that, in the absence of a solution, resistant infections could surpass cancer in total annual deaths by 2050[3].

This problem is coupled with the fact that antibiotic discovery has largely declined[1]. Only one new antibiotic class has been discovered in over 30 years[4]. Analogous of existing drugs have mitigated the impact of this lack of discovery but even their rate of development can no longer adequately compete with the rate of resistance emergence[5]. A major contributor to the paucity of antibiotics is that pharmaceutical companies have shifted away from antibiotic research for reasons including increased regulatory expenses, research challenges, and low returns on investment[1].

The threat of antimicrobial resistance has received global attention, with the U.S. implementing the *National Action Plan for Combating Antibiotic-Resistant Bacteria* in 2015. This plan outlines goals to reduce microbial infections in half by 2020. This plan focuses on promoting the research of new therapeutic and diagnostic methods, strengthening surveillance efforts, and fostering international collaboration to combat resistance emergence. With the overuse of antibiotics being a root cause of resistance development, this plan also emphasizes reducing the unnecessary application of antibiotics throughout healthcare and agriculture[1].

Epidemiological studies have found a direct relationship between antibiotic use and the emergence and dissemination of resistant strains. When antibiotics are applied to a microbial population, they apply a selective pressure which breeds resistance development by eradicating the drug-sensitive population and allowing the resistant subset to thrive and pass on their resistance markers to succeeding and/or neighboring microbes. Resistance can be acquired through spontaneous mutation, clonal expansion, or through horizontal gene transfer from mobile elements[6].

The over-prescription of antibiotics in the clinic is one avenue for resistance development that requires reform. In some U.S. states, the number of prescribed courses of treatment with antibiotics each year exceeds the state's population[7]. In other countries, antibiotics are available over-the-counter enabling unrestricted and unmonitored application. Studies have indicated that in 30-50% of cases, prescriptions are incorrect in the antibiotic agent chosen or in duration prescribed[6].

Antibiotics are also extensively used in the agricultural sector, administered to animals for the purposes of growth promotion and disease prevention. In the U.S., an

estimated 80% of the antibiotics sold are used for animal production purposes. This practice causes a multi-faceted problem as these antibiotics can select for resistant strains which can be transferred to consumers through food consumption and handling. Up to 90% of the antibiotics administered to livestock are excreted through animal waste, which affects the environmental microbiome, by making their way into groundwater, fertilizers, and surface runoff[6].

The challenge and burden resistant infections pose to the global healthcare system calls for the development of new antibiotic technologies, along with reform in the distribution and use of existing therapies. Without immediate and coordinated action, the director of the Centers for Disease Control and Prevention noted 'the medicine cabinet may be empty for patients with life-threatening infections in the coming months and years.'

1.2 Antimicrobial Peptides (AMPs): A Potential Antibiotic Alternative

In light of the resistance crisis, antimicrobial peptides (AMPs) have gained increasing attention as potential antibiotic alternatives. AMPs are small peptides, typically less than 100 amino acids in size, which are produced by organisms across all domains of life as part of their innate immune response against microbial challenge[8]. Around 5,000 AMPS have been identified to date, displaying a large range in structural and functional diversity[9].

The subset of bacterially produced AMPs, called bacteriocins, are especially attractive in the fight against antibiotic resistance. Bacteriocins are produced by microbes to ward of competing strains when resources are scarce[10]. It is estimated that the vast majority of bacteria produce at least one AMP[10]. The widespread dissemination of bacteriocins is likely linked to the fact that the genetic determinants underlying bacteriocin production tend to be found on mobile genetic elements such as conjugative plasmids and transposons. Their ubiquity in the bacterial kingdom, despite their associated production costs, emphasizes their functional utility[11].

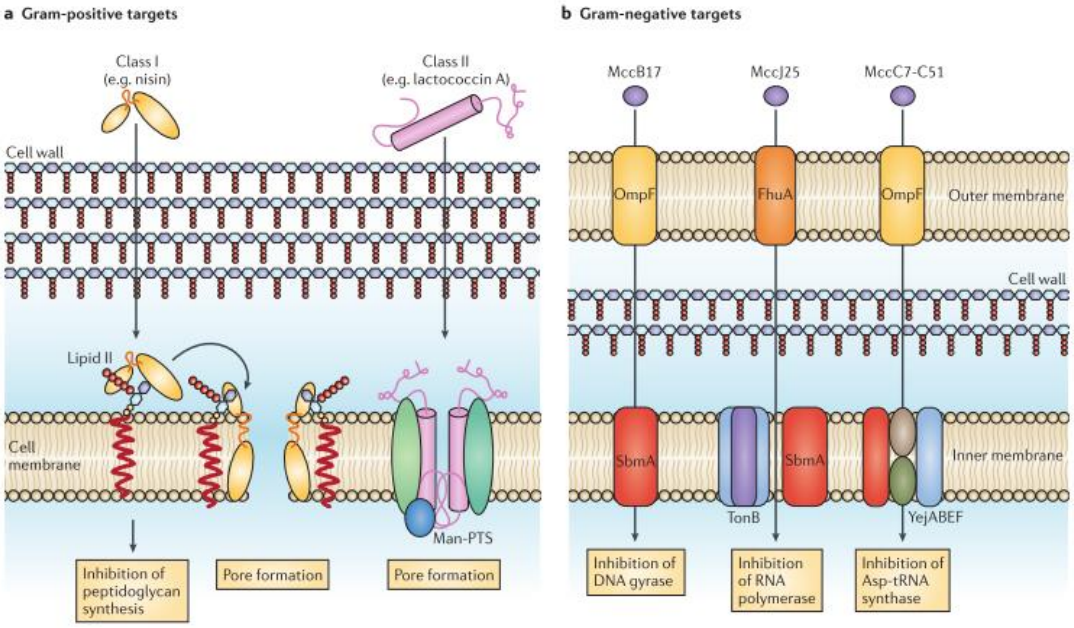

Figure 1-1 *Select AMPs mechanism of action*. Mechanism of entry and action of several AMPs against (a) Gram-positive and (b) Gram-negative bacteria. (Reproduced from Duquesne et al. *Nat. Prod. Rep.*, 2007, 24 with permission from The Royal Society of Chemistry.)

Unlike eukaryotic AMPs, which tend to have broad spectrum activity and require micromolar concentrations for antibiotic effects, bacteriocins tend to have potent activity in the pico to nanomolar ranges against species within the same phylogenetic category as the producer[11]. The host strain is typically equipped with dedicated immunity genes to

combat the toxic effect of the peptide. The fact that many bacteriocins have narrow spectrum activity offers the advantage that they won't disrupt the commensal microbiota through off-target activity or apply a wide selective pressure for resistance development upon treatment, which are common drawbacks of broad spectrum antibiotics[12].

Figure 1 captures some of the diversity of bacteriocins and how they can differ from the level of target-cell entry down to their actual mechanism of antibacterial action[13]. Bacteriocins have been identified that exhibit specific activity against many clinical targets, including those which are antibiotic-resistant, such as methicillin-resistant *Staphylococcus aureus* and vancomycin-resistant *Enterococci*[12].

However, despite all the therapeutic promise of AMP-therapy, there has been a large lack of clinical success. There are many challenges associated with AMP-based treatments, notably their susceptibility to proteolytic degradation and the costs associated with chemical synthesis. The primary commercial applications of AMPs have been limited to topical applications such as their use in dermal creams and mucosal delivery[14]. In this work, we propose a new technology to overcome the transport barriers of AMP-therapeutics for use in treating bacterial infections that spring from the gastrointestinal (GI) tract.

1.3 Recruiting Probiotics to Treat Enteric Infections

1.3.1 Enteric Infections and Foodborne Illness

Each year enteric infections, or those associated with the intestinal tract, cause an estimated 1.5 billion episodes of diarrheal disease and 2.2 million deaths worldwide. Enteric infections are the 5th leading cause of death among all ages globally, while the majority of fatalities occur in children under 5 years of age in developing countries.

These infections can be caused by an array of bacterial, viral, parasitic, and fungal agents that disrupt normal intestinal function[15].

Seventy percent of microbial diarrheal diseases are attributed to foodborne illnesses. The CDC estimates that in the U.S alone, there are 45 million cases of foodborne illness annually, which result in 128,000 hospitalizations and 3,000 deaths. The CDC predicts that 44% of the resulting hospitalizations and deaths are caused by 31 known pathogens[15].

Effective vaccines have not been developed for many key enteric pathogens and antimicrobial therapy is complicated due to the resistance crisis. In agriculture, antibiotics have played a key role in controlling enteric infections in livestock, but many countries have imposed stricter regulations or banned the use of antibiotic in stock feeds to reduce microbial resistance emergence[16].

In light of the public health concerns with enteric infections, attention has been directed to the control, prevention, and detection of foodborne pathogens. The World Health Organization (WHO) has prioritized 22 agents for surveillance based on their higher prevalence, mobility, and mortality rates. These pathogens include *Brucella* spp., *Campylobacter* spp, Enteropathogenic *E. coli*, and *Salmonella* spp. (non-typhoidal). In the search for control strategies, the use of probiotic bacteria has been proposed as an antibiotic-alternative strategy to reduce and control foodborne pathogens[15].

1.3.2 The Role of Probiotics in Gastrointestinal (GI) Health

Probiotics are live microorganisms that are believed to confer health benefits to their hosts upon consumption of adequate doses[17]. Although the beneficial effects of

probiotics have been speculated for centuries, they have recently gained increasing research attention with over 6,000 publications being released in the past two decades. Several mechanisms of actions that contribute to the positive effects of probiotics have been described, including their abilities to strengthen the intestinal barrier, modulate the host immune response, and produce antimicrobial substances[18].

The most common probiotics in use today are lactic acid bacteria (LAB), including Lactobacilli and Bifidobacteria, and non-pathogenic *E. coli* strains. During acute infections, the administration of probiotics may help combat pathogenic microbes through competitive exclusion and/or direct antagonism. There has been promising data elucidating the benefits of probiotics in combating enteric pathogens. For example, Lactobacilli and Bifidobacteria have been shown to enhance colonization resistance in mice infected with *Campylobacter jejuni* and *Salmonella*. Experimental administration of a strain of probiotic *L. acidophilus* was able to prevent cholera in both, mice and suckling rabbits[15].

Probiotics have additional benefits as a livestock feed additive. The use of probiotics as an animal feed supplement dates back to the 1970's, with studies demonstrating their ability to increase performance and feed conversion efficacy in poultry and swine[19].

1.3.3 Engineered Probiotics as AMP-delivery vehicles

With all the promise of both AMPs and probiotics for their individual potential as antibiotic alternatives in combatting enteric pathogens, we propose combining these two avenues and engineering probiotic bacteria as AMP-delivery vehicles.

Probiotics are attractive delivery platforms for AMPs as they are safe-to-consume, can survive transit to the GI tract, and naturally reside alongside the host's intestinal microflora. Probiotics are amenable to genetic engineering and can be manipulated to produce and secrete these peptides at the local site of infection, overcoming the transport barriers associated with AMP-therapy. This work-flow enables a modular technology where the probiotic host and secreted AMPs can be combinatorially interchanged for different hosts and pathogens of interest.

From an engineering standpoint, modified probiotics can enable tunable AMP expression, the production of multicistronic peptide constructs, and dosing regimens can be altered for both preventative and treatment methods. This proposed technology enables the therapeutic power of AMPs to be harnessed while utilizing the historic benefits of probiotics.

1.4 Scope and Organization of Thesis

This work details our recent advances on engineering probiotics for the treatment of pathogenic microbes. The work in this dissertation focuses on using the probiotic *E.coli* strain, Nissle 1917 (EcN), as a delivery vehicle for AMPs that target Enterobacteria, such as *Salmonella* and *E. coli.* We chose to focus on gram-negative pathogens as they remain notorious for antimicrobial resistance due to the presence of their outer membrane, which serves as an additional hurdle for antibiotic entry. The foundation of the work detailed in this dissertation focuses on incorporating and expanding upon existing synthetic biology tools and techniques for technological advancement. Although not the focus of this work, applying peptide engineering and

computational methodologies would greatly complement and enhance the improvement of engineered probiotics and opportunities for these methods are noted when applicable.

In Chapter 2, we describe our development of a synthetic-hybrid promoter system, termed ProTeOn+, which enables robust and well-characterized gene expression. We focus on the application of this promoter network in modifying AMP biosynthetic gene clusters to increase secreted AMP titers from *E. coli*. However, it has many attractive features that could be used in general protein production when exogenous induction is undesirable.

In Chapter 3, we describe our construction of an engineered probiotic, EcN(J25), for *Salmonella* control in poultry. We focus on the application of this system in the agricultural space, a sector where we believe engineered probiotics may have the most potential due to decreased regulatory barriers and an immediate need with stricter regulations being imposed on antibiotic use in livestock. In this work, we demonstrate the first *in vivo* success of AMP-producing probiotics, with our system reducing 97% of *Salmonella* carriage in infected turkey poults 14-days post treatment. A manuscript detailing this work is available in Nature's *Scientific Reports.*

Chapter 4 describes our collaboration with Dr. James Johnson of the Veterans Affairs (VA) Medical Center of Minneapolis in developing engineered probiotics for clinical applications. In this section we describe an engineered EcN derivative we developed, EcN(C7), that elicits strong antagonistic activity against the extraintestinal pathogenic *E. coli* strain, ST131, via production of Microcin C7 (Mcc7). Within the ST131 population, there is a resistant subset that is capable of evading the toxic effect of

Mcc7. We describe approaches we took to understand how this subset was exhibiting resistance, in hopes of finding and developing methods to eradicate this population.

Chapter 5 describes our development and iterations of a modular peptide expression system that enables the release of multiple AMPs through a single AMP-export system. The success of this system could enable the development of broader-spectrum probiotics by releasing AMPs that target a multitude of pathogens or it could be used to release peptides with orthogonal mechanisms of action against a single target to decrease the chances of resistance development.

Collectively, this thesis lays a foundation for future work in the field of engineered probiotics and discusses some of the challenges and potential that lay ahead. Along the way, we describe novel synthetic biology tools we have developed that can contribute to engineering bacteria for future applications outside of AMP-therapy.

Chapter 2 ProTeOn+: A Synthetic Promoter for the Delivery of Antimicrobial Peptides

2.1 Scope

With antibiotic-resistant pathogens emerging in the clinic with disconcerting frequency, the development of new antimicrobial technologies is sorely needed. Antimicrobial peptides (AMPs) offer a promising alternative to traditional antibiotics but remain largely limited in their utility due to their high costs of synthesis and susceptibility to proteolytic degradation. Engineering probiotic organisms as AMP production and delivery vehicles may overcome the barriers associated with AMP-therapy, allowing peptide release at the local site of infection. In this work, we describe a novel synthetic promoter system, termed ProTeOn+. This promoter demonstrates promise in improving titers of AMPs from engineered probiotics when incorporated in AMP biosynthetic gene clusters. ProTeOn+ has been characterized through a combination of experimental assays and stochastic kinetic models, eliciting well-defined and predictable behavior. We focus on using ProTeOn+ to re-engineer the Microcin V (MccV) operon, successfully increasing secreted MccV titers. ProTeOn+ is a useful tool in synthetic biology applications, laying a foundation for rationally designed promoters. Its well-defined behavior could help mitigate concerns over the use of live bio-therapeutics in disease control.

2.2 Introduction

Antimicrobial peptides (AMPs) are secreted natively from organisms across all evolutionary domains and constitute a principal defense mechanism against microbial challenge[11]. In the past few decades investigators have discovered hundreds of AMPs,

many of which elicit potent antimicrobial activity against clinically-relevant bacterial pathogens[8]. With a wide spectrum of structure and function, AMPs have been identified that effectively target bacteria by a multitude of molecular mechanisms, from compromising membrane integrity to targeting conserved intracellular components[13].

With the paucity of antibiotics in the drug-discovery pipeline coupled with the continuing emergence of antibiotic-resistant pathogens, AMPs have been proposed as a therapeutic alternative to conventional antibiotics[20,21]. However, despite their therapeutic promise, the medicinal power of AMPs has yet to be harnessed. The associated production costs, limited bioavailability profiles, and their propensity for proteolytic degradation has widely hampered the clinical success of AMP-therapy[22,23].

A host of bacterial infections spring from the intestinal tract, and AMP-releasing probiotics that prohibit or reverse pathogen colonization may constitute an effective antimicrobial strategy. Numerous examples are now available of probiotic organisms modified to express and secrete AMPs *in vitro*[24–26]. In the past few years, work has begun demonstrating the utility of these 'antimicrobial probiotics' at reducing pathogens such as *Salmonella* and *Pseudomonas* in the intestinal tracts of animals. These successful *in vivo* models have used the probiotic organism, *E. coli* Nissle 1917 (EcN), as the delivery strain[27,28].

Interest in this technology has focused on its application as an animal feed supplement to reduce pathogen colonization in the intestinal tract of animals to replace antibiotic use in the feed. In lieu of tighter regulations on antibiotic use in food-production, this could provide the agricultural industry with an alternative strategy to

protect livestock, improve food safety, and reduce microbial resistance development to clinically-relevant antibiotics[29].

There are many regulatory hurdles associated with the use of genetically modified live bio-therapeutics in animal feed formulations. Aside from implementing biocontainment strategies, the use of a well-characterized promoter system that allows predictive and defined behavior of the engineered component may help mitigate these concerns. Traditional *E. coli* promoters are challenging for *in vivo* applications as they can compromise cellular growth rate[30], their induction can elicit bimodal population distributions[31], and their performance can be affected by the carbon sources in the external environment[32]. In native AMP biosynthetic gene clusters, peptide expression is often activated by stress stimuli, such as glucose or iron depletion, to give bacterial hosts a competitive advantage in acquiring resources from the environment[33]. In the context of a therapeutic delivery system, an ideal promoter should enable robust peptide production that bypasses growth phase limitations and does not require expensive exogenous induction.

In this work, we describe a novel synthetic promoter, termed ProTeOn+, which addresses many of the challenges associated with AMP-expression from *E. coli*. The ProTeOn+ promoter network is a strong constitutive promoter that has been extensively characterized through experimental assays and stochastic simulations. This promoter system enables strong peptide expression in all phases of growth but is designed to reach peak expression levels upon entry into stationary phase. Many AMPs enter sensitive cells through receptors that mediate nutrient transport, many of which are upregulated in nutrient limiting environments, such as stationary phase. This upregulation of AMP

importers likely contributes to the increased susceptibility of target cells to AMPs in these environments, and ProTeOn+ capitalizes on this feature by increasing production in this phase of growth.

The ProTeOn+ promoter has been used successfully in engineering EcN to produce a variety of different AMPs, and led to the first *in vivo* success of engineered EcN at reducing pathogens in the gastrointestinal (GI) tract of animals[34]. Herein, we describe the mechanics of the ProTeOn+ promoter and compare its expression capacity to commercial and native AMP promoters. We also show how redesigning the operon of Microcin V, one of the most studied AMPs to date, with this system can lead to improvements in secreted AMP titers.

2.3 Results

2.3.1 ProTeOn+ Network Mechanics

A schematic of the ProTeOn+ promoter system is depicted in Figure 2-1a. The core component of this network is the synthetic-hybrid activator protein, ProTeOn, which was first developed by Volzing et al.[30].

ProTeOn is a synthetic protein that was constructed using components of the native bacterial tetracycline resistance (*tet*) and luminescence (*lux*) operons. ProTeOn consists of two functional domains, linked together by a flexible polypeptide chain. The N'-terminal region of ProTeOn serves as the DNA-binding component and is composed of the reverse-tetracycline repressor (rTetR). rTetR is a reverse phenotype mutant of the regulatory tetracycline repressor (TetR) and binds specifically to the *tetO* DNA operator site[35]. The C'-terminal region of ProTeOn consists of LuxRΔN(2-162) (LuxRΔN), which is the constitutive activating component of the full-length LuxR regulatory protein. LuxR

is a well-studied transcriptional activator derived from the quorum-sensing luminescence operon of *Vibrio fischeri* [36]. LuxR binds specifically to the *luxbox* operator site and upregulates downstream gene expression through RNA polymerase (RNAP) recruitment to the promoter region.

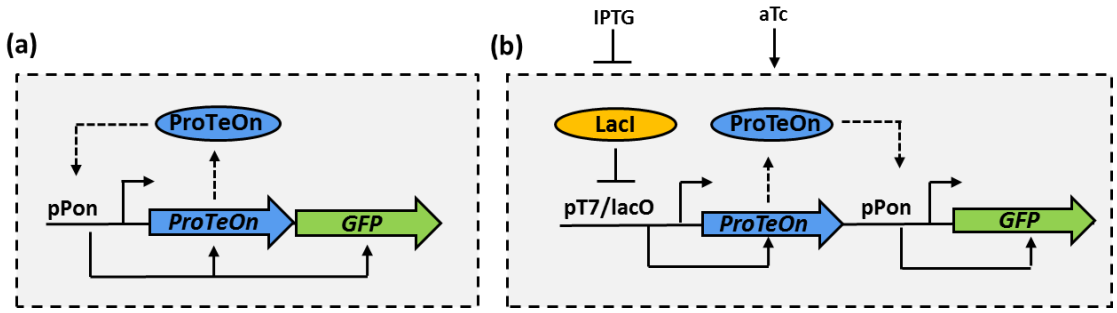

Figure 2-1. *Schematics of network configurations*. (a) ProTeOn+ (b) ProTeOn AND-Gate

The associated synthetic promoter, Pon, contains *tetO* and *luxbox* binding regions that are optimally spaced to facilitate strong interactions with the ProTeOn activator[37]. Upon binding Tc, or equivalently, anhydrotetracycline (aTc), the rTetR domain of ProTeOn undergoes a conformational change that enables stronger binding with the *tetO* site. This DNA binding event brings the attached LuxRΔN component in contact with the *luxbox* operator to promote its activating effect.

In the original AND-gate design (Figure 2-1b), expression of the output signal, green fluorescent protein (GFP), relies on induction with both isopropyl β-D-1-thiogalactopyranoside (IPTG) and aTc. In the ProTeOn+ network described herein, the activator is placed under the control of its own dedicated promoter site (Pon), generating a positive feedback control element. In this configuration, the ProTeOn activator overcomes the requirement for exogenous induction for protein expression. We anticipated a stronger expression profile with this configuration than the predecessor

system and expected the ProTeOn activator to accumulate in cells allowing for dramatic increases in protein production upon deceleration of cellular growth rate. Using GFP as a reporter gene, we compared the expression profiles of the ProTeOn AND-Gate and the ProTeOn+ promoter systems using kinetic spectrophometric measurements.

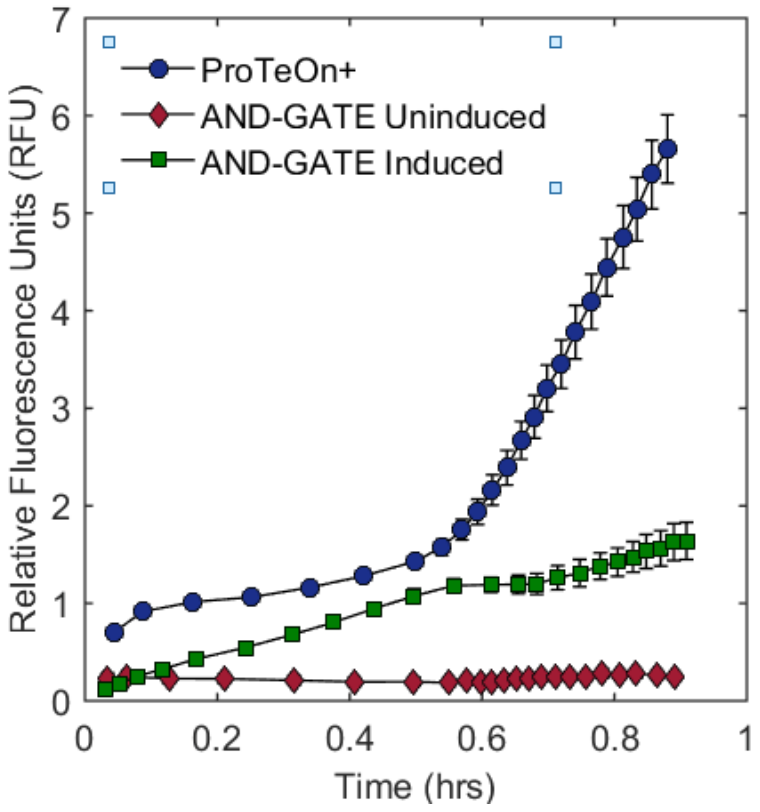

Figure 2-2. *Comparison of ProTeOn+ and AND-Gate expression profiles.* The AND-Gate shows tight inducible expression with negligible expression in the uninduced state (0mM IPTG, 0ng/ml aTc) and significant increases in the 'ON' state (0.5mM IPTG, 100ng/ml aTc). ProTeOn+ (no inducer) outcompetes the fully induced AND-gate across all measurements. The error bar represent the standard error of 3 replicates.

Figure 2-2 shows the expression profiles of the AND-gate in the 'ON' (0.5mM IPTG, 100ng/ml aTc) and 'OFF' (0mM IPTG, 0ng/ml aTc) states in comparison to ProTeOn+ over a range of cell densities. The ProTeOn-AND gate elicits tight inducible expression, while the ProTeOn+ system consistently outperforms the predecessor system

in terms of fluorescence and swells to remarkable output levels in late logarithmic phase. Between OD 0.5 and 1, the fluorescent signal of ProTeOn+ increases 4-fold. A comparison of these two systems with more experimental conditions is available in Appendix A (Figure 8-1).

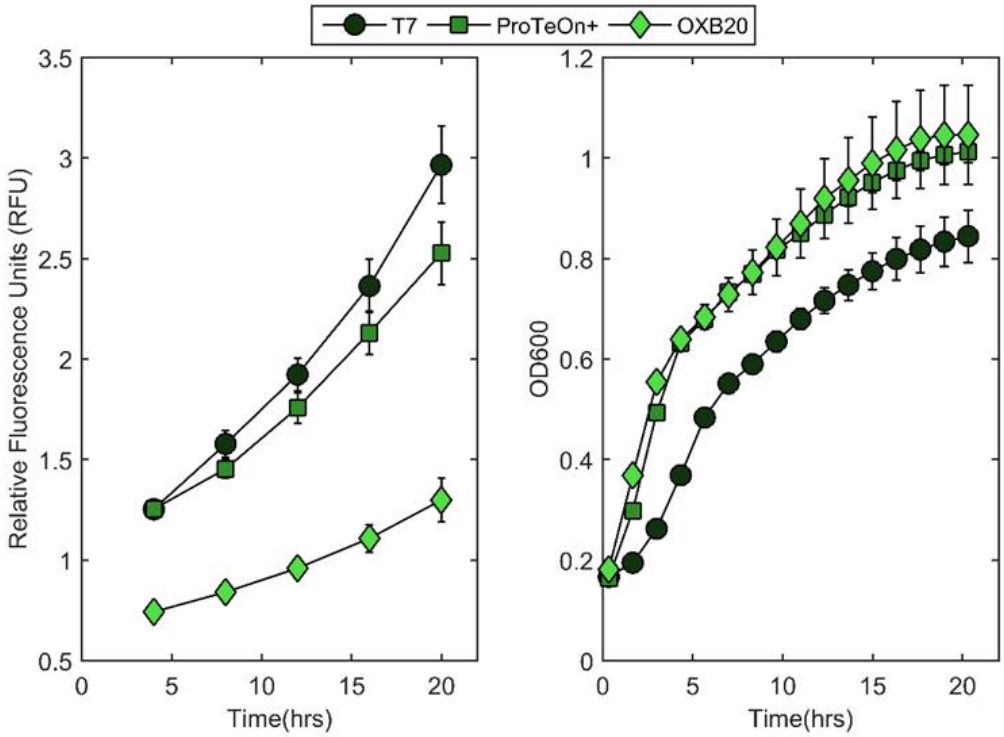

Figure 2-3. *Comparison of ProTeOn+ to commercially available promoters*. GFP expression was kinetically monitored from T7express cells under the control of the ProTeOn+, OXB20, and T7 promoters. The T7 promoter is fully-induced with 1mM IPTG. Fluorescence readings (left) were measured every 4hrs and OD600 readings (right) were taken on 80min intervals for 20hrs. Error bars are standard error of four replicates.

To put the expression strength of ProTeOn+ in context, Figure 2-3 shows a comparison of ProTeOn+ to two commercially available promoters, OXB20 and the fully-induced T7 RNAP/promoter system. OXB20 is a derivative of the LexA-dependent RecA promoter and is the strongest constitutive promoter available from Oxford Genetics. The T7 system is a highly efficient and tightly-inducible promoter system that

is widely-used for expression of cloned genes in *E. coli*. The system utilizes the T7 phage RNAP promoter which selectively transcribes from a dedicated T7 promoter site[38].

In this comparison, ProTeOn+ is competitive with the fully-induced T7 system in the resulting fluorescence signal without the associated growth burden. Although T7 does slightly outcompete ProTeOn+ in production, the primary advantage of ProTeOn+ is that is does not require external induction; which in the context of AMP-expressing probiotics eliminates issues with inducer cost and potential toxicity *in vivo.*

2.3.2 Stochastic-Kinetic Simulations of ProTeOn+

The network components of the ProTeOn+ expression circuit are well-characterized, and many of the known functional interactions have readily available kinetic information[39–45]. Using these values, it is possible to model the molecular mechanisms that underlie the observed phenotype, offering a more detailed understanding of system behavior. To our knowledge, this level of detail is not available for any other bacterial promoter system, making ProTeOn+ an attractive platform for genetically modified organisms and therapeutic technologies.

As biological reactions tend to occur away from the thermodynamic limit, we conducted stochastic simulations to describe the expression profiles of ProTeOn+. These simulations generate probability distributions of molecular concentrations which are directly comparable to experimentally observed fluorescence populations[46].

The model presented in this work takes into account each bimolecular interaction event that underlies the resulting GFP output signal. As aTc is capable of strengthening ProTeOn's interactions with the *tetO* site within the promoter, we chose to include aTc-

induced samples in our simulations to capture any effects induction would have on system output to give better insight into the sensitivity of the *in silico* analysis. The theoretical reaction network used in these models is displayed in Table 2-1 and details each reaction involved in GFP output, from the initial induction step to final protein maturation.

Table 2-1 *Biomolecular Reaction Network*

Biochemical Reaction	Kinetic Constant
Anhydrotetracycline administration	
1. aTcEx → aTc	0.00033 [a,36]
Interactions between PROTET and aTc	
2. PROTET + aTc → PROTET:aTc	552 [b,40]
3. PROTET:aTc → PROTET + aTc	1 [a,40]
4. PROTET:aTc + aTc → PROTET:aTc2	1.38 10^{8} [b,40]
5. PROTET:aTc2 → PROTET:aTc + aTc	2 [a,40]
Interactions between PROTET and tetO	
6. PROTET + tetO → PROTET:tetO	4 10^{3} [b,35]
7. PROTET:tetO → PROTET + tetO	0.1 [a,35]
Interactions between PROTET, tetO and aTc	
8. PROTET:tetO + aTc → PROTET:tetO:aTc	2.76 10^{6} [b,40*]
9. PROTET:tetO:aTc → PROTET:tetO + aTc	1 [a,40]
10. PROTET:tetO:aTc + aTc → PROTET:tetO:aTc2	1.38 10^{8} [b,40]
11. PROTET:tetO:aTc2 → PROTET:tetO:aTc + aTc	2 [a,40]
12. PROTET:aTc + tetO → PROTET:tetO:aTc	4 10^{8} [b*]
13. PROTET:tetO:aTc → PROTET:aTc + tetO	0.1 [a*]
14. PROTET:aTc2 + tetO → PROTET:tetO:aTc2	4 10^{8} [b,40]
15. PROTET:tetO:aTc2 → PROTET:aTc2 + tetO	0.1 [a,40]
Transcription of genes when tetO is free	
16. RNApol + pro + tetO → RNApol:pro:tetO	4 10^{-6} [c,*]
17. RNApol:pro:tetO → RNApol + pro + tetO	1 10^{-6} [a,*]
18. RNApol:pro:tetO → RNApol:pro:tetO_c	2.5 [a,37*]
19. RNApol:pro:tetO_c → RNApol:DNA_c + pro + tetO	30 [a,38]
Transcription of genes when tetO is occupied only by PROTET	
20. RNApol + pro + PROTET:tetO → RNApol:pro:PROTET:tetO	5 10^{-6} [c,*]
21. RNApol:pro:PROTET:tetO → RNApol + pro + PROTET:tetO	1 10^{-6} [a,*]
22. RNApol:pro:PROTET:tetO → RNApol:pro:PROTET:tetO_c	2.5 [a,37]
23. RNApol:pro:PROTET:tetO_c → RNApol:DNA_c + pro + PROTET:tetO	30 [a,38]
Transcription of genes when tetO is occupied by PROTET:aTc2	
24. RNApol + pro + PROTET:tetO:aTc2 → RNApol:pro:PROTET:tetO:aTc2	6 10^{-2} [c,35*]
25. RNApol:pro:PROTET:tetO:aTc2 → RNApol + pro + PROTET:tetO:aTc2	1 10^{-6} [a,35]
26. RNApol:pro:PROTET:tetO:aTc2 → RNApol:pro:PROTET:tetO:aTc2_c	2.5 [a,37*]
27. RNApol:pro:PROTET:tetO:aTc2_c → RNApol:DNA_c + PROTET:tetO:aTc2 + pro	30 [a,38]
mRNA production	
28. RNApol:DNA_c → RNApol + mRNAp + mRNAg	30 / 1782 [d,38]
Translation of GFP	
29. Rib + mRNAg → Rib:mRNAg	1 10^{5} [b,41]
30. Rib:mRNAg → Rib:mRNAg_c + mRNAg	100 [a,39]
31. Rib:mRNAg_c → Rib + GFP	100 / 239 [a,8]
Translation of PROTET	
32. Rib + mRNAp → Rib:mRNAp	1 10^{5} [b,41]
33. Rib:mRNAp → Rib:mRNAp_c + mRNAp	100 [a,39]
34. Rib:mRNAp_c → Rib + PROTET	100 / 355 [d,39]
GFP protein maturation	
35. GFP → GFPm	0.2 [a,*]
Degradation	
36. GFP →	1.2 10^{-3} [41]
37. PROTET →	1.2 10^{-3} [a,41]
38. mRNAg →	2 10^{-3} [a,41]
39. mRNAp →	2 10^{-3} [a,41]

The kinetic constants displayed were found from a review of the literature[39–45]. [a]First order reaction rates have units of s^{-1}, [b]second order reaction rates have units of $(MS)^{-1}$, [c]third order reaction rates have units of 1/s, [d]transcription and translation reactions are Gamma distributed[109]. The GFP and PROTET genes have 717 and 1065 base pairs, or 239 and 355 amino acids, respectively[37,110]. Hence, the total amount of transcribed base pairs is 1782. The reaction rate units are s^{-1}, [*]reaction rates have been modified to fit the experimental results.

The model was used to generate the fluorescent population dynamics of cells containing ProTeOn+ upon induction with 0, 10, and 200ng/ml of aTc at 1, 3, 5, and 7 hours post-induction during exponential growth phase. The results were compared to experimentally observed fluorescence populations under the same conditions.

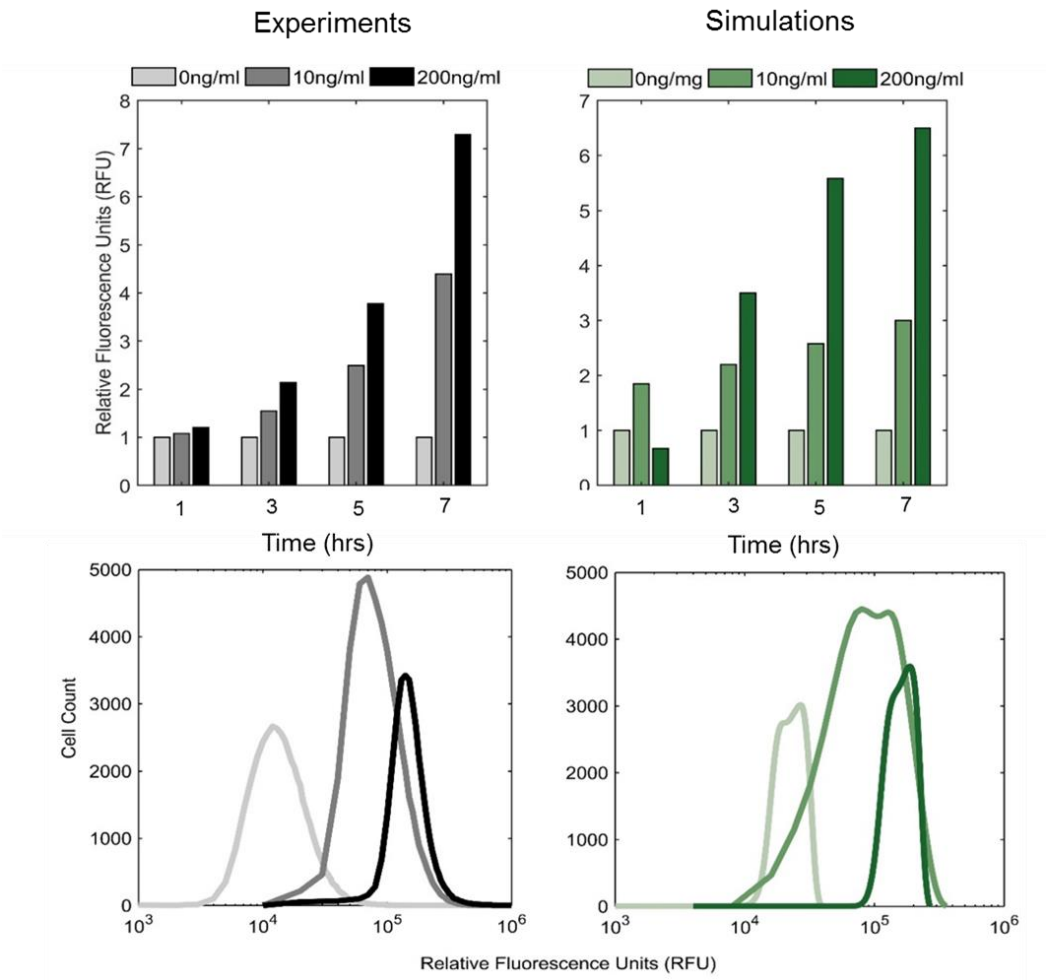

Figure 2-4. *Comparison of ProTeOn+ GFP expression from flow cytometry and stochastic simulations.* The figures on the left are the experimental results and the figures on the right show the simulation predictions. The top panel shows the average intracellular fluorescence of cells induced with 0, 10, and 200ng/ml aTc at 1, 3, 5, and 7hrs post-induction. The simulation results match the relative behavior of the experimental results across all time points. The bottom panel shows the population distributions obtained by the simulations and flow cytometry when they reach their steady-state profiles at 7hrs.

As shown in Figure 2-4, the *in silico* results match both the dynamic behavior of the GFP production dynamics observed experimentally and the absolute production at steady state (7hrs). Although the feedback control element mitigates the induction effect of aTc and leads to only modest increases in GFP signal, these signal changes were accurately captured in our models. More detailed information on the model development can be found in Appendix A.

2.3.3 Incorporate ProTeOn+ into MccV-gene cluster

Most promoters driving AMP expression in native constructs are activated by stress signals to give producers a competitive advantage in survival. MccV, formerly known as Colicin V, was the first antibiotic substance reported to be produced by *E. coli* and elicits antagonistic activity against closely related species[13]. MccV elicits antibiotic activity on sensitive cells by targeting the outer membrane Cir receptor and disrupting membrane potential[13].

The genetic organization of the MccV operon is depicted in Figure 2-5. The MccV gene cluster is 4.2kb long and contains two converging operons. One operon dictates expression of the genes, *cvaC* and *cvi,* which encode for the MccV precursor and self-immunity gene, respectively. The second operon contains the sequences for the

export machinery, including *cvaB*, the ABC transporter, and *cvaA*, the required accessory protein[13].

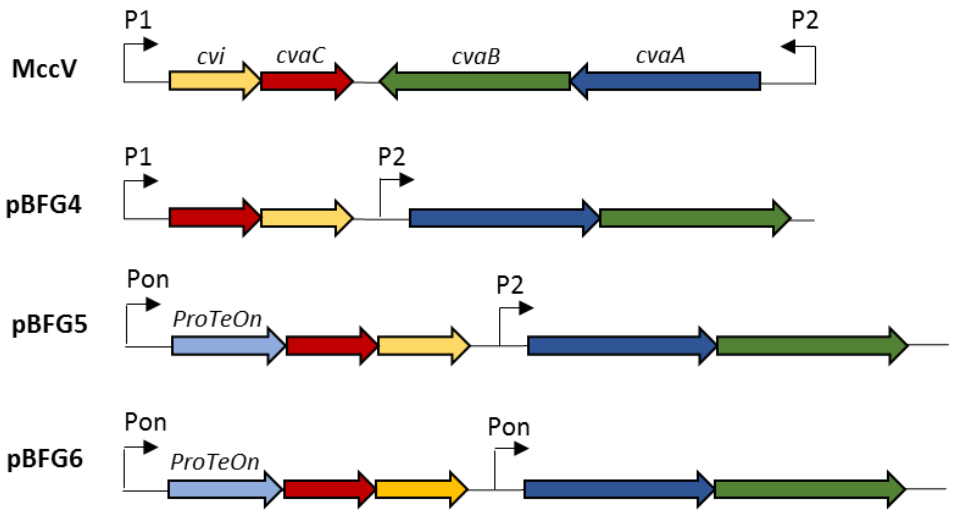

Figure 2-5. *Engineered Gene Clusters for MccV Production.*

Previous work has demonstrated that the promoters upstream of *cvi*, i.e., P1, and *cvaA*, i.e., P2, are both iron regulated[47]. In this work, we compared the promoter strengths of ProTeOn+, P1, and P2 using GFP (Figure 2-6). Using the same spectrophometric growth assay described previously, we measured the fluorescence of each cell culture over time as function of cell density. The results of this assay are shown in Figure 2-6 comparing MC1061 *E. coli* cells expressing GFP from both, ProTeOn+ and P1. ProTeOn+ maintains consistently higher fluorescence levels, whereas P1 demonstrates minimal levels of expression until cells reach a higher optical density (OD~0.8-0.9). At

late logarithmic phase, the P1 promoter abruptly increases its production capacity. The results for the ProTeOn+ and P2 comparison can be found in Appendix A (Figure 8-2).

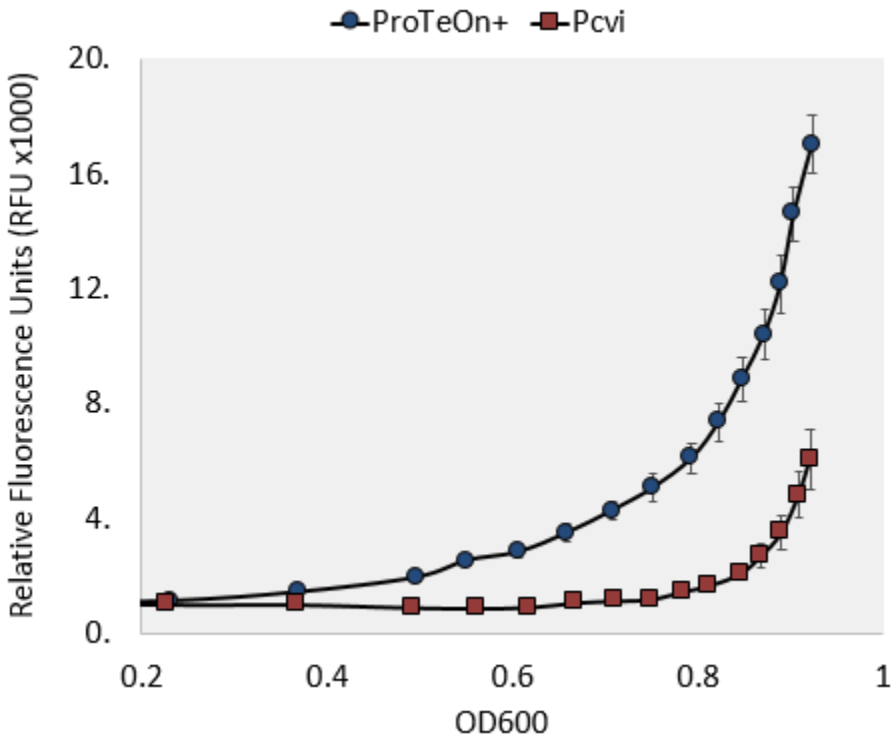

Figure 2-6. *Comparison of ProTeOn+ and P1 promoters*. GFP was placed downstream of ProTeOn+ and P1 and fluorescence was measured at 30min intervals for 24hrs and plotted as function of OD600. Error bars are standard error of four replicates.

We calculated the promoter strengths of ProTeOn+ and P1 in both exponential and stationary phase using the method detailed by Mutalik et al.[48]. From these results, it was determined that the exponential phase promoter strength of ProTeOn+ was over 7.5-fold higher than P1. In stationary phase, the strength of both promoter increases dramatically with 6x and 19x increases for ProTeOn+ and P1, respectively (Figure 2-7). However, even with the sharp activation of the P1 promoter in late-logarithmic phase, the ProTeOn+ system continues to elicit higher expression levels at all times.

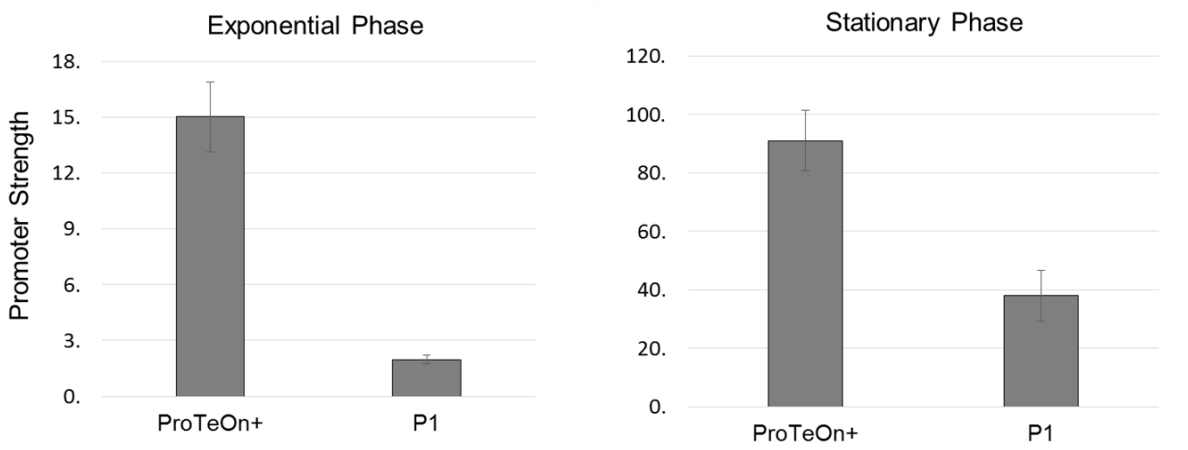

Figure 2-7. *Promoter Strength of ProTeOn+ and P1.* Strength calculated in exponential (left) and stationary (right) phases.

To test if these increases in promoter strength could translate to higher levels of secreted MccV when using ProTeOn+ to drive expression, we created the plasmids pBFG4 and pBFG5 which contain the corresponding gene clusters, depicted in Figure 2-5. These respective gene networks were cloned into a pMS expression vector containing a Spectinomycin resistance marker and ColE1 origin of replication (Appendix A).

Compared to the native construct, we swapped the organization of the four genes of the MccV operon into a linear organization with all genes being encoded in the same orientation. We interchanged the respective positions of *cvaC* and *cvi* and altered the upstream ribosomal binding sites on each. The only difference between pBFG4 and

pBFG5 is the presence of the promoter upstream of *cvi*.

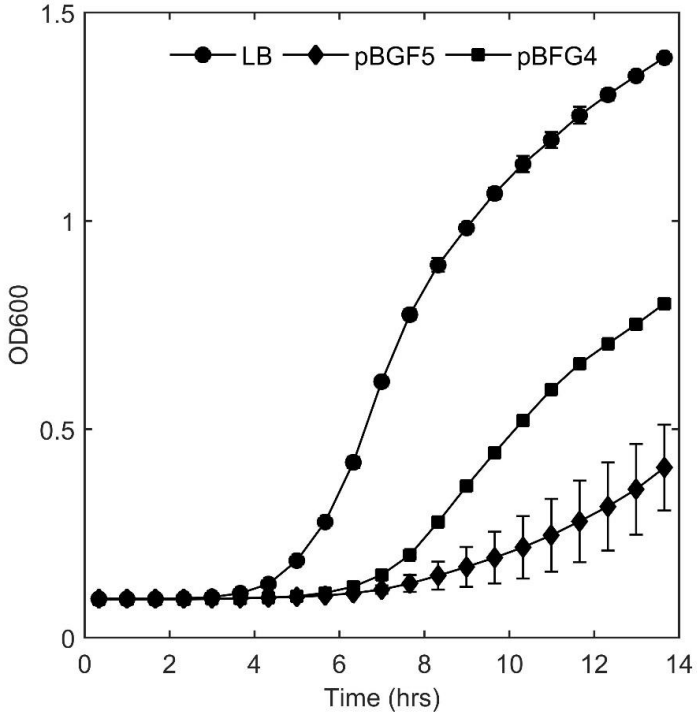

Figure 2-8. *Inhibitory activity of MccV secreted by strains BFG4 and BFG5 during exponential phase growth.* Supernatant containing secreted MccV was collected from BFG4 and BFG5 at OD~2. 10% supernatant was applied to DH5α from BFG4, and BFG5 and growth was monitored by OD600 readings for 14hrs. A control group was treated with 10% supernatant collected from empty MC1061 cells (LB). The errors bars are standard error of three replicates.

To test the secretion capacity of these constructs, we expressed pBFG4 and pBFG5 in M1061 *E. coli* (strains BFG4 and BFG5, respectively) and evaluated the relative levels of external MccV at the end of exponential and stationary phase. To evaluate the amount of MccV secreted in exponential phase, we inoculated washed BFG4 and BFG5 cells to OD~0.1. When the cultures reached the end of growth phase (set at OD~2), the supernatant was collected and tested for antimicrobial activity using liquid supernatant inhibition assays. The supernatant from each producer was applied to a culture of DH5α, a sensitive indicator strain, at 10% of the total volume and growth was

monitored for evidence of inhibition. The resulting growth curves are shown in Figure 2-8. From this assay, the treatment with the supernatant collected from BFG5 led to the greatest inhibition of DH5α indicating higher concentrations of MccV.

To test the secreted MccV at the end of stationary phase, we used an agar diffusion assay. At 16hrs post inoculation, we collected the supernatant from BFG4 and BFG5. The supernatant was serially diluted and spotted on agar plates seeded with DH5α. Using the method described by Solbiati et al., we were able to calculate the minimum inhibitory concentration (MIC) of supernatant required for growth inhibition in terms of Bacteriocin Units (BU)[49]. A BU is defined as the reciprocal of the final dilution that inhibits growth of the indicator strain. For BFG4 the MIC was 6 BUs and for BFG5 was 2 BUs, consistent with our previous results.

We note that we developed the construct, pBFG6, by placing the Pon promoter upstream of both, *cvi* and *cvaA*. However, this arrangement dramatically decreased peptide secretion as determined by an agar diffusion assay. We hypothesize that increasing the transporter levels may affect membrane permeability and integrity making this an unfeasible engineering route.

2.4 Discussion

AMPs are a largely untapped reservoir of antibiotic activity that remain hindered in their therapeutic application due to their inherent economic and transport barriers. In this work, we propose recruiting and redesigning bacteria as peptide delivery vehicles to enable localized production of otherwise undeliverable AMPs.

The success of AMP-producing bacteria lies largely in the underlying gene expression circuits that dictate peptide expression and secretion. Herein, we describe our development of a new synthetic biology tool, the ProTeOn+ promoter, for use in AMP-delivery applications. ProTeOn+ is competitive with commercial promoters in terms of protein production but has the advantage of being fully characterized through a combination of experimental and computational techniques eliciting well-defined and predictable behavior.

We have used ProTeOn+ to improve MccV titers from its native biosynthetic gene cluster. The use of ProTeOn+ in this context enables increased peptide secretion in both primary phases of growth, which translates to greater inhibitory activity. With the recent advances in the successful use of AMP-producing probiotics, this study offers a stepping stone in the pathway of rationally designing AMP gene clusters.

2.5 Materials and Methods

2.5.1 Bacterial Strains and Plasmid Construction

The Pon promoter, ProTeOn activator, and GFPmut3 sequences were synthesized by GENEART in a pMS expression vector containing a ColE1 origin of replication and Spectinomycin resistance gene (pBFmut3). A detailed plasmid map is available in Appendix A. The ProTeOn AND-Gate vector maps and construction methods are detailed in ref. 30. Both networks were transformed into chemically competent BL21(DE3) cells (Sigma Aldrich) via heat-shock for the fluorescence assays.

Plasmids pBFG4, pBFG5, and pBFG6 (maps in Appendix A) were constructed by amplifying *cvaA* and *cvaB* from pHK22 (donated by Professor Kolter, Harvard University) and inserting them into pBFmut3 in place of GFP using NEBuilder® HiFi

DNA Assembly Master Mix (HiFi, NEB). A gene fragment was synthesized from Integrated DNA technologies (IDT) containing *cvaC* and *cvi* with the ribosomal binding sites (AGGAGGA) upstream of both genes. This gene was inserted downstream of ProTeOn to create pBFG5. The ProTeOn+ promoter site was removed and replaced with the P1 promoter, which was synthesized by IDT for the development of pBFG4 via HiFi. For pBFG6, the Pon promoter sequence was synthetized by IDT and inserted in place of P1 via HiFi assembly. pBFG4, pBFG5, and pBFG6 were expressed in MC1061 *E. coli* (Lucigen) for all work presented (strains BFG4, BFG5, BFG6, respectively).

2.5.2 Spectrophotometer Fluorescence Assays

BL21(DE3) cells containing the ProTeOn AND-Gate and ProTeOn+ networks were grown overnight in selective Luria-Bertani (LB) media at 37°C with agitation at 225rpm. 1.5ml of the overnight cultures were transferred to a 2ml microcentrifuge tube. The cells were washed twice by centrifuging for 2 min @ 2.5rcf and resuspended in 500µl of fresh LB. Cultures were diluted to 10^4 CFU/ml and transferred to a sterile, black-walled 96-well plate (CellVis) in 10µl volumes. LB media containing varying levels of IPTG and aTc (0-1mM IPTG, 0-200 ng/ml aTc) were added, bringing the final volume to 350µl/well with four replicates per treatment.

Fluorescence (Ex 485, Em 528, gain 100) and optical density (600nm) measurements were taken every 15-20 mins in a Biotek Synergy H1 microplate reader maintained at 37°C in double-orbital mode. Wells containing empty cells and LB-only were assayed in parallel to correct for auto-fluorescence and background absorbance from the media. The OD600 reading of each sample was blanked to correct for LB background and the

fluorescence was corrected by subtracting the average reading of the empty BL21 cells as a function of OD.

For the OXB20, ProTeOn+, and T7 promoter comparison, T7-express cells containing the pSF_PonMut3, pSF_OXBmut3, and pSF_T7mut3 plasmids (Appendix A) were grown in selective LB media containing 50µg/ml Kanamycin overnight. OD readings were taken every 80 mins and fluorescence on 4hr intervals. OD600 and fluorescence measurements are shown without additional corrections.

2.5.3 GFP Quantification via Flow cytometry

Overnight cultures of BL21(DE3) cells containing the ProTeOn+ network were diluted 1:10 in selective LB media. After 2 hours of growth, the cells were inoculated in LB media containing 0, 10, or 200 ng/ml aTc at an OD~0.1 with 4 replicates per treatment. All cultures were maintained at 37°C with agitation at 225rpm for the duration of the experiment. Samples were monitored for growth by OD600 and were diluted 1:10 on 2-hour intervals to restrict growth to logarithmic phase. At 0, 1, 3, 5, and 7 hours post-induction, 0.1ml of cells was collected from each sample. The harvested cells were centrifuged for 3min @2.5rcf and fixed with 4% paraformaldehyde (PFA, Affymetrix) for 30 mins to halt GFP production and degradation following harvest. Samples were then centrifuged and resuspended in 0.25ml of phosphate buffer saline (PBS, Teknova) and stored at 4°C until analysis.

GFP fluorescence was measured using a BD Accuri C6 flow cytometer. For each sample, 25,000 gated events were collected and analyzed using BD Biosciences software.

2.5.4 Stochastic chemical reaction simulations

The theoretical reaction network (Table 2-1) was created in order to simulate the experimentally observed behavior of the ProTeOn+ promoter system. To simulate the kinetic equations, a hybrid stochastic-discrete and stochastic-continuous algorithm, Hy3S, was implemented[50,51]. In the past, Hy3S has been employed for the simulation of multiple different biological systems[35-39]. Hy3S solves the system by coupling chemical Langevin equations with discrete kinetic Monte Carlo methods[52]. Milstein's method was used and 100,000 trajectories were simulated per aTc treatment[50,51]. More detailed information on model development and parameters in available in Appendix A.

2.5.5 Liquid Supernatant Activity Assays

1ml of overnight cultures of BFG4, BFG5, and empty MC1061F' cells were collected and centrifuged for 3min @ 2.5rcf. The supernatant was decanted and the pellet was resuspended in 2ml LB. Replicate cultures of each strain were diluted to an OD~0.1 in 2ml LB. When the cultures reached an OD~2, 1ml of each culture was transferred to a microcentrifuge tube and centrifuged for 1min @13.5rcf. The supernatant was collected and sterilized using a .22µm filter.

In a 96-well plate, 180µl of 10^4 CFU/ml DH5α was transferred to each well. The collected supernatant from each strain and replicate was diluted in spent media from MC1061 and applied to DH5α bringing the total supernatant treatment to 10%. The OD600 was measured on 20-min intervals using a Biotek Synergy H1 microplate reader that was maintained at 37°C in double-orbital mode.

2.5.6 Agar Diffusion Assay

Supernatant was collected from replicate overnight cultures (16hrs) of BFG4, BFG5, BFG6, and empty MC1061 cells. The supernatants from BFG4, BFG5, andBFG6 were two-fold serially diluted into spent media from MC1061. LB agar plates containing 200µl of OD~0.5 DH5α per 40ml media were spotted with 10µl of each subsequent serial dilution. The plates were incubated for 24 hours and zones of inhibition were evaluated.

Chapter 3 Antimicrobial Probiotics Reduce *Salmonella enterica* in Turkey Gastrointestinal Tracts

Adapted from "Forkus, B., Ritter, S., Vlysidis, M., Geldart, K., & Kaznessis, Y. N. (2017). Antimicrobial Probiotics Reduce *Salmonella enterica* in Turkey Gastrointestinal Tracts. *Scientific Reports, 7*."

3.1 Scope

Despite the arsenal of technologies employed to control foodborne nontyphoidal *Salmonella* (NTS), infections have not declined in decades. Poultry is the primary source of NTS outbreaks, as well as the fastest growing meat sector worldwide. With recent FDA rules for phasing-out antibiotics in animal production, pressure is mounting to develop new pathogen reduction strategies.

We report on a technology to reduce *Salmonella* enteritidis in poultry. We engineered probiotic *E.coli* Nissle 1917, to express and secrete the antimicrobial peptide, Microcin J25. Using *in vitro* experiments and an animal model of 300 turkeys, we establish the efficacy of this technology. *Salmonella* more rapidly clear the ceca of birds administered the modified probiotic than all other treatment groups. Approximately 97% lower *Salmonella* carriage is measured in the treated group, 14 days post-*Salmonella* challenge.

Probiotic bacteria are generally regarded as safe to consume, are bile-resistant, and can plausibly be modified to produce a panoply of now-known antimicrobial peptides. The reported systems may provide a foundation for platforms to launch

antimicrobials against gastrointestinal tract pathogens, including ones that are multi-drug resistant.

3.2 Introduction

Foodborne gastrointestinal (GI) tract infections exact a vast global health toll, with nearly one in ten individuals falling ill each year [53]. In the U.S., non-typhoidal *Salmonella* (NTS) is responsible for the highest incidence of foodborne disease among bacterial pathogens, causing one million infections, 19,000 hospitalizations and over 400 deaths annually [54,55].

Poultry is a major reservoir for NTS, with more than half of outbreaks linked to the consumption of contaminated poultry products [54]. In particular, *Salmonella* enterica serovar Enteritidis (SE) is the most common NTS strain in the U.S. food supply [54]. Poultry are asymptomatic carriers of SE, which allows rapid transmission through flocks. Subsequent spread to the community can occur at many stages along the food-production chain, but primarily at the consumption level [56].

A related public health concern is the continuing emergence of antibiotic-resistant foodborne pathogens. The Centers for Disease Control and Prevention have estimated that 5% of NTS infections are already resistant to 5 or more antibiotics, and have classified NTS as a 'serious threat' to public health [55]. Resistant infections complicate patient treatment leading to prolonged illnesses, increased mortality rates, and higher medical expenses [55].

This widespread resistance development is partly attributed to the heavy use of antibiotics in animal production [57]. Over 70% of the antibiotics produced in the U.S. are

incorporated in livestock feed [58]. It is plausible that this continuous, sub-therapeutic administration applies selective pressures that facilitate the evolution of resistance development. Resistant strains may then be released to the environment through fecal shedding, human handling, and consumed foods[57]. This microbial release is concerning because there is considerable overlap between the antibiotics listed by the World Health Organizations as 'critically important' for human health and animal health.

With these concerns, pressure is mounting to phase out the nontherapeutic use of antibiotics in U.S. food production [29]. Proposals to legislate feed-grade antibiotic removal have been met with significant opposition because a complete ban could lead to increased food prices and strain current agricultural practices [57]. Instead, the FDA issued a rule on livestock use with the agreement of animal pharmaceutical companies. According to this plan, drug companies will voluntarily revise the FDA-approved labeled use conditions, and change the marketing status from over-the-counter to Veterinary Feed Directive for drugs administered through feed or to prescription status for drugs administered through water. The ultimate goal is to promote the judicious use of medically important antimicrobial drugs in food animals and to remove the use of antimicrobial drugs for production purposes [29].

Antibiotics in animal feed prevent or reduce the incidence of infectious disease [57]. Therefore, it may be surmised that with the imminent phasing-out process, alternative, affordable pathogen reduction technologies are needed to help mitigate consumer risk and exposure to foodborne pathogens.

We present tests of a modified probiotic *E. coli* strain, Nissle 1917 (EcN), with the capacity to reduce SE counts in the GI tract of turkeys. Using recombinant DNA technology, we modified EcN to produce and secrete the antimicrobial peptide (AMP), Microcin J25 (MccJ25). We show in two repeat studies that the modified probiotic (EcN(J25)) can substantially reduce SE counts in the ceca of turkeys. With the administration of a single dose, we observe markedly improved SE clearance rates over a two-week period compared to treatment with the antibiotic, enrofloxacin (ENR), or the unmodified EcN.

Beneficial bacteria have been used in the agricultural industry for years to improve animal health and limit pathogen colonization. Often administered as competitive exclusion products, commercial treatments have been developed that are routinely administered to newly hatched birds [59]. Probiotic formulations have also been tested as feed additives. When incorporated in livestock diets, probiotics can improve animal growth, feed conversion efficiency [60], and reduce shedding of enteric pathogens [61].

Herein we show in two repeat trials that a modified probiotic (EcN(J25)) can substantially reduce SE counts in the GI tract of turkey poults. We observe markedly improved SE clearance rates over a two-week period compared to the traditional antibiotic enrofloxacin or the unmodified EcN.

3.3 Design of System for AMP Production and Secretion

Our objective is to lower SE carriage in the GI tract of poultry by employing probiotic EcN as the production and delivery vehicle of MccJ25. MccJ25 is a 21-residue peptide [62] natively secreted from the human *E. coli* isolate AY25[49]. MccJ25 elicits a

strong antagonistic affect against SE. Mature MccJ25 forms a lasso structure[62], affording remarkable stability against unfolding and degradation. The peptide inhibits bacterial growth primarily by binding to RNA polymerase and obstructing nucleotide uptake [63].

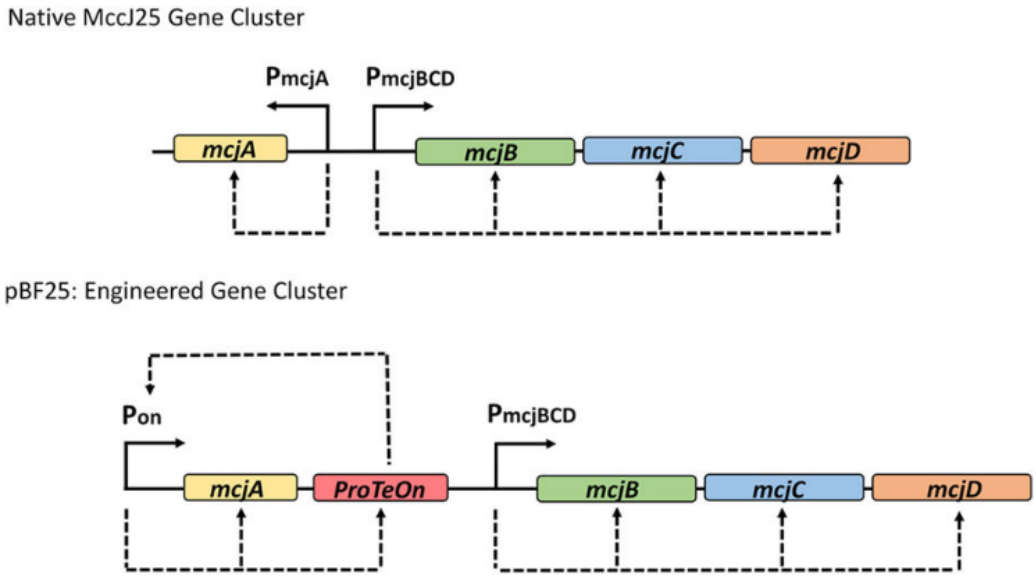

Figure 3-1 *Schematic of native and engineered MccJ25 operons.* In the natural gene cluster, *mcjA* is divergently expressed from its dedicated processing and transport enzymes. Expression of *mcjA* is activated in stationary phase while *mcjBCD* are constitutively expressed by a σ^{70}-like promoter. pBF25 is the engineered construct used in this study where *mcjA* production is under the control of the ProTeOn+ system and all genes are convergently expressed.

The four genes facilitating production of the microcin, i.e., *mcjA*, *mcjB*, *mcjC*, and *mcjD*, are located adjacently on a native plasmid-borne operon (Figure 3-1)[49]. *mcjA* encodes the MccJ25 precursor that is processed into the active form by enzymes, McjB and McjC [64]. The immunity protein, McjD, enables the active efflux of the peptide to the extracellular space [64]. Natively, *mcjA* expression is governed by an ill-defined promoter that initiates production upon entry into stationary phase, with maximal expression in conditions of nutrient depletion. The other genes are hypothesized to be constitutively expressed [65] .

In this work, we engineered a strong promoter system to bypass native limitations on *mcjA* production. Expanding upon the synthetic ProTeOn system, a hybrid protein-promoter pair developed by Volzing and co-workers [37], we designed 'ProTeOn+', a new genetic circuit, which enables constitutive, high-level production of downstream genes. ProTeOn is a synthetic activator protein constructed by physically linking the reverse tetracycline repressor protein to the activating domain of the LuxR transcription factor of *Vibrio fischeri*. ProTeOn makes strong contacts within the engineered DNA promoter site (Pon), which contains optimally spaced tetracycline and LuxR operator binding regions. This system recruits RNA polymerase and strengthens the holoenzyme-DNA interactions to strongly up-regulate gene expression [37].

In ProTeOn+, we incorporated the ProTeOn protein in a positive-feedback control loop, allowing it to amplify its own production while driving expression of a target protein (Figure 3-1). We incorporated ProTeOn+ upstream of *mcjA* and reorganized the genes to be convergently expressed, creating pBF25 (Appendix B). This system achieves more robust gene expression than previously afforded and has a markedly stronger expression capacity than the strong, commercial promoter, OXB20 (Chapter 2).

3.4 Results

3.4.1 *In Vitro* SE Growth Inhibition

To evaluate the antimicrobial potency of the engineered gene expression cassette, pBF25 was expressed in Nissle (EcN(J25)). As shown in Figure 3-2a, EcN(J25) exhibits clear microcin activity after just 2 hours of culture growth and the peptide continues to accumulate in the supernatant over time. In contrast to the native promoter, the ProTeOn+ system affords microcin production across all stages of growth.

Figure 3-2a demonstrates that microcin-containing supernatant (SN) produced by EcN(J25) inhibits SE growth. The assay shows kinetic growth curves of SE in the presence of small volume fractions of MccJ25-rich SN. The two microcin-containing treatments (0.5 and 1%) exhibit considerable growth suppression compared to the control (0%) after just 4 hours of exposure ($p<0.05$).

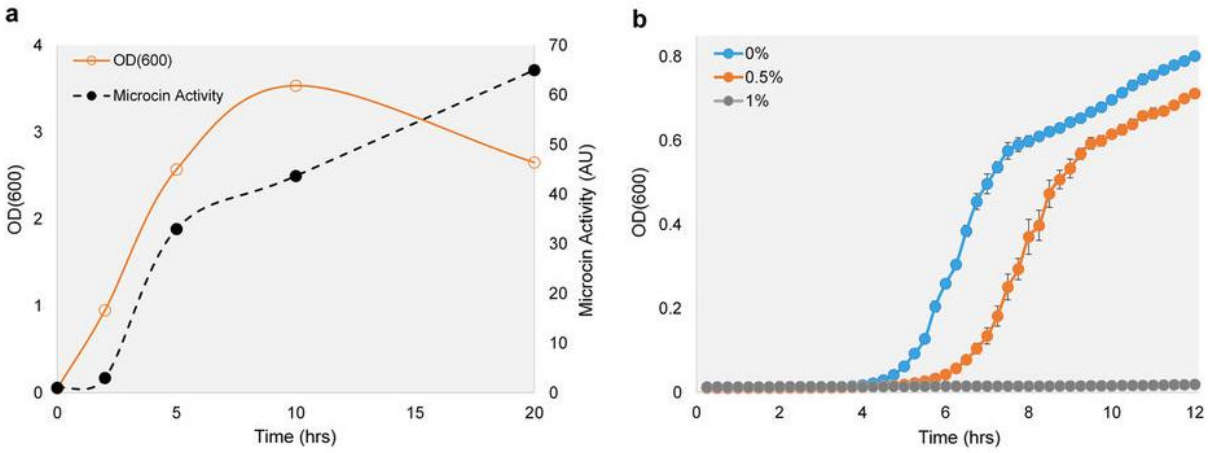

Figure 3-2 *Modified probiotic elicits strong antagonistic activity against SE* (a) pBF25 enables growth phase independent production of MccJ25. The growth (OD600) of EcN(J25) is shown as a function of time. Supernatant was collected from EcN(J25) at 0, 2, 5, 10 and 20hrs following inoculation in fresh media. Two-fold serial dilutions of the supernatant were plated on SE-agar plates and the reciprocal of the final dilution with a visible halo was denoted as the activity units (AU). Microcin production from the modified Nissle commences immediately upon inoculation with visible activity after just 2 hrs. (The connecting lines used are for visualization purposes and are not interpolations of the data points.) (b) Kinetic growth inhibition of SE in the presence of supernatant from the modified probiotic strain. SE is grown in the presence of 0, 0.5, and 1% volume fractions of supernatant collected from EcN(J25), demonstrating a strong antimicrobial effect.

3.4.2 SE reduction in turkey ceca following EcN(J25) treatment

To test the efficacy of the modified probiotic at reducing colonization of SE in the GI tract, we performed two independent treatment trials in turkey poults. We focused on pathogen clearance in the ceca because they are the primary area of bacterial residence within the poultry GI tract, harboring over 10^{11} organisms per gram of digesta [66]. The function of the ceca is to provide a stable bacterial ecosystem, and aid in feed fermentation and digestive processes. The ceca are the principal colonization site of *Salmonella* and are a major source of contamination in processing facilities [67,68]. Reducing *Salmonella* levels in the ceca at the pre-harvest stage may decrease the amount that initially enters the food chain.

We challenged turkey poults at 4 days post-hatch with a 1ml oral gavage of 10^8 colony forming units (CFU) of SE (day 0), followed on day 1 by treatment with 1ml of either 10^8 CFU EcN, 10^8 CFU EcN(J25), or PBS (phosphate buffer saline). These primary treatment groups allowed for comparison between the modified probiotic's engineered antimicrobial activity and any inherent competitive exclusion or native antagonistic effect of the unmodified strain. The SE strain used, MH91989, was previously isolated from a chicken GI tract and is known to colonize poultry intestines.

Over a two-week period, we extracted the ceca from birds at 5 time points post SE-infection and enumerated the SE and Nissle count densities. Figure 3-3 shows the trajectories of the SE counts for each individual treatment group throughout each of the studies. In both trials, all SE counts declined for all groups over the two-week trial.

In Trial 1, the SE counts in the EcN(J25)-treated birds were significantly reduced compared to the untreated birds (p=.03, see Materials and Methods). By the final time point (day 14), the SE counts were reduced by over an order of magnitude, with SE being reduced by a factor of 25 compared to the SE-control group. Trajectories displaying individual bird counts for both challenge strains can be found in Appendix B.

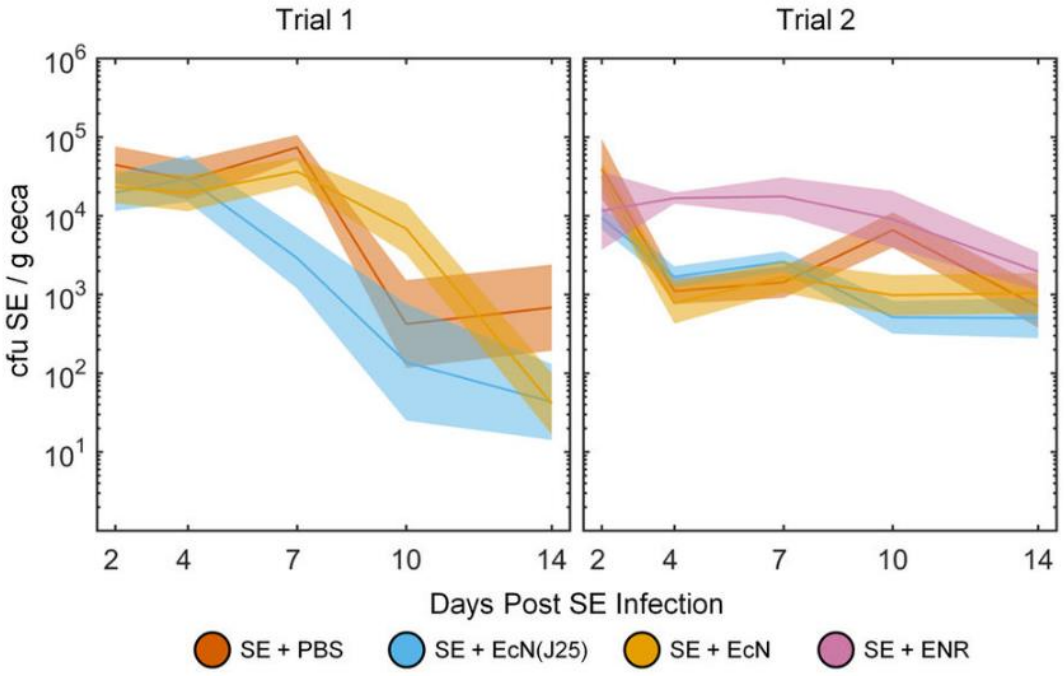

Figure 3-3. *SE reduction in the ceca of turkey poults administered the EcN(J25) treatment.* Turkey poults at 4 days post-hatch (day 0) were challenged with 10^8 CFU of SE. On day 1, birds were treated with PBS, EcN(J25), EcN, or ENR (Trial 2 only). 3–8 birds were euthanized from each treatment group 2, 4, 7, 10, and 14 days post-infection. SE and EcN were enumerated using selective plating to determine CFU per gram of ceca. The average SE counts at each necropsy point are shown for each treatment group at each time point for both trials. Time course line thickness represents the standard error. Both trials were analyzed separately using ANOVA and post-hoc analysis was performed for pairwise comparisons. More detailed descriptions of the statistical analysis can be found in the Materials and Methods.

The differences between the SE-reduction trends in the two trials can be attributed to slightly different experimental parameters. In Trial 2, the crinoline flooring in the isolator units was removed on day 1 to mitigate any reinfection process caused by coprofagia. In Trial 1 this flooring was removed on day 4. The earlier removal in Trial 2 may explain the rapid 10x reduction of SE observed at the first collection point in the EcN(J25)-birds, absent in Trial 1. We note that fecal shedding within housing facilities and subsequent ingestion have been implicated as the primary route of horizontal pathogen transmission [69]. We hypothesize that any SE-reduction effect attributed to the more sanitary conditions created by the removal of the crinoline flooring may be more efficacious than the probiotic treatment in controlling SE. In Trial 2, all treatment groups, excluding the ENR-group, experience a dramatic decrease in SE counts by day 4, alluding to expedited pathogen shedding in this more hygienic environment.

In both trials, the unmodified Nissle did not by itself yield a significant reduction in SE counts. This result demonstrates that MccJ25 activity was responsible for the faster clearance rate from the ceca.

In Trial 2, we compared the efficacy of the EcN(J25) treatment to the activity of a single dose of enrofloxacin (ENR), a fluoroquinolone antibiotic. As shown in Figure 3-3, the ENR treatment led to significantly higher SE levels than all other treatment groups ($p \leq .02$, see Materials and Methods).

To monitor animal health and assess any adverse effects of the probiotic treatments, we included a PBS control group, as well as a group administered EcN(J25) in the absence of SE. These control treatments enabled us to examine cecal score and bird

weight as indicators of overall health. All treatments showed no adverse effects, and bird weight remained nearly identical across all groups (Appendix B). In addition, we observed no visible changes between any of the groups in the morphology of the GI tract and the nature of the cecal contents.

The probiotic does not colonize the intestinal tract as strongly as SE. The levels of the modified and unmodified probiotic were monitored throughout the course of the study. EcN and EcN(J25) passed through the intestines with a residence time of 3-5 days before counts dropped below the level of detection (Appendix B).

Notably, none of the tested SE isolates exhibited microcin resistance following their passage to the cecum (Appendix B).

3.4.3 Microbiome Analysis

The poultry GI tract is developmentally very active in the early post-hatch period. Because intestinal health is critical to bird development, for years commercial poultry producers have used antibiotics to achieve and maintain GI stability and consistency within flocks[70]. Previous studies suggest that EcN enhances early GI tract maturation[71], reduces shedding of enteric pathogens, and may improve body weight gain[72]. We performed a microbiome analysis on 258 ceca samples to ensure that our modification on Nissle did not adversely affect intestinal health.

In Figure 3-4a, it is evident that the microbiota profiles in groups treated with the modified or unmodified EcN have no major differences. This implies that the microcin does not significantly alter the native gut microbial distribution, a challenge routinely encountered with standard antibiotic regimens [73]. Consistent with previous work, we

observe clear temporal shifts in bacterial populations, with Clostridia spp. dominating the microflora [74].

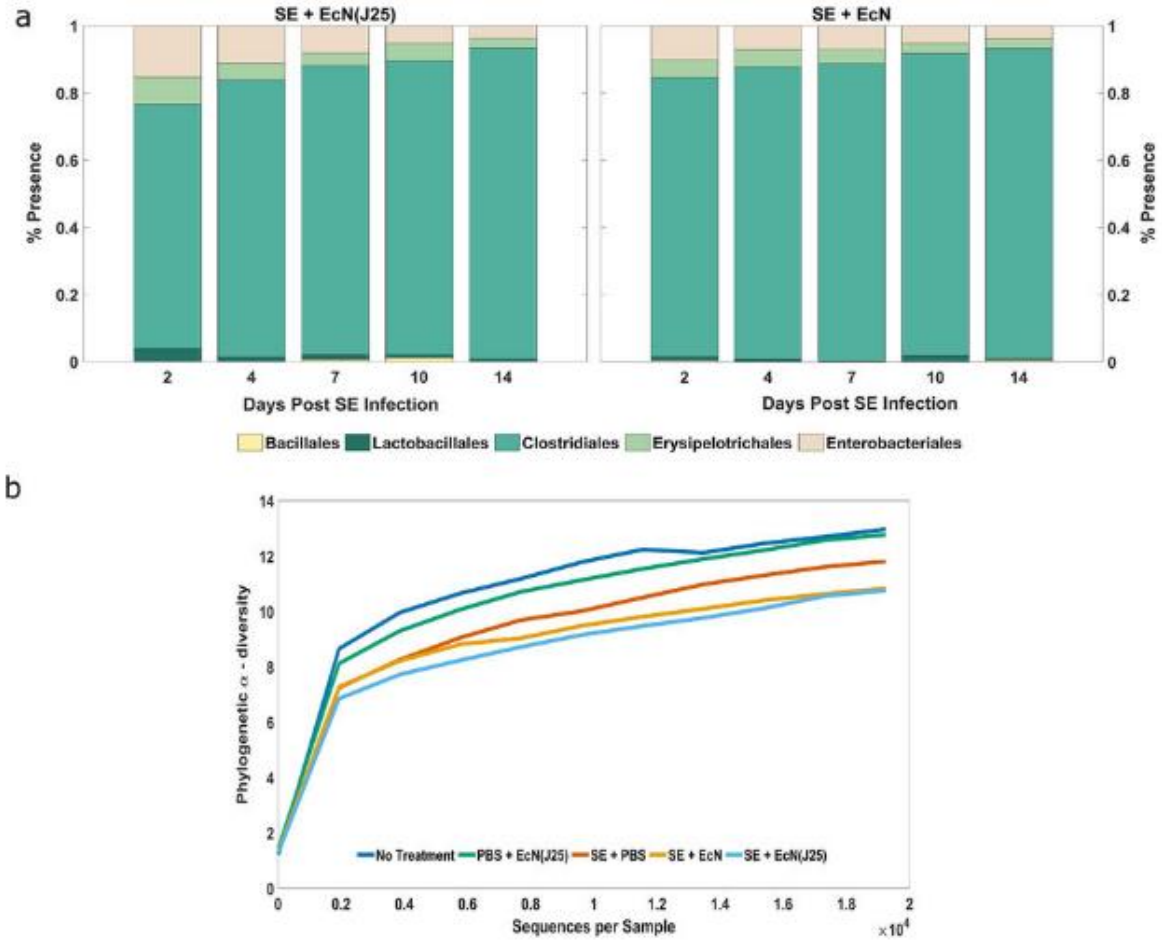

Figure 3-4. *Modified probiotic has no discernible impact on microbial diversity* (a) Presence of microbial species in the bird's microbiota in the 'order' taxonomic category. The ceca samples extracted from poults challenged with SE and treated with the modified probiotic (left) and unmodified probiotic (right) were averaged across both trials. The percent presence (×100) of the microbial species are shown for each collection point. (b) Alpha-diversity plot for Trial 1 at day 14 post-infection. UniFrac phylogenetic diversity was used as a criterion.

In accord with recent literature [75], SE significantly reduces microbial diversity across all infected groups. The untreated control birds and those administered solely EcN(J25) have markedly similar α-diversity profiles at day 14 (Figure 3-4b). The

presence of the pathogen appears to have a more appreciable effect on diversity than the modified probiotic alone. In the SE-treatment models, EcN and EcN(J25) have similar effects further substantiating our conclusion. More detailed microbiota analysis is available in Appendix B.

3.5 Discussion

The presented technology reduced cecal SE carriage, taking advantage of the remarkable character of MccJ25, a naturally occurring AMP. AMPs are ancient host defense effector peptides, produced by organisms across all biological domains as part of the innate immune response against microbial challenge[21]. AMPs, for all their promise as alternatives to antibiotics, have failed in translational success, largely due to their high synthesis costs and rapid degradation in the body [21].

The use of a probiotic delivery vector appears to overcome these economic and transport hurdles, enabling localized production of AMPs at the site of infection. EcN has demonstrated numerous health benefits in poultry [71,72] and is equipped with several fitness factors that allow it to persist in the intestinal environment, making it a prime candidate for this delivery platform [76].

The brief period of colonization by EcN allows for a tunable treatment regime, enabling continuous administration through feed. The delivery of antimicrobial molecules may then be sustained for hours, or even days, localized at the site of infection.

Several key questions concerning the delivery of peptides by bacteria remain. The most pressing ones are perhaps the ones related to the use of modified organisms. In

particular, the levels of release to the environment and the rate of DNA transfer of engineered components to other microbiota species have not been studied. There are ways to mitigate these risks, including suicide genes that will destroy the cells outside host GI tracts. This study's favorable proof-of-concept results suggest that larger programs that focus on the safety of antibiotic probiotics are warranted.

From a practical viewpoint, a critical question is the influence of numerous alternative dosing regimens on SE carriage, bird health, and host microflora. A single, 1ml inoculum proved sufficient to alter the trajectory of SE carriage and expedite shedding. Continuous administration by incorporation in the water or feed may have the potential of rapidly clearing SE in pre-harvest poultry.

There are multiple engineering choices impacting the performance characteristics of antibiotic probiotics, including the choice of the bacterial strain and its colonization profile, the antimicrobial peptides, the expression strength, and the secretion pathways, to name a few. Optimizing the efficacy of antibiotic probiotics and determining the best dosing regimen may be best addressed through a combination of carefully designed field studies and smaller scale animal experiments.

Finally, we note that the described strategy does not follow the traditional drug discovery and delivery process. Instead of identifying new therapeutic targets in pathogenic bacteria and developing new classes of drug molecules, probiotic bacteria can be recruited in the fight against pathogens. With available libraries of organisms, AMPs, and vectors for peptide production and secretion, this technology may be developed for numerous GI tract pathogens in a variety of hosts. Fine-tuning antibiotic probiotic

systems may offer an alternative to antibiotics used in agriculture for pathogen reduction. This strategy can also potentially offer sorely needed solutions in the growing fight against antibiotic-resistant strains that infect and sicken humans.

3.6. Materials and Methods

3.6.1 Bacterial strains and plasmid construction

The Pon promoter and the ProTeOn activator protein were synthesized by GENEART in a pMS expression vector that contains a ColE1 origin of replication and a Spectinomycin selection marker. Using standard molecular biology techniques, the *mcjABCD* operon was PCR amplified from the PJP3 vector (donated by J. Link, Chemical and Biological Engineering, Princeton University) and cloned into the pMS plasmid between the EcorI and SacI restriction sites. The final construct, pBF25, is illustrated in Supplemental Figure 1. pBF25 was transformed into EcN by electroporation for characterization (EcN(J25)).

3.6.2 Zone of Inhibition Activity Assay

EcN(J25) was cultured in Luria-Bertani (LB) media at 37°C with agitation at 225rpm. 1ml of duplicate overnight cultures were transferred to a 2ml microcentrifuge tube and centrifuged for 3min @ 2.5rcf and the pellet was washed with 0.5ml of 1x PBS. At t=0hrs, the washed EcN(J25) was inoculated in 2ml of fresh LB to an OD of 0.05 in 5 sterile culture tubes, allowing one tube per time point. At each point (0, 2, 5, 10, and 20hrs) post-inoculation, 1.5mls of culture supernatant was collected from the respective tube and centrifuged for 1min at 15.8rcf. The supernatant was sterile filtered and stored at 4°C. OD600 was measured at each time point.

M9 minimal agar plates (15g/L) were overlaid with 10ml of soft M9 agar (6.5g/L) containing 10^7 CFU of SE. The supernatant was serially diluted in two-fold steps and 10µl of each dilution was spotted on the SE-agar plates. The reciprocal of the last dilution with a visible halo was taken as the activity units of MccJ25.

3.6.3 *In vitro* supernatant activity assay

Cultures of EcN(J25) and unmodified EcN were grown in LB and the supernatant was collected at 16hrs. Exponential phase SE was diluted to 10^3 CFU/ml and transferred to a 96-well plate. Microcin-rich supernatant from EcN(J25) was applied to the SE at varying volume concentrations (0, 0.5, and 1%). The wells were blanked with spent media from the unmodified Nissle supernatant to obtain a final volume of 340 µl/well. The growth assays were obtained by shaking the plate at 37°C and taking OD600 measurements every 15 mins in a BioTek Synergy H1 microplate reader.

3.6.4 Bacterial challenge/treatment of turkey poults

All experiments were performed in accordance with relevant guidelines and regulations. This project was approved by the Institutional Biosafety Committee and by the Institutional Animal Care and Use Committee (IACUC) at the University of Minnesota. Day-of-hatch Hybrid Converter Breed Tom poults, free of vaccinations, were transported from a commercial hatchery. Birds were randomly transferred to isolator units with incandescent lighting, crinoline flooring, and *ad libitum* access to antibiotic and probiotic-free food and water. Three birds were taken to the University of Minnesota Veterinary Diagnostic lab prior to each trial to confirm they were *Salmonella*-free. The remaining birds were left in the units for a 3-day acclimation period following transport.

3.6.5 Bacterial Challenge Strains

The SE and EcN challenge strains were both made resistant to antibiotics prior to inoculation so they could be recovered from the intestinal tract of the birds for enumeration. SE and EcN were both made resistant to 100μg/ml Rifampicin for this antibiotic concentration proved effective in limiting bacterial background from the poults. To differentiate the challenge strains, SE was additionally made resistant to 30μg/ml Nalidixic acid and EcN to 100μg/ml Streptomycin. On days 1 and 2 post-hatch of both trials, fecal samples were collected from each isolator unit and resuspended in PBS to make a final 10x dilution. The fecal samples were plated on the respective antibiotic agar plates to ensure there was no background bacterial growth in any of the units. Bacterial resistance was achieved using a ramping up and repeated exposure protocol[77].

3.6.6 Animal trial 1

On day 0 (4-days post-hatch), 140 birds were randomly selected to make 5 groups of 28 birds, with one group for each treatment ((5 birds per treatment per time point x 5 time points) + 3 extra birds per treatment to account for potential early losses). The birds were randomized at this stage to mitigate any early microbiome diversification that may have occurred during the acclimation period. Each group of 28 birds was placed into one of five isolator units and each unit underwent a different experimental treatment. The 5 treatment groups evaluated in this study were: (1) SE-control, (2) SE + EcN(J25), (3) SE + EcN, (4) EcN(J25)-control, and (5) PBS-control.

On day 0, groups 1, 2, and 3 were orally inoculated with 10^8 CFU SE. Groups 4 and 5 were inoculated with 1ml of 1x PBS. The birds were monitored for any signs of distress

for 2 hours post-challenge. On the following day the birds were inoculated in the same fashion with 1ml of their respective treatments, groups 1 and 5 with PBS, groups 2 and 4 with 10^8 CFU EcN(J25), and group 3 with 10^8 CFU EcN. All bacterial treatments were suspended in 1ml PBS.

On days 2, 4, 7, 10, and 14, five birds from each isolator unit were euthanized, weighed, and necropsied. We note that we added 3 surplus birds per unit to account for natural bird losses that are common in the first few days following hatch. At the final time point any remaining birds also were necropsied and data were collected.

3.6.7 Animal trial 2

Similar to trial 1, on day 0, birds were randomized from the isolator units they stayed in during their adjustment period to make 4 new groups of 38 birds. In this study, we used two isolator units per treatment, with 19 birds per unit. The 4 treatment groups in this study were: (1) SE control, (2) SE + EcN(J25), (3) SE + EcN, and (4) SE + .15mg ENR/(kg of bird weight).

On day 0, all 4 groups were orally inoculated with of 10^8 CFU SE. On day 1, groups 1-4 were treated with 1ml PBS, 10^8 CFU EcN(J25), 10^8 CFU EcN, and 1.5mg of ENR, respectively. On days 2, 4, 7, 10, and 14, 3-4 birds per unit (6-8 birds per treatment) were euthanized, weighed, and necropsied from each unit. At the final time point, any remaining birds were also necropsied and data were collected for all birds.

3.6.8 Enumeration of *Salmonella* and Nissle in cecal contents

On post-inoculation days 2, 4, 7, 10, and 14, birds were randomly selected and euthanized from each isolator unit. Body weight was recorded and both ceca pouches were extracted. Ceca samples were weighed and transferred to sterile 7ml Precellys tubes (Bertin Corp) containing ten 2.8mm zirconium oxide (Bertin Corp) beads. Each sample tube was processed by adding 2ml PBS and using a Minilys® homogenizer for 15s at low speed.

The homogenate for each sample was serially diluted in 10x increments and plated on selective media for SE and EcN enumeration. The plates were incubated overnight at 37°C and then the colonies were counted.

3.6.9 Statistical analysis of cecal counts

CFU/g cecal tissue was determined for both SE and EcN from each bird at each time point. The data were log10 transformed and all data points with an enumerated CFU below the limit of detection were given a value of 0.5 CFU/g ceca. Extended discussion of the normality testing is discussed in Appendix B.

Trials 1 and 2 were analyzed separately via ANOVA. In both trials, the 'Treatment' and 'Day' were described as categorical variables, as well as, their interactions to account for different time-dependent responses.

Table 3-1. *ANOVA results for Trial 1 and Trial 2*

Trial	Treatment F-value	p-value
1	3.96	0.02
2	8.19	<0.01

Given these results, the null hypothesis that all treatments had the same effect was rejected. Therefore, pairwise post-hoc analysis was done between all treatments across all times using the Tukey-Kramer method (with) the computed confidence intervals (CI) of the differences of the transformed data.

Table 3-2. . *Pairwise analysis for Trial 1 treatments*

Trial 1					
Treatment		Transformed 95% CI			
i	j	Lower	Center	Upper	p-value
PBS	EcN(J25)	0.07	0.69	1.30	0.03
PBS	EcN	−0.47	0.15	0.78	0.83
EcN(J25)	EcN	−1.15	−0.53	0.09	0.11

Table 3-3. *Pairwise analysis for Trial 2 treatments*

Trial 2					
Treatment		Transformed 95% CI			
i	j	Lower	Center	Upper	p-value
PBS	EcN(J25)	−0.12	0.29	0.69	0.27
PBS	EcN	−0.24	0.17	0.57	0.71
PBS	ENR	−0.88	−0.46	−0.05	0.02
EcN(J25)	EcN	−0.52	−0.12	0.29	0.87
EcN(J25)	ENR	−1.17	−0.75	−0.33	<0.01
EcN	ENR	−1.05	−0.63	−0.22	<0.01

3.6.9 Microbiome Extraction and Analysis

DNA was extracted from ceca samples using the MoBio Powersoil kit (Mo Bio Labs). Sequencing of the samples was performed at the University of Minnesota Genomics Center using Illumina MiSeq paired-end 2x300 bp technology of the V4 region of the 16S rRNA. The pair reads were assembled using PandaSeq [782]. The quality threshold for PandaSeq was set at 0.9. After the assembly, sequences were trimmed and converted from fastq to fasta format. ChimeraSlayer's USEARCH 6.1 method [79,80] was used to remove potential chimeras. For the operational taxonomic unit (OTU) picking, QIIME's [80,81] open reference method was employed. For the closed-reference OTU picking, the Greengenes library [82] was employed through QIIME. For the unclassified sequences, de novo Uclust OTU picking [79] was used. QIIME was also used for the alpha diversity analysis using UniFrac [37].

3.6.10 Vertebrate Animal Experiments

The University of Minnesota Institutional Animal Care and Use Committee has reviewed and approved protocol 1409-31793A involving all live vertebrate animals described herein, ensuring compliance with federal regulations, inspecting animal facilities and laboratories and overseeing training and educational programs.

Chapter 4 Engineered Probiotics to Target Multidrug-Resistant *E. coli*

4.1 A Rising Superbug: *E. coli* Sequence Type ST131

E. coli inhabit the intestines of human and animals making up a large portion of the facultative anaerobic intestinal population[84]. Although most *E. coli* are commensal inhabitants of the microbiota, there are several pathogenic strains of *E. coli* that can cause a variety of infections within their hosts. Based on the location of infection and type of resulting disease, the pathogenic variants are largely classified as either intestinal (InPEC) or extraintestinal pathogenic *E. coli* (ExPEC). InPEC strains tend to cause diarrheal diseases, while ExPEC strains cause infections at a variety of locations outside of the intestinal tract. ExPEC *E. coli* are the major cause of bacteremia and meningitis in neonates, and are responsible for 80% of urinary tract infections (UTIs)[85]. It is estimated that ExPEC *E. coli* cause 50% of hospital-acquired and 70-95% of community-acquired UTIs[86].

The treatment of pathogenic *E. coli* infections is complicated by their increasing spectrum of antibiotic resistance. Resistance to fluoroquinolones and trimethoprim-sulfamethoxazole limit outpatient treatments while extended-spectrum cephalosporin resistance complicates treatment options in the hospital. Extended-spectrum cephalosporin resistance typically arises from bacteria harboring extended-spectrum β-lactamases (ESBLs). ESBLs are enzymes that enable bacteria to hydrolyze β-lactam antibiotics, including penicillins, cephalosporins, and the monobactam aztreonam. This leaves only last resort antimicrobial therapies such as carbapenems[87].

Most ESBL-associated *E. coli* infections are due to a recently emerged and globally disseminated ExPEC clone, ST131[88]. This previously unidentified clone was first reported in 2008 as having been found among ESBL-producing *E. coli* isolates from nine countries across 3 continents. Since then, ST131 has risen to dominance across the globe, with studies suggesting that the pandemic emergence of ST131 took place over less than 10 years[89]. Surveys indicate that ST131 accounts for 10-27% of the total clinical *E. coli* population in several locations and between 52 and 67% of all ESBL-producing or fluoroquinolone resistant *E. coli*[88].

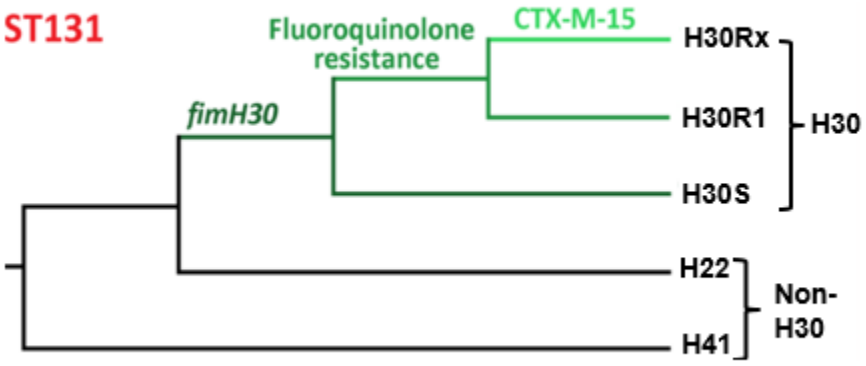

Figure 4-1. *ST131 genetic groups and acquisition of drug-resistance changes*

Recent studies using whole genome sequencing have investigated the population structure of ST131. As shown in Figure 4-1, ST131 has several important sublingeages; notably the H30 subclones which contain the H30S, H30R, and H30Rx groups. The *H*30 subclones are defined by the presence of a specific fimbrial adhesion allele, *fimH30.* Studies suggest that the expansion of ST131 in the U.S. has been driven primarily by the *H*30 group.

Within *H*30, *H*30R branched off from *H*30S due to the acquisition of fluoroquinolone resistance, arising from mutations in the *gyrA* and *parC* genes. *H*30R strains constitute an estimated 58% of the total ST131 isolates[86,90]. The *H*30R strains contain further fine structure where the *H*30Rx subclones contain the same FQ resistance-conferring mutations as does H30R1, but are also associated with ESBL production, typically of CTX-M-15[90]. The expansions of *H*30R and *H*30Rx reportedly began around 25 years ago, when fluoroquinolones and extended-spectrum cephalosporins were first introduced for widespread clinical use[90].

ST131 infections manifest primarily as UTIs, most of which originate from intestinal colonizers[86]. In this work, we teamed up with Dr. James Johnson of the Veterans Affairs Medical Center to determine if engineered probiotics could be used to reduce the intestinal colonization of ST131 in carriers. Dr. Johnson has extensive experience in studying the epidemiology and resistance patterns of ST131. In this aim, we focused on an ST131 *H*30Rx isolate, JJ1886, which was recovered from a patient with fatal urosepsis. Dr. Johnson was part of a team that reported the whole genome sequence of this isolate[91].

In this work, we screened AMPs for activity against JJ1886, engineered EcN to elicit antibiotic activity against the isolate, and began to study the resistance mechanisms of JJ1886 to the AMP, Microcin C7 (Mcc7).

4.2 Microcin C7: A Trojan Horse Antimicrobial Peptide

Microcin C7 (Mcc7), the smallest microcin known, is a 21bp gene produced by *E. coli* isolates that harbor a plasmid-borne synthesis and immunity cassette containing the *mccABCDEF* gene cluster[92]. Mcc7 undergoes extensive post-translational modifications

during its biosynthesis, leading to a potent peptide antibiotic that inhibits aspartyl-tRNA synthetases (AspRS)[93].

Amino-acyl tRNA synthetases (aaRSs) catalyze the attachment of amino acids to cognate tRNAs, which are then transferred to growing peptide chains. aaRSs are promising targets for antimicrobial agents because they are critical for translating the genetic code[94]. Mcc7 structurally mimics an aspartyl adenylate, the native binder of AspRS, but exists in a nonhydrolysable form. Mcc7 thus binds to AspRS and essentially clogs the machinery, preventing further protein synthesis[94].

Mature Mcc7, which in this context refers to the form that is exported from the host cell but not yet internalized by the target, consists of a MRTGDAD heptapeptide with a covalently attached C-terminal adenosine monophosphate, a propylamine group attached to the phosphate, and an N-terminal formylated methionine (Figure 4-2).

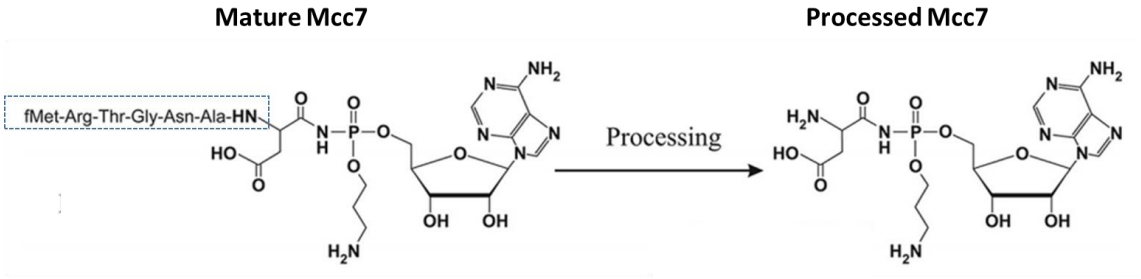

Figure 4-2. *Mature (unprocessed) Mcc7 and Processed (Toxic) Mcc7.* Adapted from Novikova et al. *The Journal of Biological Chemistry*. 2010; 285(17).

Mcc7 is imported into sensitive cells via the inner membrane transporter, YejABEF (YejF), which recognizes the leading hexapeptide portion of Mcc7. The biological function of YejF is not yet understood, but it presumably plays a role in the transport of oligopeptides, particularly those containing an N-terminal formyl-

methionine[92]. Upon cell entry, the N-terminal formyl methionine is removed by peptide deformylase and then the peptide portion is cleaved sequentially by intracellular peptidases. This cleavage process releases the toxic aspartyl adenylate analogue into the target cell (Figure 4-2). Mcc7 is therefore actively transported into sensitive cells, where the portion for facilitated transport is subsequently removed to release the entry-incapable peptide antibiotic, making Mcc7 a bona fide 'Trojan Horse' inhibitor. Other naturally occurring aminoacyl adenylate-based antibiotics use similar strategies, including the leucyl-tRNA synthetase inhibitor, agrocin 84, and the seryl-tRNA synthetase inhibitor, albomycin[92].

Despite the small size of Mcc7, five enzymes spanning a ~6kb region are required for the processing, transport, and host immunity of the peptide. The keys steps in this sequence, from the host cell's processing of Mcc7 to target-cell inhibition, are depicted in Figure 4-3[95].

The biosynthetic gene cluster governing Mcc7 production contains two opposing operons. The first dictates the expression of *mccABCDE* while *mccF* is transcribed independently in the reverse direction. The promoter upstream of *mccA*, Pmcc, is a CAP (catabolite activator protein)-dependent promoter, which is activated in the decelerating phase of growth or in nutrient-limiting environments.

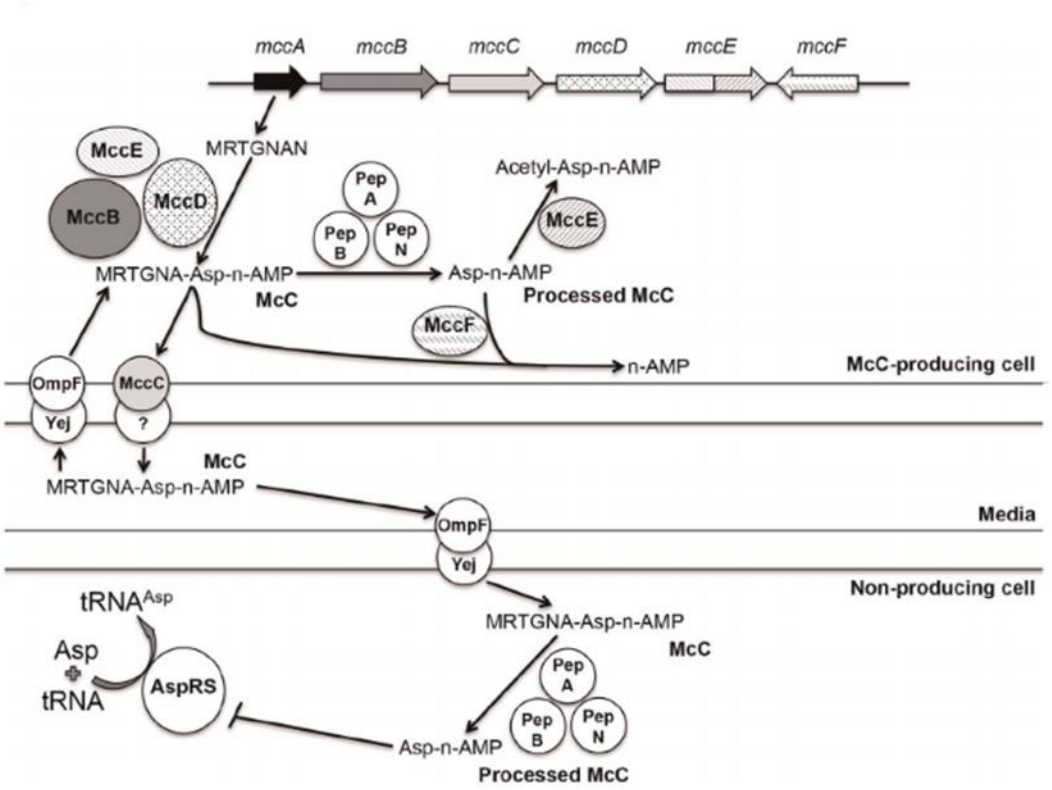

Figure 4-3. *The mechanism of action of Mcc7.* Reproduced with permission from Piskunova et al. *Molecular Microbiology*, 104.

The biosynthesis of Mcc7 begins with the product of *mccA,* a heptapeptide consisting of MRTGNAN and is the initial precursor of Mcc7. This peptide is converted into a biologically active intermediary form by an adenylation reaction catalyzed by the MccB enzyme. MccD and MccE then jointly contribute to modifying the MccB-catalyzed product with propylamine, increasing the biological activity of the peptide by ~10 fold. This mature Mcc7, and some intermediary forms, are exported by a major facilitator superfamily efflux pump encoded by *mccC*[93].

Unprocessed Mcc7 can be processed into the toxic form by the intrinsic peptidases of the producing bacterial cell. Such host cell toxicity is avoided because the Mcc7 gene cluster includes built-in methods to detoxify the peptide. Three gene products

contribute: MccE, MccF, and MccC. MccE is an acetyltransferase that acetylates processed Mcc7, thereby detoxifing it[96]. MccF is a serine peptidase that cleaves the isopeptide bond in Mcc7 that connects the AMP moiety. MccC is capable of exporting both intracellularly produced and externally acquired Mcc7[92].

4.3 Development of a Mcc7-Producing Probiotic

4.3.1 Analysis of the Mcc7 Promoter

Mcc7 was donated to the Kaznessis lab by Dr. Konstantin Severinov of the Rutger's Wacksman Institute. In this study, we used the donated pp70 plasmid, which is about 9kb and contains the native Mcc7 gene cluster in a pBR322-based vector with an Ampicillin resistance marker (Figure 4-4).

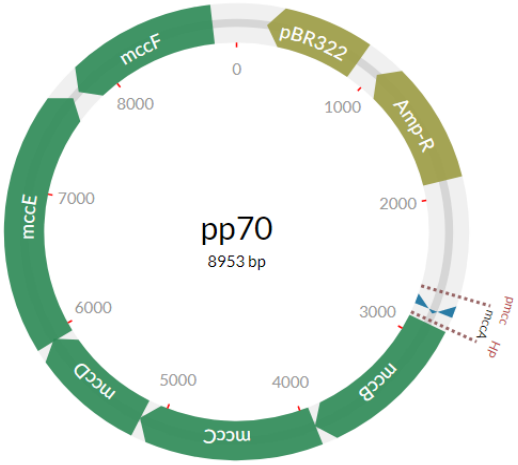

Figure 4-4. *Plasmid map of pp70*

In my initial efforts to improve Mcc7 titers from *E. coli* containing pp70, I focused on swapping out the native Mcc7 promoter, Pmcc, with staple promoters developed in the Kaznessis lab such as ProTeOn+ and TTL[97]. In previous work, these promoters had led to successful increases in secreted peptide titers from AMP-producing

E. coli. However, here all these constructs failed to compete with the native genetic operon of Mcc7 leading to overall reductions in antimicrobial activity. This led me to characterize the Pmcc promoter to better understand its strength and expression profiles, thereby clarifying system behavior.

The Pmcc promoter is CAP-activated and exhibits growth-phase-dependent regulation[92]. In a previous study, Pmcc was shown to activate expression during the decelerating phase of cell growth, upon transition into stationary phase. Regulation of the promoter depends on a complex interplay of at least four global regulators of transcription including the σ^s-subunit of RNA polymerase and the CRP, H-NS, and LRP proteins. It is hypothesized that the H-NS and LRP regulators are involved in the repression of Pmcc expression in exponential phase[65].

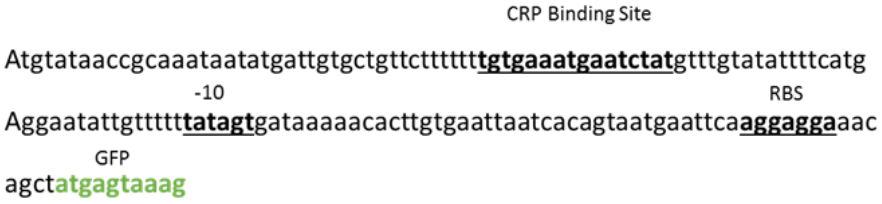

Figure 4-5. *Sequence of the Pmcc promoter*. The Pmcc promoter was isolated from pp70 and placed upstream of GFP. Key features of this sequence, including the CRP binding site, -10 element, RBS, and start of GFP, are denoted.

Here, the Pmcc promoter was isolated from the pp70 plasmid and placed upstream of GFPmut3 (GFP). Promoter strength was compared to the native MccV (Pcvi), MccJ25 (Pmcja), and ProTeOn+ promoters in parallel with Pmcc. The Pmcc promoter sequence is show in Figure 4-5. The sequences of the other AMP promoter regions tested are available in Appendix C. As shown in Figure 4-6, although Pmcc was activated more strongly at later stages of growth, it consistently exhibited higher

expression levels than any of the tested promoters, including ProTeOn+. This explains the decrease in activity we had observed with our systems when different promoters were used in place of Pmcc. Therefore, in subsequent work we used Pmcc for gene expression.

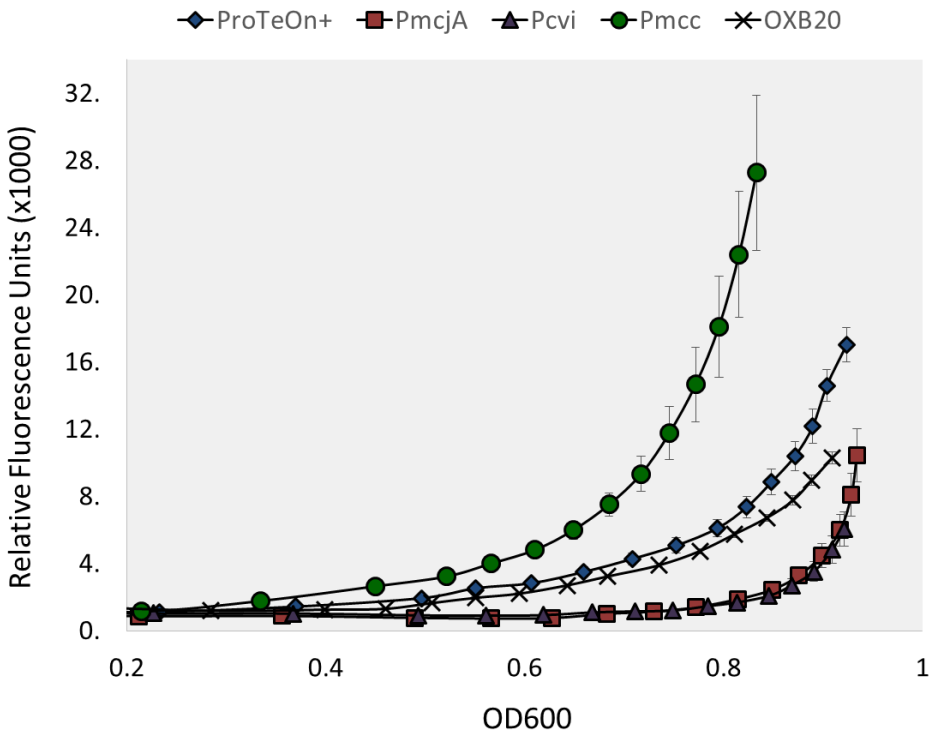

Figure 4-6. *Expression profiles of native AMP promoters, OXB20, and ProTeOn+.* ProTeOn+, OXB20, and the native MccV (Pcvi), MccJ25 (PmcjA), and Mcc7 (Pmcc) promoters were placed upstream of GFP. MC1061 was used as the host strain for all constructs tested. In a kinetic spectrophometric assay, OD600 and fluorescence readings were measured at 30-min intervals. Fluorescence was plotted as a function of OD600. Error bars represent standard error of four replicates.

All the AMP promoters showed steep activation during the later stages of growth. OXB20 was included as a control for the accumulation rate that a constitutive promoter exhibits upon entering stationary phase. Between 11 and 19 hours, the ProTeOn+,

OXB20, Pcvi, Pmcja, and Pmcc promoters increase their fluorescence by 7.5, 6.5, 12.5, 22, and 11.5-fold, respectively.

4.3.2 *In Vitro* activity of Mcc7 producing *E. coli*

We screened the activity of several microcins, including Microcin V, Microcin L, Microcin N, and Microcin J25, against a panel of ST131 isolates provided by Dr. Johnson. Binary results of these screens are shown in Table 4-1. This screen leaves open the potential for future engineering efforts against these isolates. Results of a zone-of-inhibition assay showing the inhibitory activity of Microcin J25 and Microcin V against ST131 strains JJ1901 and MVAST020 are available in Appendix C. However, Mcc7 had significantly more potent activity against the target of interest, JJ1886, than did the other microcins.

Table 4-1. *Binary Screening Results of Microcins J25, V, L, and N for activity against ST131 isolates*

Isolate	ST131 subgroup	Microcin J25	Microcin V	Microcin N	Microcin L
JJ2547	H30Rx	+	+	+	-
JJ1886	H30Rx	+	+	+	+
JJ2050	H30Rx	+	+	+	-
JJ2528	H30R1	+	+	+	-
MVAST0036	H30R1	-	+	-	-
MVAST014	H30R1	+	+	+	-
H17	"H22" (H27)	+	+	+	-
JJ1901	H22	+	+	+	+
JJ2087	H22 (FQR)	+	+	+	-
JJ1999	H22	+	+	+	-
MVAST020	H41	+	+	-	+
MVAST167	H41	+	+	+	-

With Pmcc being the strongest constitutive promoter tested, for subsequent assays we used the unmodified pp70 plasmid containing the native Mcc7 operon. For characterization, we transformed pp70 into EcN and used liquid supernatant assays to measure the inhibitory effect on the growth kinetics of JJ1886. The Mcc7-producing

Nissle derivative (EcN(C7)) was grown in LB media for 13 hours, at which time the Mcc7-rich supernatant was collected and applied to seed cultures of JJ1886 in different volume fractions in a 96-well plate. We screened serial two-fold dilutions, from 40% to 0.625%, of the studied Mcc7-containing supernatants (e.g., Figure 4-7). Treatment with 40% Mcc7 supernatant suppressed growth of JJ1886 for ~9 hours, while treatment with 0.625% suppressed growth for 7 hours. In this assay, we did not dilute sufficiently to capture the MIC. However, based on the range of volume fractions tested, this peptide/pathogen combination appears to be the most potent system developed in the Kaznessis lab thus far, outcompeting MccJ25 vs SE.

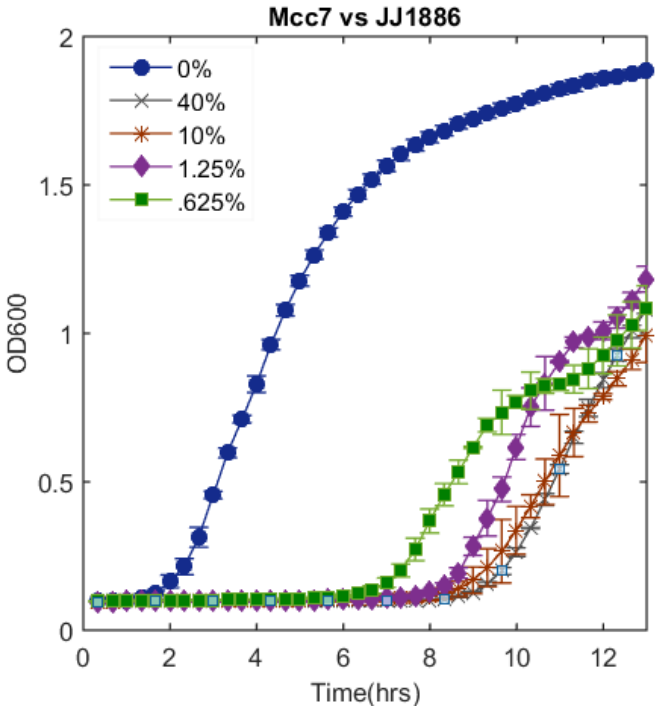

Figure 4-7. *In vitro activity of Mcc7 against JJ1886.* Supernatant was collected from EcN(C7) at 13hrs and applied in different volume fractions ranging from 0.625% to 40% to JJ1886 (OD~0.01). A kinetic spectrophometeric assay was run for 12hrs and OD600 readings were measured periodically. The error bars represent standard error of 3 replicates.

The susceptibility of JJ1886 to Mcc7-containing supernatant was tested in different media conditions to determine if any shifts occurred when nutrient composition was altered. It is hypothesized that many transporters, possibly YejF, are upregulated when nutrients are scarce, increasing the amount of entry points for AMPs. JJ1886 growth was tested in the presence of Mcc7-containing supernatant during growth in rich (LB) and limiting (M9) media

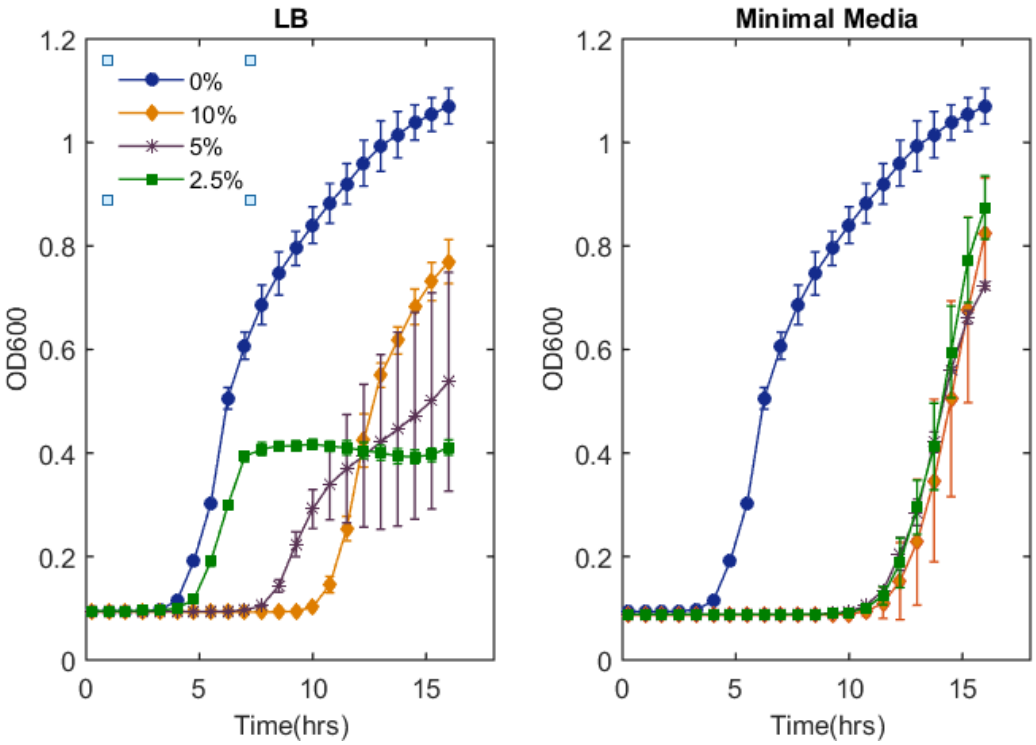

Figure 4-8. *JJ1886 susceptibility to Mcc7 during growth in different nutrient conditions*. Mcc7 supernatant was collected from MC1061 cells containing pp70 at 16hrs. The supernatant was applied to JJ1886 (OD~0.001) at different volume fractions ranging from 10-2.5%. JJ1886 growth was monitored via OD600 upon treatment in LB and M9 media. The error bars are the standard error of 3 replicates.

As shown in Figure 4-8, the susceptibility of JJ1886 shifts to higher inhibitory levels upon treatment in M9 media exhibiting a lower MIC. In M9 media, with all Mcc7 treatments tested, the growth curves of JJ1886 were superimposed with growth only

beginning at 12hrs. In contrast, the LB group displayed growth curves that begin less than 10hrs after treatment with 2.5 and 5% supernatant. These shifts indicate that JJ1886 is likely more susceptible to Mcc7 when nutrients are scarce.

4.4 Mechanism of Resistance in JJ1886

Resistance is an inevitable side effect of antimicrobial therapies. Despite the potency of Mcc7 against JJ1886, there remains a resistant subset within the population that is unaffected by the toxic peptide. We chose to explore this resistant subset to gain better insight into the mechanisms of resistance. Understanding the peptide evasion process could aid in the development of combination therapies to create more effective treatments.

Mcc7 resistance could arise due to several distinct types of mutations. For example, mutations could affect the intracellular target (AspRS), the peptidases of the sensitive cells that process Mcc7 into its toxic form, or the import or export mechanisms of Mcc7 from the target cell. Mutations in AspRS are likely difficult for cells to acquire and maintain because AspRS is an essential enzyme; mutations that confer Mcc7 immunity could alter binding with the native substrate and thus affect cell viability. Mutations in the peptidases would also be challenging for cells to achieve because there are many redundant and non-specific peptidases in the *E. coli* genome[98]. This led us to focus on the import/export mechanisms of Mcc7 for their role in Mcc7 resistance.

In a previous study, the YejF transporter was determined to be essential for Mcc7 sensitivity and deletion of any of the four genes of the operon is sufficient for resistance[98]. We hypothesized that down-regulation of this transporter would be the resistance mechanism of the resistant subpopulation of JJ1886. If this transporter were

down-regulated on some targets, the peptide could have less opportunities to enter the cells and exert its antibiotic effect, yielding a resistant phenotype.

The YejF transporter is produced by four genes that are transcribed as a single operon, *yejABEF*. *yejA* encodes a putative periplasmic binding protein, *yejB* and *yejE* encode for putative permease components, and *yejF* encodes for the ATPase component[99].

We determined the frequency of resistance of JJ1886 to Mcc7 to be 1×10^{-6} CFU. We then isolated spontaneous mutants of JJ1886 that had stable a resistance pattern. We classified mutants as 'stably resistant' if they grew in rich media without selection pressure and exhibited a similar survival rate on LB agar plates in the presence and absence of Mcc7.

We then used Real-Time Quantitative Reverse Transcription PCR (qRT-PCR) to assess *yejF* expression by wild-type JJ1886 and its Mcc7-resistant mutants during exponential-phase growth in LB media. Preliminary results are shown in Figure 4-9. Reevaluation of these preliminary results, with the JJ1886 *gapA* and *hca*t housekeeping genes used as controls, is ongoing.

In these preliminary results, six out of seven resistant mutants had significant downregulation of *yejF* compared to the susceptible group. The transcript levels of *yejF* show between a 3 and 6x reduction compared to the susceptible group. These results are consistent with our hypothesis that JJ1886 resistance involved down-regulation of the YejF transporter.

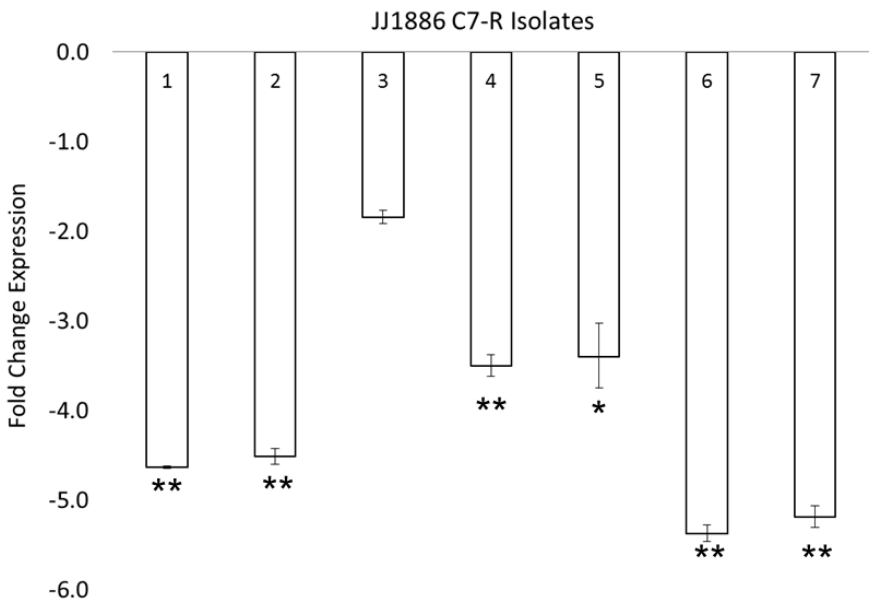

Figure 4-9. *yejF down-regulation in Mcc7-resistant JJ1886 mutants*. *yejF* transcript levels were measured using qRT-PCR. Six out of seven Mcc7-resistant mutants exhibit significantly lower *yejF* transcript expression compared to the susceptible population. Each isolated was tested in biological replicates with technical duplicates. The fold change and error was calculated using the ΔCt method. *p<.05, **p<.01.

The YejF transporter has been found to contribute to the virulence of *Salmonella Typhimurium* and *Brucella melitensis*. *Salmonella* and *Brucella* stains with mutations or deletions in the YejF transporter showed increased susceptibility to AMPs and peptide antibiotics including, protamine, melittin, polymyxin B, human beta defensins (HBD)-1 and (HBD)-2, and restricted invasion of and replication in macrophages. In mouse models, as compared to the parental strains *Brucella yejF* mutants showed more rapid clearance rate from the spleen of infected mice and S*almonella yejF* mutants demonstrated decreased virulence when administered intragastrically [99,100]. If the Mcc7-resistant population of JJ1886 does down-regulate YejF, this subset might be inherently less virulent and may not be capable of causing reinfection if left behind following

EcN(C7) treatment. It is also possible to follow EcN(C7) treatment with peptide antibiotics such as polymyxin B to eradicate this resistant population *in vivo.*

4.5 Future Directions

4.5.1 Test EcN(C7) in mouse decolonization models

Dr. Johnson has established colonization models of ST131 *E. coli* in the GI tract of mice. In these models, colonization is established and maintained using Streptomycin selection and Streptomycin-resistant test strains. Using these models, we will test our engineered Nissle, EcN(C7), as a decolonization measure. For this, we will challenge mice with JJ1886 via oral gavage and treat them with EcN, EcN(C7), and PBS in the drinking water. EcN(C7) has been made resistant to Rifampicin (100ng/µl) and Streptomycin (100ng/µl), and JJ1886 is intrinsically resistant to Ciprofloxacin (10ng/µl) and has been made resistant to Streptomycin (100ng/µl), which enables us to get colony counts of bacteria in the GI tract via selective plating.

4.5.2 Peptide Engineering of Mcc7

A possible future direction in this project would be to apply rationale peptide engineering techniques to broaden the spectrum of activity of Mcc7. Mature Mcc7 is capable of functioning through a 'Trojan Horse' mechanism due to its modular structure, whereby the non-hydrolyzable apartyl adenylate is attached to a hexapeptide carrier that facilitates transport into sensitive cells upon recognition by YejF.

It could be possible to capitalize on these modular components to either (1) attach other toxic molecules to the hexapeptide carrier or (2) change the hexapeptide carrier to allow the transport of Mcc7 into cells through alternate entry point. Previous studies have demonstrated that substitutions in the seventh amino acid of MccA prevent Mcc7

production, likely due to preventing interactions with the enzymes involved in post-translational modifications[101]. However, chemically synthesized Mcc7-like compounds can exhibit antibiotic activity after cellular uptake via the Mcc7 import mechanism. Vijver et al. linked aminoacyl-sulfamoyl adenosines, which are nanomolar inhibitors of their cognate aspartyl-tRNA synthetases (aaRS), to the hexapeptide carrier. Synthetic compounds such as these could specifically target the aaRSs for which they were designed[94].

This study by Vijver et al. shows promise in exploiting the modular nature of Mcc7 to enable the carriage of other toxic molecules. However, although such an approach may be possible, we suspect that the extensive post-translational modifications that occur during Mcc7 processing will make it challenging to identify C' terminal analogues that are compatible with the processing enzymes required for production from engineered probiotics. Accordingly, this approach may be best suited for chemical synthesis applications. Mcc7 exhibits broad activity on AspRSs from a wide variety of organisms; resistance is attributed largely to restricted cellular uptake. We propose focusing on modifying the hexapeptide carrier to target alternative importers. Such synthetic Mcc7 compounds could be tuned to target specific pathogens that lack YejF, or administered as part of a cocktail for broader activity. The ability to expand the activity spectrum of the Mcc7 platform through either of these mechanisms would greatly increases its value and potential as a novel antibiotic, with or without the use of engineered probiotics.

4.6 Materials and Methods

4.6.1 Promoter assays with GFP

The Pcvi, Pmcja, and Pmcc promoters were synthesized by IDT and inserted into pBFmut3 using HIFI assembly (NEB). The promoter sequences including the HIFI assembly homology sites are available in Appendix C. The plasmids developed – pBFG10, pBFG11, and pBFG12 – were transformed into MC1061 via electroporation for characterization, leading to strains BFG10, BFG11, and BFG12, respectively.

Strains BFG10, BFG11, BFG12, MC1061(psF_OXB20Mut3) (positive control)), MC1061 (negative control), and MC1061(pBFmut3) were cultured for 12hrs in 2ml LB, supplemented with antibiotics when necessary (100ng/ul Spectinomycin or 50ng/ul Kanamycin). Overnight cultures were diluted in LB to OD~0.5. 5µl was then transferred to 5ml selective LB. 300µl of each dilute culture was transferred to a black-walled 96-well plate in four replicates. Using a BioTek Synergy H1 microplate reader, the plate was maintained at 37C in double-orbital mode. Fluorescence intensity and OD600 were measured at 30 min intervals for 20hrs. Background fluorescence was corrected for by subtracting out the average background fluorescence of MC1061F at the respective OD600 values of the sample reading.

4.6.2 Kinetic supernatant inhibition assays

MC1061 or EcN containing pp70 were grown for 12-16hrs in antibiotic-free LB media. 1.5ml of the overnight cultures were centrifuged for 3min at 2.5rcf and the supernatant was sterilized using a .22µm filter. The supernatant was two-fold serially diluted in spent MC1061 media. 180µl JJ1886, diluted to OD~0.001 in LB or M9 minimal media, was transferred to a 96-well plate and treated with 120µl of each serially diluted supernatant

treatment. In the BioTek Synergy H1 microplate reader, OD600 was measured at 20-30 min intervals, while the plate was maintained at 37C in double-orbital mode. Each treatment was tested in 3 or 4 replicates.

4.6.3 Isolation of JJ1886 mutants stably resistant to Mcc7.

LB agar plates were supplemented with 20% Mcc7 supernatant collected from MC1061(pp70). 30µl of an overnight JJ1886 culture in LB media underwent 10x serial dilution in phosphate-buffered saline (PBS). 10µl of the serial dilutions were plated on LB plates with and without 20% Mcc7. Plates were incubated overnight at 37C and the colonies on LB +/- Mcc7 were counted. The frequency of resistance (FOR) was calculated as shown below:

$$Frequency\ of\ resistance\ (FOR) = \frac{\frac{CFU}{ml}\ viable\ on\ 20\%\ Mcc7\ plates}{\frac{CFU}{ml} viable\ on\ LB\ plate}$$

Colonies that grew on Mcc7+ plates were cultured in LB media with no selective pressure and the above protocol was repeated twice. Mutants were determined to be stably resistant if colony counts on plates with and without Mcc7 were constant.

4.6.4 qRT-PCR analysis of *yejABEF*

Triplicate colonies of both JJ1886-S (i.e., Mcc7-susceptible) and each JJ1886-R (i.e., Mcc7-resistant) mutant were inoculated from LB agar plates into LB media without selection pressure and incubated overnight at 37C with 225rpm. The overnight cultures of each replicate were diluted to OD~0.1 in LB and incubated for an additional 3hrs. In the preliminary study in this thesis, the samples were submitted to the University of

Minnesota Genomics Center for RNA extraction, cDNA preparation, and qRT-PCR of *yejF*. Each sample was tested with two technical replicates.

Chapter 5 Microcin V: Foundation for modular AMP-expression systems

5.1 Introduction

In our previous work, we demonstrated the potential and versatility of EcN as an AMP-delivery system. However, when using an engineered probiotic that produces only a single AMP, several challenges may arise throughout the course of treatment.

For one, microcins tend to have very specific activity that is confined to a narrow subset of bacterial species[13]. This presents the issue that the pathogen underlying disease may need to be identified prior to administration of the engineered probiotic for the treatment to be effective. Identification of the causative agent typically requires a few days to a week which would delay treatment onset[102]. This is in contrast to many small molecule antibiotics which are broad-spectrum and can be administered with successful outcomes without knowing the precise species underlying the illness.

There is also the issue we discussed previously, that within a bacterial population there typically exists a resistant subset that is immune to the activity of the peptide and can survive the AMP treatment. These resistant strains can persist in the gut environment, passing on their resistance genes to neighboring organisms. This makes future treatments more difficult and can give rise to new strains of resistant bacteria.

To overcome these challenges, we have explored the possibility of developing engineered probiotics that can simultaneously produce multiple AMPs. The ability to deliver multiple peptides in parallel can enable the development of broader-spectrum probiotics that can elicit activity against a wider range of bacteria or they could be

engineered to express peptides that have orthogonal mechanisms of action against a single target to decrease the size of the resistant population.

One of the major hurdles associated with peptide expression from probiotic organisms stems from secretion barriers. In many cases, AMPs are exported by dedicated secretion pathways or rely on extensive post-translational modifications prior to release. In this work, we focused on releasing multiple peptides from the well-studied Microcin V (MccV) secretion pathway.

5.1.1 Heterologous Secretion of Antimicrobial Peptides

Previous work has explored the possibility of releasing AMPs from alternate secretion pathways and in heterologous hosts with promising results. In one notable study, Borrero et al. were seeking methods to produce Enterococcal AMPs, or enterocins, from *Lactococcus lactis* (*L.lactis*) due to concerns over *Enteroccocus* associated infections. To do this, they replaced the native signal peptides of two enterocins, Enterocin P (EntP) and Hiracin JM79 (HirJM79), to the signal peptide of Usp45. Usp45 is a Lactococcal protein released by the Sec-dependent pathway, a conserved export system that transports unfolded proteins across the cell membrane through a pore formed by the SecYEG complex. Usp45 is the major Sec-dependent protein secreted by *L.lactis*. Fusions of Usp45 to EntA and HirJM79 successfully enabled the production, secretion, and expression of these peptides in the extracellular space of the engineered *L. lactis*[103].

In a similar study, it was shown that divergicin A, a bacteriocin produced by *Carnobacterium divergens* LV13, could be exported through the pathways of leucocin A and lactococcin A by exchanging the leader peptide of divergicin A with those for leucocin A and lactotoccin A, respectively. In this study, it was found that expression of

divergicin A was maximized when the attached leader peptide was expressed in the host it was derived from[104].

Related to the study presented in this work, it was demonstrated that the MccV leader peptide (Vsp) could be used to transport divergicin A out of *E.coli* and *L. gelidium*[104]. In this work we expand upon this foundation in developing a modular expression cassette for the expression of multiple AMPs using MccV's pathway.

5.2 Genetic Organization of Microcin V

The simplicity of Class IIa microcins, such as MccV, makes them an ideal model system for the development of polycistronic constructs. Class IIa microcins reside on gene clusters that only require four genes for peptide synthesis and export and their post-translational modifications are limited to disulfide bonds. MccV, the focus of this study, was the first antibiotic substance reported to be produced by *E.coli* and is one of the best studied microcins to date. MccV acts on sensitive cells by targeting the Cir iron receptor and disrupting membrane potential of the target cell[13].

The genetic organization of the MccV operon is shown in Figure 5-1a. The MccV gene cluster is 4.2kb long and contains two converging operons. MccV is first produced as a precursor peptide encoded by *cvaC*. This 103-amino acid precursor contains an N-terminal leader sequence, which is a common feature among secreted proteins, and is responsible for directing the precursor to its dedicated transport system (Figure 5-1b). c*vi* encodes for a self-immunity protein that protects the host cells from the toxic effect of MccV[13].

The MccV export system is composed of three essential genes, *cvaB, cvaA*, and *tolC*. The ABC transporter, CvaB, and the accessory protein, CvaA, are plasmid-encoded genes expressed from the MccV operon[105]. TolC is a chromosomally expressed outer membrane protein which plays a fundamental role in many *E. coli* export systems. A schematic of the proposed organization of the full transporter is shown in Figure 5-1c.

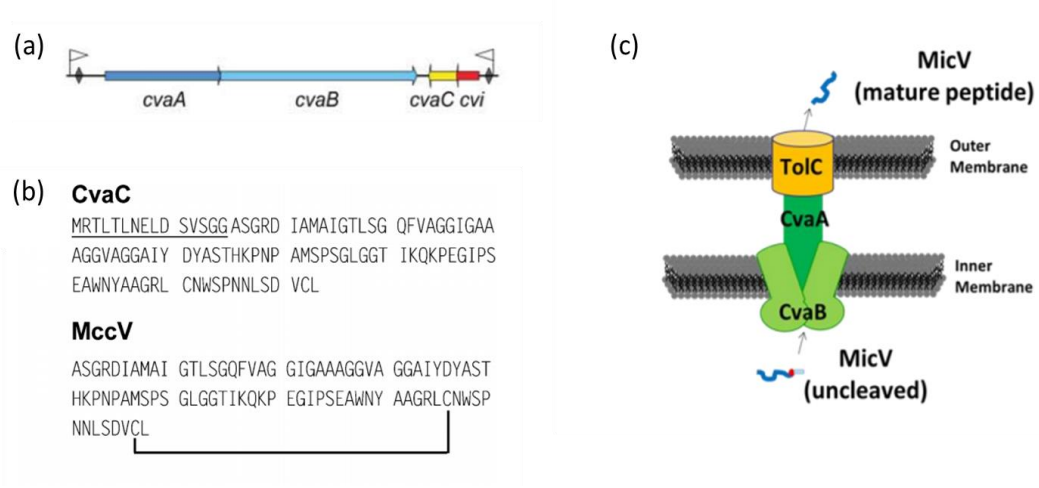

Figure 5-1. *Key elements of MccV development.* (a) The native operon of MccV contains four plasmid borne genes. *cvaC* encodes for the microcin precursor, *cvi* encodes for the immunity gene, *cvaA* and *cvaB* encode for components of the ABC transporter. (b) cvaC contains an N-terminal leader peptide (underlined) which is cleaved during export to release the mature MccV. (c) Proposed schematic of the ABC transporters organization for MccV export. (Adapted from Duquesne et al. *Nat. Prod. Rep.*, 2007, 24 with permission from The Royal Society of Chemistry.)

The leader peptide of CvaC contains a double glycine motif which is a conserved attribute of many secreted bacteriocins. The processing of the precursor peptide occurs concomitantly with export through the ABC transporter[106]. The transporter contains an N-terminal cysteine protease domain which cleaves the leader peptide directly after the glycine motif. This occurs on the cytoplasmic side of the membrane during MccV export.

5.3 Results

5.3.1 Development of pMPES 1.0

The design, construction, and testing of pMPES 1.0 was carried out by myself along with Madeline McCue, Evelyn McChesney, and Kathryn Geldart. A manuscript detailing this work is available in MDPI Pharmaceuticals[26], however in this dissertation I will focus on the portions of the project that were advanced primarily by my contributions with the goal of developing advanced engineered probiotics.

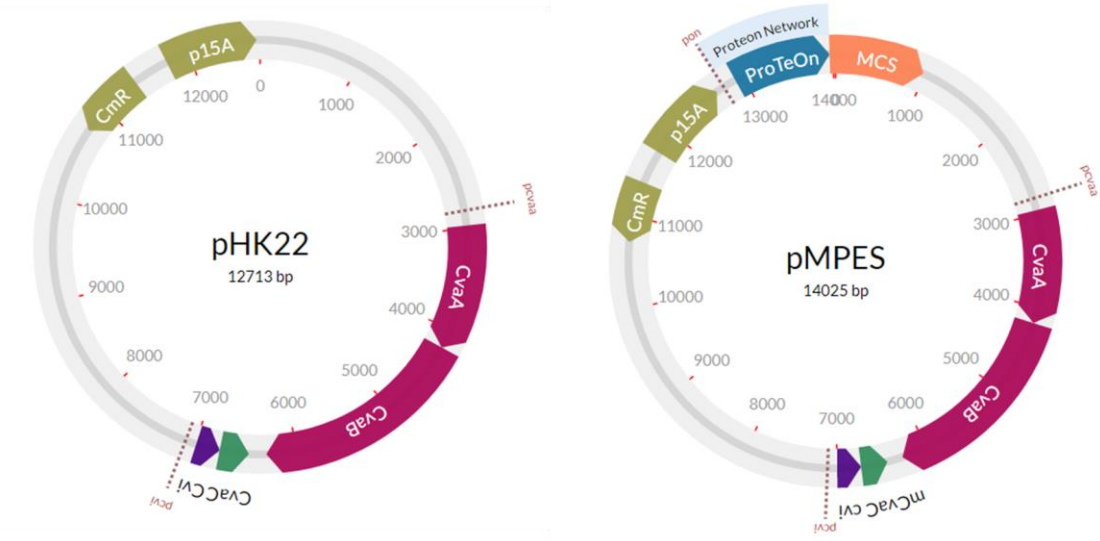

Figure 5-2. *Plasmid maps of pHK22 and pMPES 1.0*

In previous work, Professor Kolter's group at Harvard University developed the plasmid, pHK22[107]. As shown in Figure 5-2, pHK22 harbors a 9.4kb subcloned region which contains all the genes required for MccV production and secretion in a pACYC184 backbone. In our proof of concept studies, pMPES 1.0 was developed by mutating the start codon of the MccV structural gene (denoted as mCvaC) to abolish any activity produced by the peptide at this location (Figure 5-2). At an alternate site we inserted the ProTeOn+ promoter upstream of a multiple cloning site so we could easily add different

peptides with variable signal sequences to determine if they could be successfully exported by the MccV secretion pathway.

5.3.2 Bacteriocins tested for secretion

In this study we chose to attempt to export a wide variety of bacteriocins to determine the limits and potential of this system. We initially began with alternative *E .coli* class IIa microcins including Microcin L (MccL) and Microcin N (MccN), due to their similarity to MccV. We then expanded the screen to include class II enterocins, including EntA, HirJM79, Enterocin P (EntP), and Enterocin B (EntB).

AMP	Signal Peptide	Mature Peptide	Transporter (CvaB)	Accessory (CvaA)
MccL	60%/86.7%	44.1%/51.0%	95.4%/97.3%	97.6%/99.3%
McnN	41.2%/47.1%	20.8%/26.4%	71.5%/85.0%	69.4%/84.5%
EntA	22.2%/50%	10.3%/14.0%	24.8%/43.4%	18.5%/37.0%
EntB	22.2%/50%	14.9%/18.8%	NA	NA
HirJM79	10.0%/16.7%	6.0%/6.9%	NA	NA
EntP	6.5%/19.4%	5.5%/11.0%	NA	NA

NA: Comparisons for EntB, HirJM79 and EntP transporters were not applicable.

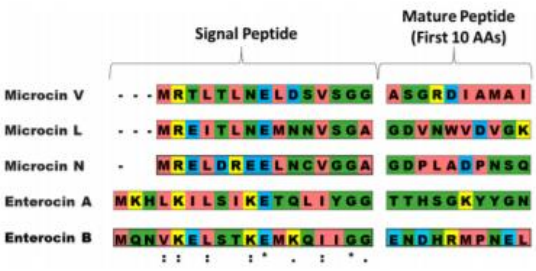

Figure 5-3. *Sequence comparisons of bacteriocins exported from the MccV secretion pathway.* The top table shows the percent identity and similarity of the leader peptide, processed peptide, and primary secretion genes of each bacteriocin studied to the corresponding feature in the MccV operon. The identity and similarity values were calculated using the EMBOSS Needle global sequence alignment program. The bottom figure shows an alignment of the signal peptides and first 10 amino acids for the mature peptide.*=fully conserved residues, :=high conservation (scoring >0.5 in the Gonnet PAM250 matrix);.=low conservation (scoring <0.5). (Reproduced from *Pharmaceuticals.* 2016, 9(4), 60.)

All of the peptides tested contained double glycine motifs in their native leader peptides, except for EntP and HirJM79, which are believed to be secreted by the Sec

protein translocation pathway. Figure 5-3 shows the percent identity and similarity of the leader peptides, processed peptides, and primary secretion genes. The secretion genes of EntB, HirJM79, and EntP were not included because they were either unknown (EntB) or belonged to the Sec pathway. The identity and similarity values were calculated using the EMBOSS Needle global sequence alignment program[26].

Additionally, the leader peptides and the first 10 amino acids of the mature peptides were aligned using the multiple sequence alignment program, Clustal Omega. Amino acid conservation scores are based on the Gonnet PAM250 substitution matrix. Residues scoring >0.5 are considered highly conserved in similarity[26]. =

Table 5-1. *Inhibitory activity of pMPES 1.0 producing bacteriocins.*

Indicator	Construct (pMPES:)	Bacteriocin Units (BU) [1]	Previously Reported MIC
E. coli DH5α	V	120.9 ± 86.2	0.1 nM (*E. coli* MH1) [44]
	L	>170.7	160 nM (*E. coli* ML-35p) [12]
	VL	142.2 ± 49.3	160 nM (*E. coli* ML-35p) [12]
	N	1.3 ± 0	150 nM (*S. Enteriditis*) [31]
	VspN	1.3 ± 0	150 nM (*S. Enteriditis*) [31]
E. faecium 8E9	VspA	7.2 ± 3.4	129 nM (*E. faecium* TUA 1344L) [45]
	LspA	7.2 ± 3.4	129 nM (*E. faecium* TUA 1344L) [45]
	A	1.3 ± 0	129 nM (*E. faecium* TUA 1344L) [45]
	VspH	21.3 ± 0	~0.2 nM (*E. faecium T136*) [27]
	VspP	2.7 ± 0	~0.4 nM (*E. faecium* T136) [32]
	VspB	2.7 ± 0	43.4 nM (*E. faecium* TUA 1344L) [45]

[1] One Bacteriocin Unit (BU) is defined as the reciprocal of the highest dilution of supernatant required to reduce the growth of the indicator strain; error represents the standard deviation of three biological replicates.

The peptide constructs tested and their corresponding results are displayed in Table 5-1. Although not the focus of this dissertation, we demonstrated we could export the majority of combinations tested. Vsp linked to MccV, MccN, EntA, HirJM9, EntA, EntP, and EntB could all be secreted through the MccV pathway with variable success. MccL and MccN were also expressed well from the MccV pathway when using their

native leader peptides, Lsp and Nsp, respectively. All of these constructs were tested in MC1061 cells.

Previous work has focused on secreting two or three AMPs from a single bacterial delivery organism. However, the work presented in this section builds on this foundation demonstrating the ability to combinatorically swap leader peptides and develop AMP expression systems capable of producing a wide-variety of diverse peptides.

5.3.3 Development of pMPES 3.0

pMPES 1.0 served its purpose as a proof-of-concept tool for a modular peptide expression system. However, a major downfall of pMPES 1.0 was that it elicited poor peptide expression overall. In this work, we set out to improve and optimize pMPES 1.0 to make it a more robust tool so it could feasibly be used for practical applications.

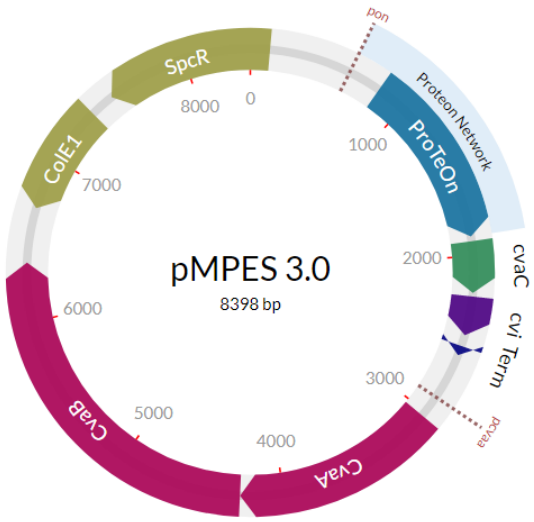

Figure 5-4. *Plasmid map of pMPES 3.0*

The optimized pMPES vector, termed pMPES 3.0, is displayed in Figure 5-4. In constructing this vector, we made several key changes that led to improved peptide production. In pMPES 1.0, the entire MccV operon was contained in the vector

backbone, including an extra ~4kb region of unnecessary sequence space. This region contained several hypothetical protein coding regions of unknown function. In pMPES 3.0, we eliminated the unnecessary sequence space and confined the cloned region of the MccV operon to include only the four essential genes required for MccV production and secretion. We removed the downstream coding region for *cvaC* and *cvi*, which were mutated in pMPES 1.0, choosing to express these proteins only from the ProTeOn+ promoter upstream. Lastly we cloned this engineered operon into the pMS vector backbone which contains a Spectinomycin resistance marker and ColE1 origin of replication.

To evaluate the strength of pMPES 3.0 vs 1.0 and quantify differences in their expression capacity, we expressed MccV from both vectors to measure relative concentrations and secretion output. We measured the differences in MccV production from each system using a combination of kinetic supernatant and zone-of-inhibition activity assays with DH5αpro (DH5α) as the indicator strain.

For the supernatant assays, we collected the supernatant from MC1061 cells producing MccV from both pMPES 3.0 and 1.0 after 16hrs of growth. We then applied this supernatant to DH5α in different volume fractions ranging from 40% to 0.625% and kinetically measured the growth profiles of DH5α. Using the growth curves collected from these assays, we were able to fit the data to Hill curves to examine shifts in the potency of the treatments. To generate these curves we used the Time to Rise (TTR) method explained in Section 5.4.4. The generated curves are shown in Figure 5-5. These curves shift to lower inhibitory concentrations of supernatant following treatment with pMPES 3.0 supernatant, indicating the presence of higher concentrations of MccV.

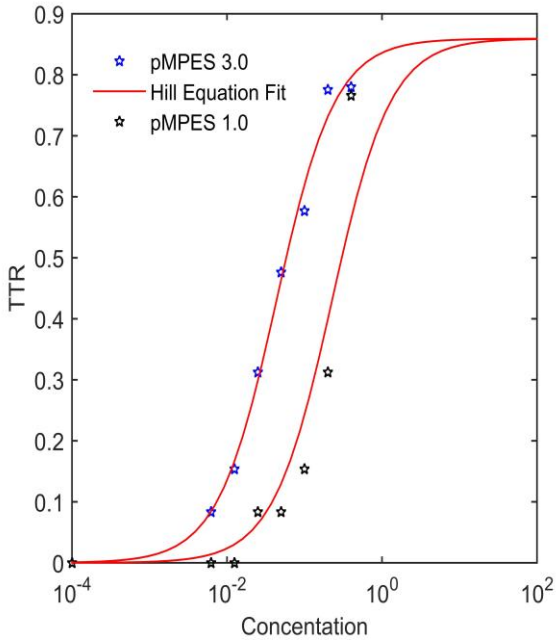

Figure 5-5. *Hill curve fitting of pMPES 1.0 and pMPES 3.0.* . The curve fits the TTR values of the indicator strain, DH5α, following treatment with serial dilutions of supernatant collected from MC1061 cells producing MccV from pMPES 1.0 and 3.0. The TTR was calculated as the average of three biological replicates.

In Figure 5-6, kinetic inhibition assays are shown where supernatant was collected from MC1061 cells producing MccV from pMPES 3.0 and 1.0. The supernatant was collected at 16hrs from both systems and DH5α growth is shown upon treatment with 1.25 to 10% supernatant collected from each. There are clear shifts in the growth profiles of DH5α in the presence of pMPES 3.0's supernatant indicating higher inhibitory concentrations. The activity, based on TTR calculations, is increased by 8x in pMPES

3.0. Additional studies producing enterocins have shown that the MIC when producing these peptides is increased over 20x in pMPES 3.0[26].

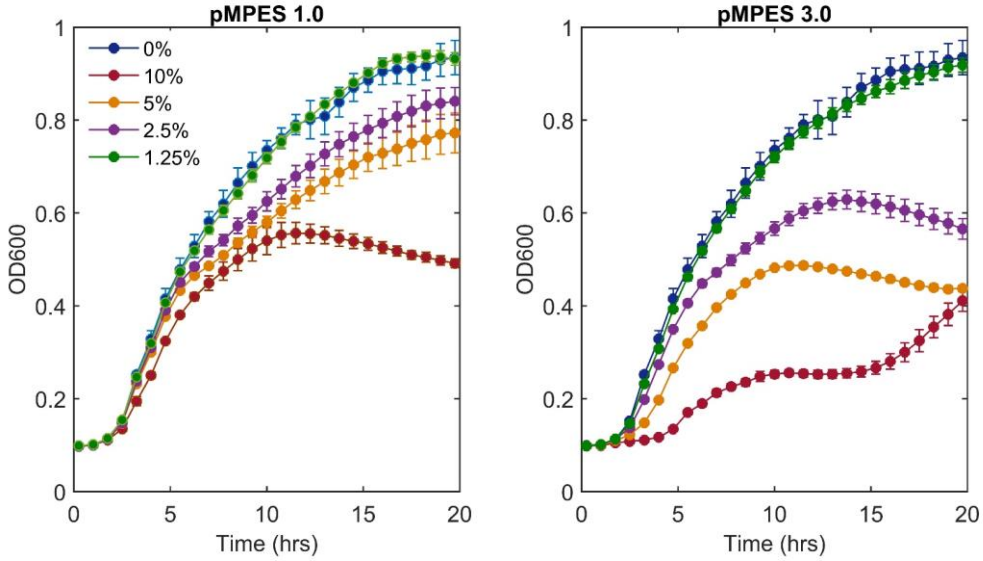

Figure 5-6. *Kinetic inhibition assay of DH5α in the presence of supernatant collected from pMPES 1.0 and 3.0 producing MccV.* DH5α growth was measured in the presence of different volume fractions of supernatant collected from MC1061 cells producing MccV from pMPES 1.0(left) and 3.0(right).

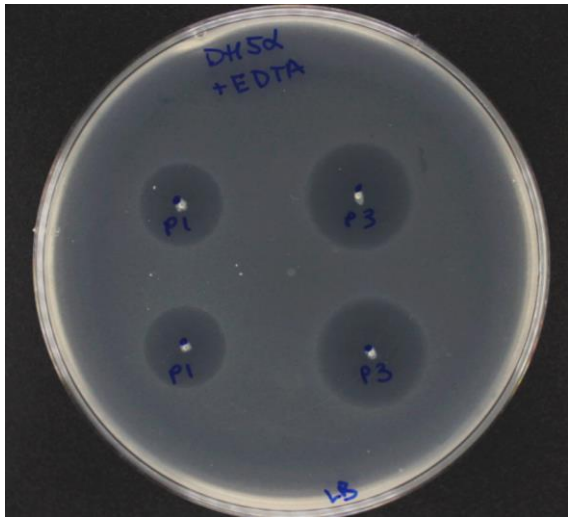

Figure 5-7. *Zone-of-Inhibition assay of pMPES 1.0 and 3.0 vs DH5α.* MC1061 cells producing MccV from pMPES 1.0 (P1) and 3.0 (P3) were spotted on an agar plate seeded with DH5α.

A halo test shown in Figure 5-7, shows the relative size of halos produced from pMPES 1.0 (P1) and pMPES 3.0 (P3) against DH5α. We note that the radius of the halos is not linearly related to peptide concentration but should increase with r^2, so a small change in halo size is a dramatic increase in peptide content.

5.4 Secretion of peptides from EcN using MccH47 Export Machinery

One of the reasons EcN is hypothesized to have powerful probiotic activity is due to its natural chromosomal carriage of two AMPs, Microcin M (MccM) and Microcin H47 (MccH47)[13]. MccH47 shares the same mode of secretion as MccV and their ABC export systems are almost identical. The two genes involved in MccH47 export, *mchE* and *mchF*, derived from EcN were found to be 98 and 99% identical to the *cvaA* and *cvaB* genes of the MccV operon[108]. In this work, we sought to determine if we could utilize the MccH47 machinery to export MccV from EcN. Being able to do this would enable us to secrete MccV, and potentially other peptides, without burdening the cells with the task of producing the bulky transporters.

To do this, we developed the plasmid pBFVI depicted in Figure 5-8. In this vector, the *cvaC* and *cvi* genes were cloned downstream of ProTeOn+ in the pMS expression system with none of the corresponding secretion genes. We then transformed pBFVI into EcN and MC1061 for testing. MC1061 does not contain homologous secretion machinery to CvaA and CvaB so MccV should not be able to be secreted to the extracellular space. We proceeded to test the secretion efficacy using zone-of-inhibition assays on both minimal media (M9) and rich media (LB). On each test we included

unmodified EcN as a negative control to compare its native antimicrobial activity. The results of these halo tests are shown in Figure 5-9.

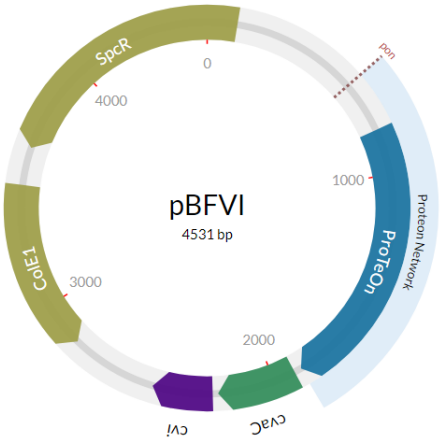

Figure 5-8. *Plasmid map of pBFVI*

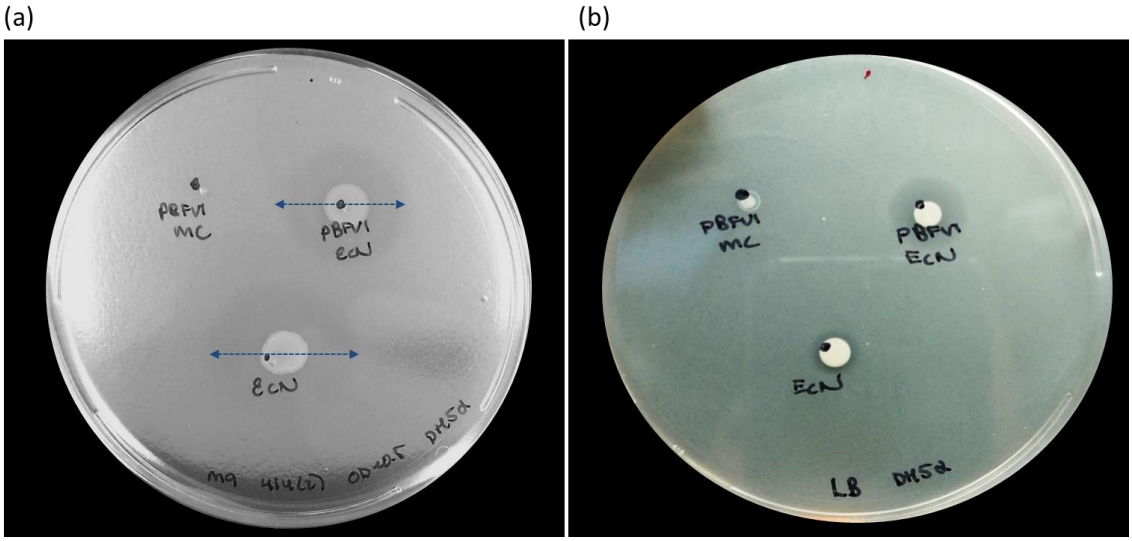

Figure 5-9. *Zone-of-Inhibition assay for MccV secretion through MccH47 export machinery.* . EcN(pBFV1), EcN, and MC1061(pBFVI) colonies were spotted on (a) M9 and (b) LB agar plates seeded with DH5α. On M9 unmodified EcN gives a large halo that is absent on the rich LB plate. EcN containing pBFV1 developed a halo on both plates while MC1061 (pBFVI) shows no halo on either plate.

From these results, we see that EcN has dramatic activity in minimal media without additional engineering due to its native antimicrobial activity. However, on LB EcN has a much smaller halo which is consistent with the idea that AMPs are activated in

times of nutrient depletion to help endowed strains in competition for survival. On LB, EcN containing pBFVI elicits a significant halo while MC1061(pBFVI) doesn't give rise to a halo in either media. This leads us to believe that MccV is being efficiently exported from EcN, likely through the MccH47 secretion genes, *mchE* and *mchF*, although this has not been explicitly confirmed.

5.5 Conclusions

In this work we describe the development of a modular secretion tool that enables the production of multiple AMPs in parallel. The development of pMPES has led to a tool that could improve engineered probiotic treatments enabling them to be broader spectrum and/or exhibit increased potency against their desired target.

The iterative development of pMPES led to an optimized construct, pMPES 3.0 that exhibits dramatic increases in peptide secretion capacity. Through this work, we have refined the MccV operon solidifying the understanding of what genes are required for MccV production and secretion allowing for further optimization and utility studies. Since most peptides typically have a dedicated transport mechanism, this tool overcomes challenges with cloning and producing the secretion machinery required for each desired protein. Further, we demonstrate that EcN is capable of exporting MccV without the addition of the transport genes, presumably being released by the chromosomal MccH47 pathway. One can envision tacking MccH47 compatible peptides to biosynthetic gene clusters for peptides such as MccJ25 and Mcc7 that require their dedicated pathways for an added antimicrobial effect with little cellular burden.

5.6 Materials and Methods

5.6.1 Development and testing of pMPES 1.0

See reference for detailed protocol:

Geldart, K., Forkus, B., McChesney, E., McCue, M., & Kaznessis, Y. N. (2016). pMPES: A Modular Peptide Expression System for the Delivery of Antimicrobial Peptides to the Site of Gastrointestinal Infections Using Probiotics. *Pharmaceuticals*, *9*(4), 60.

5.6.2 Construction of pMPES 3.0

IDT synthesized a gene fragment containing the sequence for *cvaC* and *cvi* which was inserted into the pMS expression vector using HIFI assembly making pBFV1. *cvaC* and *cvaB* were PCR amplified from pHK22 and inserted downstream of the terminator in pBFVI.

5.6.3 Kinetic Supernatant Inhibition Assays of pMPES 1.0 and pMPES 3.0

pMPES 1.0 and pMPES 3.0 producing MccV were transformed into the *E. coli* host strain, MC1061, and grown for 16hrs in LB. The supernatant of each culture was collected by transferring 1.5ml of the overnight culture to a microcentrifuge tube and centrifuging for 3min at 2.5rcf. The supernatant was sterile filtered using a .22µm filter. The supernatant was two-fold serially diluted in spent media from unmodified MC1061. DH5α (OD~0.01) was transferred to a 96-well plate and treated with each supernatant dilution, bringing the total volume to 300µl/well. The 96-well plate was transferred to a Biotek Synergy H1 plate reader and the plate was maintained at 37C in double-orbital mode. The OD600 was measured at 15 min intervals for 20hrs. Each supernatant treatment was run in triplicate and the error bars represent the standard error.

5.6.4 Time to Rise (TTR) Method

To semi-quantify the amount of MccV in the supernatant, the TTR method was developed. From kinetic supernatant inhibition assays, the average growth curves were generated for each supernatant treatment by averaging the OD600 reading of each replicate at each time point. We set a cut-off at OD~0.2 and measured the time it took for the untreated growth curve to reach this value. We considered the 'MIC' to be the lowest supernatant concentration that significantly increased the TTR compared to the control. Bacteriocin units (BUs) are defined as the reciprocal of the lowest dilution that extended the TTR.

5.6.5 Zone-of-Inhibition assays

LB or M9 agar was inoculated with 10-100µl DH5α and plates were poured and allowed to harden. A colony of the strain of interest was spotted on top of the agar plate and incubated overnight allowing a zone of inhibition to form where the peptide diffused and inhibited the seed cultures growth.

Chapter 6 Conclusions and Future Perspectives

Antibiotic resistance is a major public health concern. There is mounting global pressure to address the issue by reducing the use of antibiotics and incentivizing the development of next-generation therapies. In this thesis, we discuss the potential of engineered probiotics as an antibiotic alternative for pathogen-reduction in the clinical and agricultural sectors.

AMPs are a largely untapped reservoir of antibiotic activity that hold promise in the fight against resistant organisms. AMPs have now been identified that display diverse structures, functions, and mechanisms of action. With the expansion of biotechnological tools in protein engineering, high-throughput cloning, and next-generation sequencing, more AMPs may soon be identified or developed with even better characteristics in aspects such as stability and activity. However, the practical use of AMPs has been limited largely due to delivery and synthesis challenges. In this work, we lay a foundation for using engineered probiotics to overcome these inherent limitations, making otherwise undeliverable peptides a viable treatment option.

This thesis focuses on using synthetic biology approaches to systematically improve, understand, and engineer biosynthetic gene networks. Borne from this methodology were ProTeOn+ and pMPES, two novel synthetic biology tools that can aid in the development of future engineered organisms.

ProTeOn+ is a well-characterized and robust promoter system which enables high constitutive expression of proteins from *E. coli* (Chapter 2). ProTeOn+ has been characterized using stochastic simulations and experimental assays demonstrating

predictable and well-defined behavior. This promoter shows comparable expression capabilities to the fully induced T7 promoter system that is routinely used for protein production. Although in this work, we highlight the use of ProTeOn+ for the expression of AMPs it has many desirable qualities that could be used in other expression contexts, specifically applications where external induction is not desirable.

pMPES and its derivatives (Chapter 5) demonstrate a method for heterologous secretion of peptides through the native MccV export pathway. We focus on the utility of pMPES for the secretion of bacteriocins in the aim of developing broader-spectrum probiotics or enhancing their antagonistic effect. In next steps, it is suggested that this system be explored as a general peptide export system. With a limited number of methods available for efficient protein secretion from *E. coli*, the ability to secrete proteins other than AMPs would greatly increase the value and utility of this tool in the context of synthetic biology. As a starting point, it is suggested to study the ability of smaller proteins with an inherent capacity to refold, such as affibodies, for release through this pathway by tagging with the Vsp leader sequence.

This thesis focuses on engineering *E. coli* Nissle 1917 (EcN), a probiotic that has been studied for decades for its role in gastrointestinal health. We describe the use of EcN as a delivery vehicle for AMPs that target enteric pathogens, focusing on gram-negative bacteria as they remain one of the most challenging antibiotic-resistant subsets. In this methodology, we have developed EcN(J25) for control of *Salmonella* in poultry and EcN(C7) for decolonization of ST131 *E. coli* in the intestinal tract of human carriers. The work described in this thesis was highly translational where professional clinical and veterinary oversight was incorporated in the fundamental design stages to shape the

systems for their intended applications through strong collaborations with the VA Medical Center and Veterinary Science departments.

In light of the recent regulations on antibiotic use in food-producing animals, engineered probiotics may have a promising future in this sector as a feed additive. The cornerstone of this thesis is our demonstration of the first *in vivo* success of AMP-producing probiotics (Chapter 3). Treatment with our EcN(J25) system was capable of reducing *Salmonella* carriage by 97% in pre-harvest turkey poults 14-days post-treatment. Bioinformatic analysis demonstrated this treatment elicited no negative impacts on the microbiota of the treated birds which is critical in their development.

Although promising, further studies are suggested to optimize the use of engineered probiotics in animal feed applications. In the study presented, EcN(J25) was administered through a single oral gavage, three days following hatch; however, exploring alternative dosing regimens and administration methods could lead to a more effective treatment strategy. Co-localization studies are encouraged for currently it is not clear if EcN and *Salmonella* colonize the same part of the intestinal tract and what role their proximity plays. However, using a delivery strain that colocalizes with the target pathogen potentially could increase the treatment efficacy by limiting diffusion barriers and peptide degradation.

In the younger project involving collaboration with colleagues at the VA Medical Center, we have developed an engineered probiotic EcN(C7) for the reduction of ST131 carriage in the intestinal tract of infected individuals. The *in vitro* studies we have performed with EcN(C7) show this probiotic exhibits the strongest inhibitory effect of any probiotic/pathogen combination built previously in our lab. With the end-goal of

using this engineered probiotic in the clinic, we chose to explore the resistant subpopulation of the ST131 isolate, JJ1886, to unveil the mechanism of resistance. We have preliminary data suggesting that the YejF transporter on resistant cells is down-regulated, blocking Mcc7 entry into the intracellular space.

Looking forward, mouse trials are underway to determine the efficacy of EcN(C7) at JJ1886 reduction *in vivo*. Since the YejF transporter is known to play a role in the virulence of *Salmonella* and *Brucella*, it would be interesting to study the Mcc7-resistant isolates of JJ1886 and to quantify this subset's colonization efficacy compared to the parental strains. Since YejF contributes to cell resistance to numerous AMPs, there may also be potential for combination therapies using AMPs to eliminate the Mcc7-resistant population.

With the continual emergence of antibiotic-resistant bacteria and the challenges they present to health care, engineered probiotics are a potential method to harness the antibiotic activity of AMPs to expand our treatment options. This thesis helps build the foundation for the further growth of this field by highlighting some of the current successes, capabilities, and potential avenues for application of engineered probiotics. The modular nature of these systems enables tunable peptide expression and different pathogen/probiotic/peptide combinations can be readily developed to treat a variety of infections. Work must continue to evaluate the safety, efficacy, and optimization of engineered probiotics before they can gain widespread use. However, with the bleak outlook of a 'post-antibiotic' future upon us, engineered probiotics hold promise in the fight against microbial resistance and could re-open the medicine cabinet for future clinicians and patients.

Chapter 7 Bibliography

1. Martens, E. & Demain, A. L. The antibiotic resistance crisis , with a focus on the United States. *J. Antibiot. (Tokyo).* **70,** 520–526 (2017).

2. Frieden, T. *Antibiotic resistance threats*. *Antibiotic Resistance Threats in the United States, 2013* (2013). doi:CS239559-B

3. O'Neill, J. Antimicrobial Resistance : Tackling a crisis for the health and wealth of nations. *Rev. Antimicrob. Resist.* 1–16 (2014).

4. Ling, L. L. *et al.* A new antibiotic kills pathogens without detectable resistance. *Nature* **517,** (2015).

5. Coates, A. R. M., Halls, G. & Hu, Y. Novel classes of antibiotics or more of the same ? *Br. J. Pharmacol.* **163,** 184–194 (2011).

6. Ventola, C. L. The Antibiotic Resistance Crisis Part 1 : Causes and Threats. *Pharm. Ther.* **40,** 277–283 (2015).

7. Gross, M. Antibiotics in crisis. *Antibiotics in Crisis* R1063–R1065 (2013). doi:10.1016/j.cub.2013.11.057

8. Sang, Y. & Blecha, F. Antimicrobial peptides and bacteriocins : alternatives to traditional antibiotics. *Anim. Heal. Res. Rev.* **9,** 227–235 (2008).

9. Bahar, A. A. & Ren, D. Antimicrobial Peptides. *Pharmaceuticals* 1543–1575 (2013). doi:10.3390/ph6121543

10. Wang, S., Zeng, X., Yang, Q. & Qiao, S. Antimicrobial Peptides as Potential Alternatives to Antibiotics in Food Animal Industry. *Int. J. Mol. Sci.* **17,** (2016).

11. Hassan, M., Kjos, M., Nes, I. F., Diep, D. B. & Lotfipour, F. Natural antimicrobial peptides from bacteria: characteristics and potential applications to fight against antibiotic resistance. *J. Appl. Microbiol.* **113,** 723–736 (2012).

12. Cotter, P. D., Ross, R. P. & Hill, C. Bacteriocins — a viable alternative to antibiotics ? *Nat. Rev. Microbiol.* **11,** 95–105 (2012).

13. Duquesne, S., Destoumieux-Garzón, D., Peduzzi, J. & Rebuffat, S. Microcins, gene-encoded antibacterial peptides from enterobacteria. *Nat. Prod. Rep.* **24,** 708 (2007).

14. Mahlapuu, M., Håkansson, J., Ringstad, L. & Björn, C. Antimicrobial Peptides : An Emerging Category of Therapeutic Agents. *Front. Cell. Infect. Microbiol.* **6,** 1–12 (2016).

15. Amalaradjou, M. A. R. & Bhunia, A. K. Bioengineered probiotics, a strategic approach to control enteric infections. *Bioengineered* **4,** 379–387 (2013).

16. Paton, A. W., Morona, R. & Paton, J. C. Designer probiotics for prevention of enteric infections. *Nat. Rev. Microbiol.* **4,** (2006).

17. Dobson, A., Cotter, P. D., Ross, R. P. & Hill, C. Bacteriocin Production : a Probiotic Trait ? *Appl. Environ. Microbiol.* 1–6 (2012). doi:10.1128/AEM.05576-11

18. Fijan, S. Microorganisms with Claimed Probiotic Properties : An Overview of Recent Literature. *Int. J. Environ. Res. Public Health* 4745–4767 (2014). doi:10.3390/ijerph110504745

19. Yirga, H. The Use of Probiotics in Animal Nutrition. *J. Probiotics Heal.* **3,** (2015).

20. Luepke, Katherine H., Suda, Katie J., Boucher, Helen, Russo, Rene L., Bonney, Michael W., Hunt, Timothy D., Mohr III, J. F. Past, Present, and Future of Antibacterial Economics: Increasing Bacterial Resistance, Limited Antibiotic Pipeline, and Societal Implications. *Pharmacotherapy* (2016). doi:10.1002/phar.1868

21. Seo, M.-D., Won, H.-S., Kim, J.-H., Mishig-Ochir, T. & Lee, B.-J. Antimicrobial Peptides for Therapeutic Applications: A Review. *Molecules* **17,** 12276–12286 (2012).

22. Rotem, S. & Mor, A. Antimicrobial peptide mimics for improved therapeutic properties. *BBA - Biomembr.* **1788,** 1582–1592 (2009).

23. Eckert, R. Road to clinical efficacy: challenges and novel strategies for antimicrobial peptide development. *Future Microbiol.* **6,** 635 (2011).

24. Volzing, K., Borrero, J., Sadowsky, M. & Kaznessis, Y. Antimicrobial Peptides Targeting Gram-negative Pathogens, Produced and Delivered by Lactic Acid Bacteria. *ACS Synth. Biol.* **2,** 643–650 (2013).

25. Borrero, J., Chen, Y., Dunny, G. M. & Kaznessis, Y. N. Modified Lactic Acid Bacteria Detect and Inhibit Multiresistant Enterococci. *ACS Synth. Biol.* **4,** 299–306 (2014).

26. Geldart, K., Forkus, B., Mcchesney, E., Mccue, M. & Kaznessis, Y. N. pMPES : A Modular Peptide Expression System for the Delivery of Antimicrobial Peptides to the Site of Gastrointestinal Infections Using Probiotics. *Pharmaceuticals* **9,** 60 (2016).

27. Forkus, B., Ritter, S., Vlysidis, M., Geldart, K. & Kaznessis, Y. Antimicrobial Probiotics Reduce Salmonella enterica in Turkey Gastrointestinal Tracts. *Sci. Rep.* (2017). doi:10.1038/srep40695

28. Hwang, I. Y. *et al.* Engineered probiotic Escherichia coli can eliminate and prevent Pseudomonas aeruginosa gut infection in animal models. *Nat. Commun.* **8,** 1–11 (2017).

29. Food and Drug Administration. *Veterinary Feed Directive*. *Federal Register* **80,** (2015).

30. Bienick, M. S. *et al.* The Interrelationship between Promoter Strength , Gene Expression , and Growth Rate. *PLoS One* **9,** (2014).

31. Marbach, A. & Bettenbrock, K. lac operon induction in Escherichia coli : Systematic comparison of IPTG and TMG induction and influence of the transacetylase LacA. *J. Biotechnol.* **157,** 82–88 (2012).

32. Rosano, G. L. & Ceccarelli, E. A. Recombinant protein expression in Escherichia coli : advances and challenges. *Front. Microbiol.* **5,** 1–17 (2014).

33. Rebuffat, S. in *Prokaryotic Antimicrobial Peptides* 55–72 (2011).

34. Forkus, B., Ritter, S., Vlysidis, M., Geldart, K. & Kaznessis, Y. N. Antimicrobial Probiotics Reduce Salmonella enterica in Turkey Gastrointestinal Tracts. *Nat. Publ. Gr.* 1–9 (2017). doi:10.1038/srep40695

35. Scholz, O. *et al.* Activity reversal of Tet repressor caused by single amino acid exchanges. *Mol. Microbiol.* **53,** 777–789 (2004).

36. Choi, S. H. & Greenberg, E. P. The C-terminal region of the Vibriofischeri LuxR protein contains an inducer-independent lux gene activating domain. *Proc. Natl. Acad. Sci.* **88,** 11115–11119 (1991).

37. Volzing, K., Biliouris, K. & Kaznessis, Y. N. ProTeOn and ProTeOff, new protein devices that inducibly activate bacterial gene expression. *ACS Chem. Biol.* **6,** 1107–1116 (2011).

38. Tabor, S. in *Current Protocols in Molecular Biology* (2001).

39. Volzing, K., Biliouris, K. & Kaznessis, Y. N. proTeOn and proTeOff, new protein devices that inducibly activate bacterial gene expression. *ACS Chem. Biol.* **6,** 1107–16 (2011).

40. Kaznessis, Y. N. Computational methods in synthetic biology. *Biotechnol. J.* **4,** 1392–1405 (2009).

41. Biliouris, K., Daoutidis, P. & Kaznessis, Y. N. Stochastic simulations of the tetracycline operon. *BMC Syst. Biol.* **5,** (2011).

42. Hill, A. D., Tomshine, J. R., Weeding, E. M. B., Sotiropoulous, V. & Kaznessis, Y. N. SynBioSS : the synthetic biology modeling suite. *Bioinformatics* **24,** 2551–2553 (2008).

43. Salis, H. & Kaznessis, Y. Numerical simulation of stochastic gene circuits. *Comput. Chem. Eng.* **29,** 577–588 (2005).

44. Phillips, J. C. *et al.* Scalable Molecular Dynamics with NAMD. *J. Comput. Chem.* **26,** 1781–1802 (2005).

45. Fuqua, W. C., Winans, S. C. & Greenberg, E. P. Quorum Sensing in Bacteria: the LuxR-LuxI Family of Cell Density-Responsive Transcriptional Regulators. *J. Bacteriol.* **176,** 269–275 (1994).

46. Kaznessis, Y. N. Multiscale Models for Synthetic Biology. in *31st Annual International Conference of the IEEE EMBS* 6408–6411 (2009).

47. Boyer, A. E. & Tai, P. C. Characterization of the cvaA and cvi Promoters of the Colicin V Export System : Iron-Dependent Transcription of cvaA Is Modulated by Downstream Sequences. *J. Bac* **180,** 1662–1672 (1998).

48. Mutalik, V. K., Nonaka, G., Ades, S. E., Rhodius, V. A. & Gross, C. A. Promoter Strength Properties of the Complete Sigma E Regulon of Escherichia coli and Salmonella enterica □ †. *J. Bacteriol.* **191,** 7279–7287 (2009).

49. Solbiati, J. O., Ciaccio, M., Farías, R. N. & Salomón, R. A. Genetic analysis of plasmid determinants for microcin J25 production and immunity. *J. Bacteriol.* **178,** 3661–3 (1996).

50. Salis, H. & Kaznessis, Y. Accurate hybrid stochastic simulation of a system of coupled chemical or biochemical reactions. *J. Chem. Phys.* **122,** (2005).

51. Salis, H., Sotiropoulos, V. & Kaznessis, Y. N. Multiscale Hy3S : Hybrid stochastic simulation for supercomputers. *BMC Bioinformatics* **7,** 1–21 (2006).

52. Constantino, P. H., Vlysidis, M., Smadbeck, P. & Kaznessis, Y. N. Modeling stochasticity in biochemical reaction networks. *J. Phys. D. Appl. Phys.* **49,** (2016).

53. World Health Organization (WHO). *WHO estimates of the global burden of foodborne diseases*. (2015).

54. Gould, L. H. *et al.* Surveillance for foodborne disease outbreaks - United States, 1998-2008. *MMWR. Surveill. Summ.* **62,** 1–34 (2013).

55. Centers for Disease Control and Prevention. *Antibiotic resistance threats in the United States, 2013*. (2013). doi:CS239559-B

56. Russell, S. M. *Controlling Salmonella in Poultry Production and Processing*. (CRC Press, 2012). doi:10.1017/CBO9781107415324.004

57. McEwen, S. A. & Fedorka-Cray, P. J. Antimicrobial use and resistance in animals. *Clin Infect Dis* **34 Suppl 3,** S93–s106 (2002).

58. Food and Drug Administration. *Antimicrobials Sold or Distributed for Use in Food-Producing Animals*. *FDA Report* (2015). doi:10.1017/CBO9781107415324.004

59. Schneitz, C. Competitive exclusion in poultry—30 years of research. *Food Control* **16,** 657–667 (2005).

60. Chang, Y. H. *et al.* Selection of potential probiotic Lactobacillus strain and subsequent in vivo studies. *Antonie van Leeuwenhoek, Int. J. Gen. Mol. Microbiol.* **80,** 193–199 (2001).

61. Higgins, J. P. *et al.* Effect of lactic acid bacteria probiotic culture treatment timing on Salmonella Enteritidis in neonatal broilers. *Poult. Sci.* **89,** 243–247 (2010).

62. Blond, A. *et al.* The cyclic structure of microcin J25, a 21-residue peptide antibiotic from Escherichia coli. *Eur. J. Biochem.* **259,** 747–755 (1999).

63. Adelman, K. *et al.* Molecular mechanism of transcription inhibition by peptide antibiotic Microcin J25. *Mol. Cell* **14,** 753–762 (2004).

64. Solbiati, J. O. *et al.* Sequence Analysis of the Four Plasmid Genes Required To Produce the Circular Peptide Antibiotic Microcin J25. *J. Bacteriol.* **181,** 2659–2662 (1999).

65. Chiuchiolo, M. J., Delgado, M. a., Farías, R. N. & Salomón, R. a. Growth-phase-dependent expression of the cyclopeptide antibiotic microcin J25. *J. Bacteriol.* **183,** 1755–1764 (2001).

66. Apajalahti, J., Kettunen, a. & Graham, H. Characteristics of the Gastrointestinal Microbial Communities, with Special Reference to the Chicken. *Worlds. Poult. Sci. J.* **60,** 223–232 (2004).

67. Fanelli, M. J., Sadler, W. W., Franti, C. E. & Brownell, J. R. Localization of Salmonellae within the Intestinal Tract of Chickens. *Avian Dis.* **15,** 366–375 (1971).

68. Corrier, D. E. *et al.* Presence of Salmonella in the crop and ceca of broiler chickens before and after preslaughter feed withdrawal. *Poult. Sci.* **78,** 45–49 (1999).

69. Bowen, A., Batz, M. B., Caswell, J. A., Chittiboyina, A. G. & Dark, M. J. *Foodborne Infections and Intoxications*. *Food Science and Technology* (Elsevier, 2013). doi:10.1016/B978-0-12-416041-5.00037-8

70. Yegani, M. & Korver, D. R. Factors affecting intestinal health in poultry. *Poult. Sci.* **87,** 2052–63 (2008).

71. Moyle, J. R. *et al.* The Probiotic Escherichia coli Nissle 1917 Enhances Early Gastrointestinal Maturation in Young Turkey Poults. *Int. J. Poult. Sci.* **11,** 445–452 (2012).

72. Huff, G. R. *et al.* Oral treatment with the probiotic Escherichia coli Nissle 1917 improves body weight and modulates the stress response of poultry in respiratory challenges with avian pathogenic. in *Proceeding of the XII European poultry conference* (2006).

73. Jernberg, C., Löfmark, S., Edlund, C. & Jansson, J. K. Long-term impacts of antibiotic exposure on the human intestinal microbiota. *Microbiology* **156,** 3216–3223 (2010).

74. Danzeisen, J. L. *et al.* Temporal Relationships Exist Between Cecum, Ileum, and Litter Bacterial Microbiomes in a Commercial Turkey Flock, and Subtherapeutic Penicillin Treatment Impacts Ileum Bacterial Community Establishment. *Front. Vet. Sci.* **2,** 56 (2015).

75. Mon, K. K. Z. *et al.* Salmonella enterica Serovars Enteritidis Infection Alters the Indigenous Microbiota Diversity in Young Layer Chicks. *Front. Vet. Sci.* **2,** 61 (2015).

76. Grozdanov, L. *et al.* Analysis of the Genome Structure of the Nonpathogenic Probiotic Escherichia coli Analysis of the Genome Structure of the Nonpathogenic Probiotic Escherichia coli Strain Nissle 1917. *J Bacteriol* **186,** 5432–41 (2004).

77. Adam, M., Murali, B., Glenn, N. O. & Potter, S. S. Epigenetic inheritance based evolution of antibiotic resistance in bacteria. *BMC Evol. Biol.* **8,** 52 (2008).

78. Masella, A. P., Bartram, A. K., Truszkowski, J. M., Brown, D. G. & Neufeld, J. D. PANDAseq: paired-end assembler for illumina sequences. *BMC Bioinformatics* **13,** 31 (2012).

79. Edgar, R. C. Search and clustering orders of magnitude faster than BLAST. *Bioinformatics* **26,** 2460–2461 (2010).

80. Edgar, R. C., Haas, B. J., Clemente, J. C., Quince, C. & Knight, R. UCHIME improves sensitivity and speed of chimera detection. *Bioinformatics* **27,** 2194–2200 (2011).

81. Caporaso, J. G. *et al.* correspondence QIIME allows analysis of high- throughput community sequencing data Intensity normalization improves color calling in SOLiD sequencing. *Nat. Publ. Gr.* **7,** 335–336 (2010).

82. DeSantis, T. Z. *et al.* Greengenes, a chimera-checked 16S rRNA gene database and workbench compatible with ARB. *Appl. Environ. Microbiol.* **72,** 5069–5072 (2006).

83. Lozupone, C. & Knight, R. UniFrac : a New Phylogenetic Method for Comparing Microbial Communities UniFrac : a New Phylogenetic Method for Comparing Microbial Communities. *Appl. Environ. Microbiol.* **71,** 8228–8235 (2005).

84. Rasheed, M. U., Thajuddin, N., Ahamed, P., Teklemariam, Z. & Jamil, K. ANTIMICROBIAL DRUG RESISTANCE IN STRAINS OF Escherichia coli. *Rev. Inst. Med. Trop. Sao Paulo* **56,** 341–346 (2014).

85. Poolman, J. T. & Wacker, M. Extraintestinal Pathogenic Escherichia coli , a Common Human Pathogen : Challenges for Vaccine Development and Progress in the Field. *J. Infect. Dis.* **213,** (2017).

86. Downing, T. Tackling drug resistant infection outbreaks of global pandemic Escherichia coli ST131 using evolutionary and epidemiological genomics. *Microorganisms* **2,** 236–267 (2015).

87. Johnson, J. R., Johnston, B., Clabots, C., Kuskowski, M. A. & Castanheira, M. Escherichia coli Sequence Type ST131 as the Major Cause of Serious Multidrug-Resistant E . coli Infections in the United States. *Clin. Infect. Dis.* **51,** (2010).

88. Colpan, A. *et al.* Escherichia coli Sequence Type 131 (ST131) Subclone H 30 as an Emergent Multidrug- Resistant Pathogen Among US Veterans. *Clinical* **131,** (2013).

89. Price, L. *et al.* The Epidemic of Extended-Spectrum- ␭ -Lactamase-Producing Escherichia coli ST131 Is Driven by a Single Highly Pathogenic. *MBio* **4,** 1–10

(2013).

90. Stoesser, N. *et al.* Evolutionary History of the Global Emergence of the Escherichia coli Epidemic Clone ST131. *MBio* **7,** 1–15 (2016).

91. Andersen, P. S. *et al.* Complete Genome Sequence of the Epidemic and Highly Virulent CTX-M-15-Producing H 30-Rx Subclone of Escherichia coli ST131. *genomeA* **1,** 1–2 (2013).

92. Severinov, K. & Nair, S. K. Microcin C: Biosynthesis and mechanisms of bacterial resistance. *Future Microbiol.* **7,** 281–289 (2012).

93. Zukher, I. *et al.* Ribosome-controlled transcription termination is essential for the production of antibiotic microcin C. *Nucleic Acids Res.* **42,** 11891–11902 (2014).

94. Vijver, P. Van De *et al.* Synthetic Microcin C Analogs Targeting Different. **191,** 6273–6280 (2009).

95. Gerdes, K., Severinov, K., Piskunova, J. & Maisonneuve, E. Peptide-nucleotide Antibiotic Microcin C Is a Potent Inducer of Stringent Response and Persistence in Both Sensitive and ... Peptide-nucleotide antibiotic Microcin C is a potent inducer of stringent response and persistence in both sensitive and producing. *Mol. Microbiol.* (2017). doi:10.1111/mmi.13640

96. Novikova, M., Kasakov, T., Vondenhoff, G. H. & Semenova, E. MccE Provides Resistance to Protein Synthesis Inhibitor Microcin C by Acetylating the Processed Form of the Antibiotic MccE Provides Resistance to Protein Synthesis Inhibitor Microcin C by Acetylating the Processed Form of the Antibiotic * □. *J. Biol. Chem.* **285,** 12622–12669 (2010).

97. Ramalingam, K. I., Tomshine, J. R., Maynard, J. A. & Kaznessis, Y. N. Forward engineering of synthetic bio-logical AND gates. **47,** 38–47 (2009).

98. Novikova, M. *et al.* The Escherichia coli Yej Transporter Is Required for the Uptake of Translation Inhibitor Microcin C □. *J. Bacteriol.* **189,** 8361–8365 (2007).

99. Eswarappa, S. M., Panguluri, K. K. & Hensel, M. The yejABEF operon of Salmonella confers resistance to antimicrobial peptides and contributes to its virulence. *Microbiology* **154,** 666–678 (2008).

100. Wang, Z. *et al.* The ABC transporter YejABEF is required for resistance to antimicrobial peptides and the virulence of Brucella melitensis. *Sci. Rep.* 1–10 (2016). doi:10.1038/srep31876

101. Kazakov, T., Metlitskaya, A. & Severinov, K. Amino Acid Residues Required for Maturation , Cell Uptake , and Processing of Translation Inhibitor Microcin C □. *J. Bacteriol.* **189,** 2114–2118 (2007).

102. Zhang, T. *et al.* Detection of respiratory viral and bacterial pathogens causing pediatric community-acquired pneumonia in Beijing using real-time PCR. *Chronic Dis. Transl. Med.* **1,** 110–116 (2015).

103. Borrero, J. *et al.* Use of the usp45 lactococcal secretion signal sequence to drive the secretion and functional expression of enterococcal bacteriocins in Lactococcus lactis. *Appl. Microbiol. Biotechnol.* **89,** 131–143 (2011).

104. Belkum, M. J. Van, Worobot, R. W. & Stiles, E. Double-glycine-type leader peptides direct secretion of bacteriocins by ABC transporters : colicin V secretion in Lactococcus lactis. *Mol. Microbiol.* **23,** 1293–1301 (1996).

105. Zhang, L. H., Faith, M. J., Mahanty, H. K., Tai, P. C. & Kolter, R. Genetic Analysis of the Colicin V Secretion Pathway. *Genetics* **141,** 25–32 (1995).

106. Zhao, Z. *et al.* Microcin PDI regulation and proteolytic cleavage are unique among known microcins. *Sci. Rep.* **7,** (2017).

107. Gilson, L., Mahanty, H. K. & Kolter, R. Four Plasmid Genes Are Required for Colicin V Synthesis , Export , and Immunity. *J. Bacteriol.* **169,** 2466–2470 (1987).

108. Azpiroz, A. F. & Rodri, E. The Structure , Function , and Origin of the Microcin H47 ATP-Binding Cassette Exporter Indicate Its Relatedness to That of Colicin V. *Antimicrob. Agents Chemother.* **45,** 969–972 (2001).

109. Gibson, M. A. & Bruck, J. Efficient Exact Stochastic Simulation of Chemical Systems with Many Species and Many Channels. *J. Phys. Chem. A* **104,** 1876–1889 (2000).

110. Cormack, B. P., Valdivia, R. H. & Falkow, S. FACS-optimized mutants of the green fluorescent protein (GFP). *Gene* **173,** 33–38 (1996).

Chapter 8 Appendix

Appendix A: ProTeOn+: A Synthetic Hybrid Promoter for the Delivery of Antimicrobial Peptides

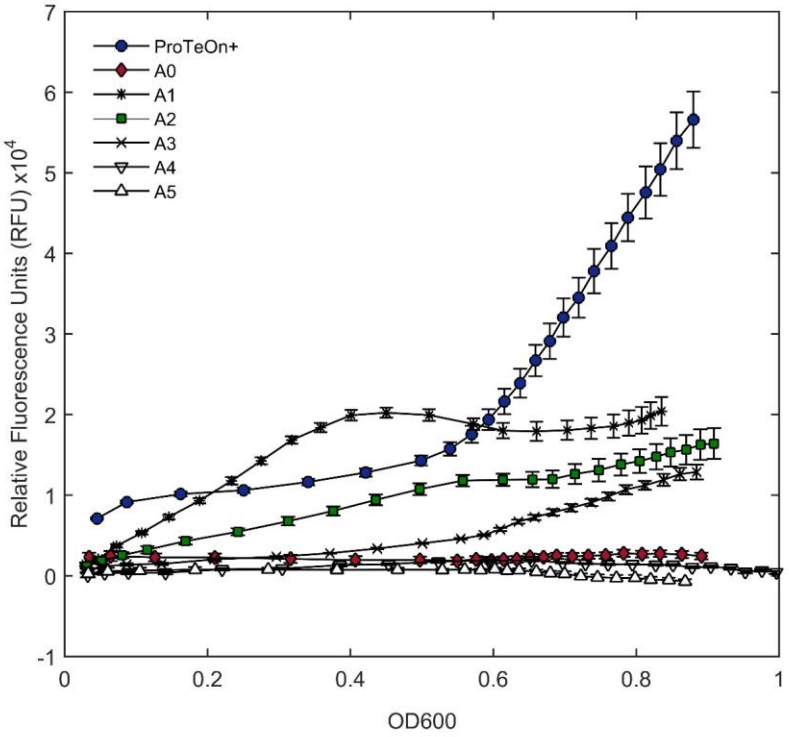

Figure 8-1 *ProTeOn+ and ProTeOn AND-Gate Comparisons.* The fluorescence of ProTeOn+ and the ProTeOn-AND gate were tested under varying experimental conditions and are represented as a function of cell density. A0-A5 are different inductions concentrations of the AND-Gate. A0: 0mM IPTG, 0ng/ml aTc, A1: 1mM IPTG, 100ng/ml aTc, A2: 0.5 mM IPTG, 100ng/ml aTc, A3: 1mM IPTG, 0ng/ml aTc, A4: 1mM IPTG, 0ng/ml aTc, A5: 0mM IPTG, 0ng/ml aTc. ProTeOn+: ProTeOn+ with no inducers.

ProTeOn+ Stochastic Kinetic Simulations

The model presented in this work is adapted from the previous model developed by Volzing et al to describe the behavior of the ProTeOn AND-gate. The molecular level events that govern the GFP-expression profiles are displayed in the bimolecular reaction network displayed in Table 2-1 of the main text. The species abbreviations used in the reaction network are displayed in

All reactions were modeled as occurring in a well-mixed volume of $10^{-1\,2}$ml to represent the size of typical *E. coli* cells (9). Cellular division times were simulated according to experimentally obtained division rates upon induction with the each respective aTc concentrations as shown in Table 8-2. Each cell was assumed to initially contain 15-20 promoter and *tetO* binding sites based on the ColE1 plasmid copy number, 450-550 available ribosomes for translation, and 150-300 RNA polymerase per cell. The initial conditions are shown in

Table 8-1. *Species Abbreviation in Bimolecular Reaction Network*

Abbreviation	Species	Abbreviation	Species
aTcEx	Extracellular anhydrotetracycline	**RNApol:pro:PROTET: tetO:aTc2**	Open RNApol and promoter site when tetO is occupied by PROTET:aTc2 complex
aTc	Intracellular anhydrotetracycline	**RNApol:pro:PROTET: tetO:aTc2_c**	Closed RNApol and promoter site when tetO is occupied by PROTET:aTc2 complex
PROTET	PROTEON dimer	**RNApol:DNA_c**	RNApol bound to DNA
PROTET:aTc	PROTET bound with one aTc molecules	**Rib**	Ribosome
PROTET:aTc2	PROTET bound with two aTc molecules	**Rib:mRNAg**	Open complex of mRNA and ribosome for the production of GFP
PROTET:tetO	PROTET bound with tetO	**Rib:mRNAg_c**	Closed complex of mRNA and ribosome for the production of GFP
PROTET:tetO:aTc	PROTET bound with tetO and one aTc molecule	**Rib:mRNAp**	Open complex of mRNA and ribosome for the production of PROTET protein
PROTET:tetO:aTc2	PROTET bound with tetO and two aTc molecules	**Rib:mRNAp_c**	Closed complex of mRNA and ribosome for the production of PROTET protein
tetO	TetR operator site	**mRNAg**	GFP mRNA transcript
RNApol	RNA polymerase	**mRNAp**	PROTET mRNA transcript
Pro	Promoter site	**GFP**	Unfolded GFP
RNApol:pro:tetO	Open RNApol and promoter site when tetO is unoccupied	**GFPm**	Folded GFP
RNApol:pro:tetO_c	Closed RNApol and promoter site when tetO is unoccupied		
RNApol:pro:PROTET:tetO	Open RNApol and promoter site when tetO is occupied by PROTET only		
RNApol:pro:PROTET:tetO_c	Closed RNApol and promoter site when tetO is occupied by PROTET only		

Table 8-2. *aTc Induction concentrations used in silico and in vivo*

aTc (ng/ml)	aTc (molecules/cell)	Cell division (±10min)
0	0	41.8
10	14	58.5
200	271	60.3

Table 8-3. *Initial Conditions Used in Stochastic Kinetic Simulations*

Species	Initial Condition (No. of species)
Pro	15-20
tetO	15-20
Rib	450-550
RNApol	150-300

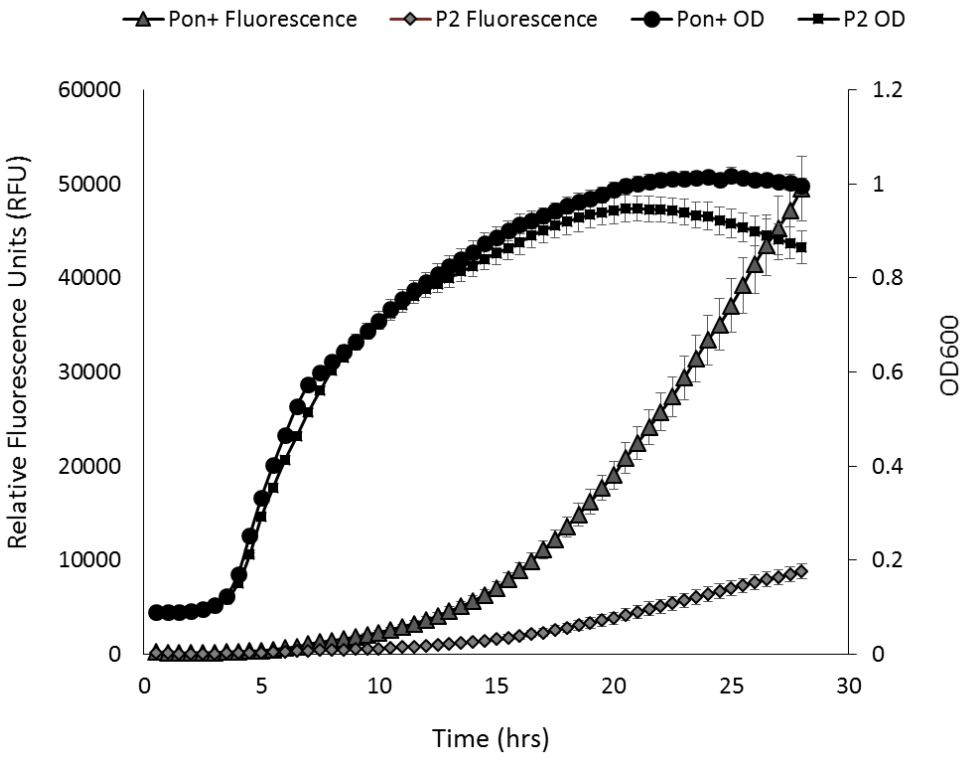

Figure 8-2 *Comparison of ProTeOn+ and P2 promoters.* Using the kinetic spectrophometric method described in Chapter 2, fluorescence and OD readings were measured from MC1061 cells expressing GFP from the P2 and ProTeOn+ promoters.

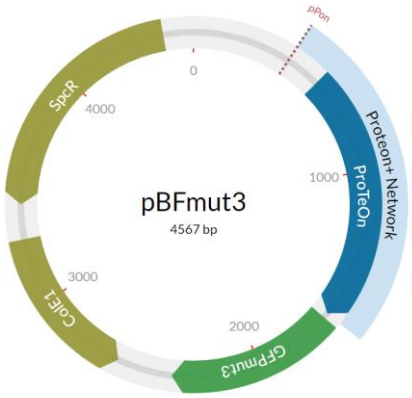

Figure 8-3. *Plasmid map of pBFmut3.* The ProTeOn and GFPmut3 genes were synthesized by GENEART. They were cloned into a pMS expression vector containing a ColE1 origin of replication and Spectinomycin selection marker.

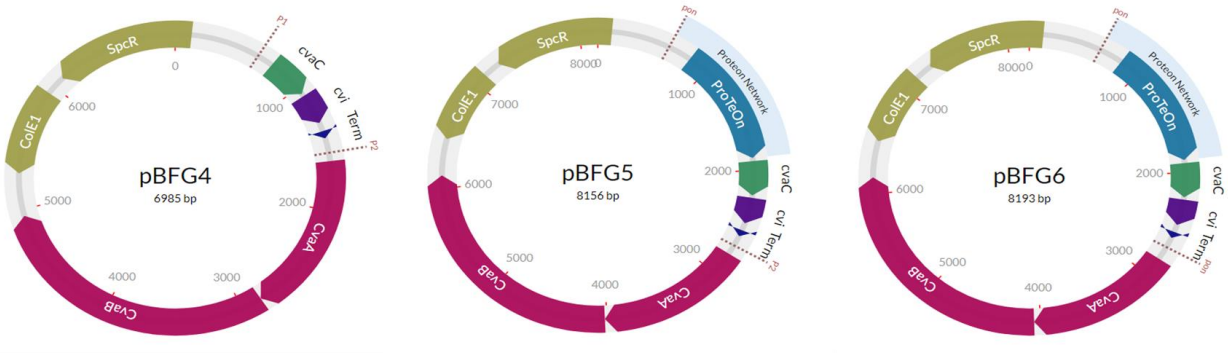

Figure 8-4. *Plasmid maps of pBFG4, pBFG5, and pBFG6*

Figure 8-5. *Plasmid maps of constructs used to produce GFP under the control of ProTeOn+, T7, and OXB20.*

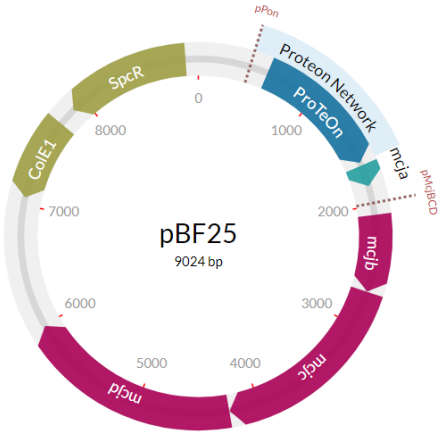

Figure 8-6. *Plasmid map of PBF25.* pMS expression vector containing a ColE1 origin of replication and Spectinomycin selection marker. *mcjABCD* was cloned from PJP3 between EcorI and SacI restriction sites via standard molecular cloning procedures to create pBF25.

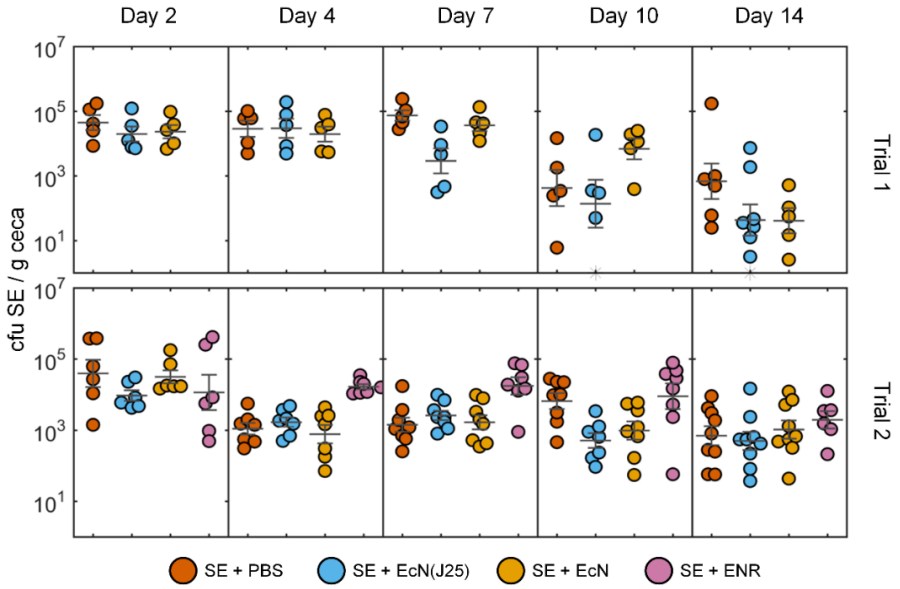

Figure 8-7. *Trajectories of individual bird SE counts.* The charts show the SE counts in the ceca for each individual bird at each collection point. The top row shows data collected for Trial 1 and the bottom shows the same data for Trial 2.

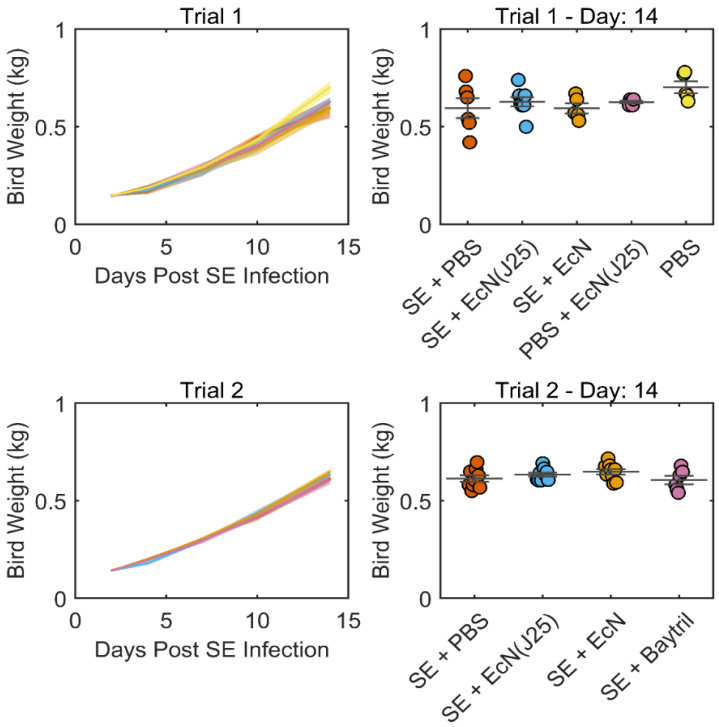

Figure 8-8. *Bird weight profiles of in vivo trials.* The left column shows the average bird weights of the euthanized birds at each time point for each respective trial. The right column shows the bird weights for the individual birds euthanized at the final time point, 14 days post SE-challenge. The width of the lines and error bars correspond to the standard error and the color represents the treatment group. The groups show no statistical difference in average bird weight across all time points.

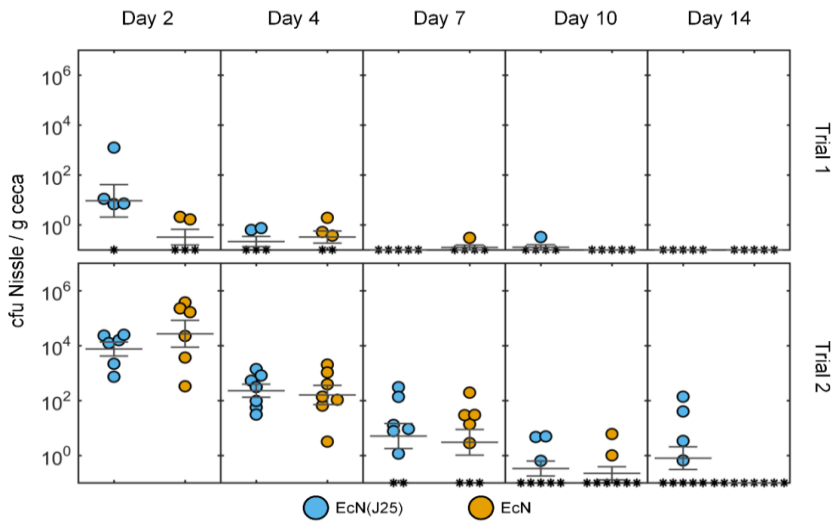

Figure 8-9. *Trajectories of individual bird Nissle counts.* The charts show the Nissle counts in the ceca for each individual bird at each collection point. The top row shows data collected for Trial 1 and the bottom shows the same data for Trial 2. Error bars represent standard error. Samples below limit of detection are plotted on the x-axis.

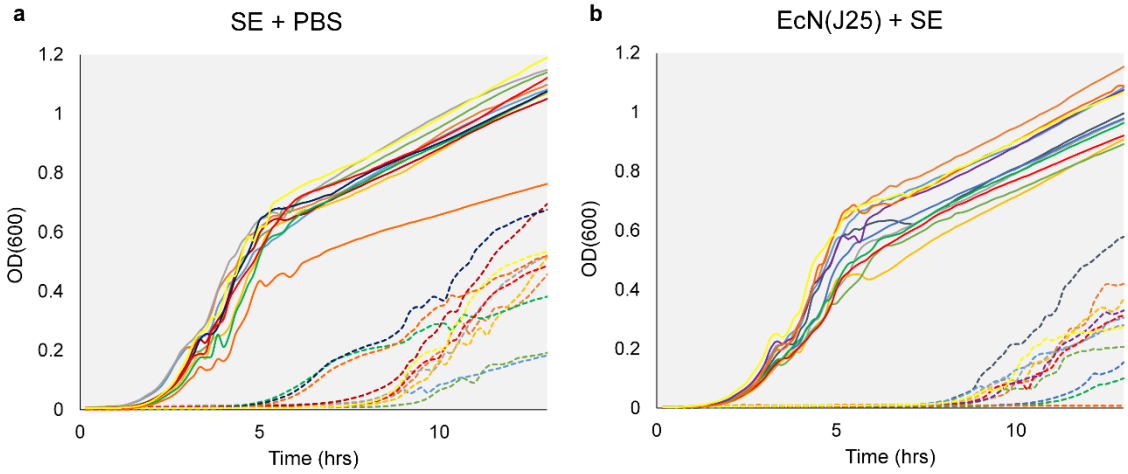

Figure 8-10. *SE-susceptibility to MccJ25 following GI passage.* 12 SE isolates were collected from birds treated with (a) SE+ PBS and (b) EcN(J25) + SE after passage to the ceca on day 14 post challenge to determine if any resistance was developed to MccJ25. The isolates were challenged with 0 and 20% by volume of EcN(J25) supernatant that was collected after 20hrs of growth. Kinetic growth curves were generated using the supernatant activity assay described in the materials and methods. Same color refers to the same isolate, solid line is growth in absence of MccJ25 and dotted line is growth in the presence of MccJ25. No resistance is observed in any of the 12 isolates in either group as clear growth inhibition is observed across all isolates in both treatment groups.

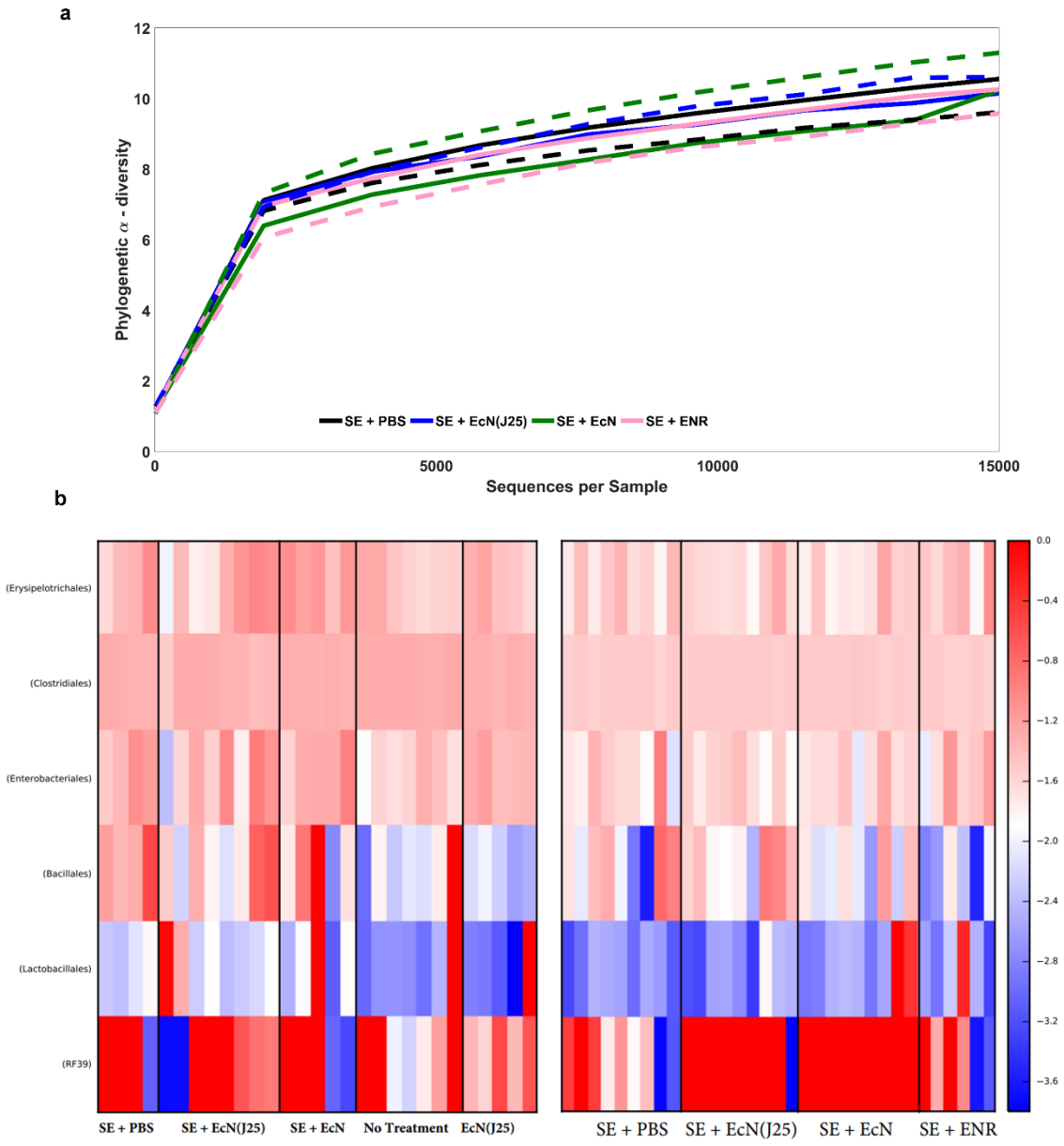

Figure 8-11. *Microbiome diversity at final time point* (a) Alpha diversity of all treatment groups in Trial 2. (b) Heat map comparing the frequencies of major bacterial species for each bird necropsied at the final time point for all treatment groups in (left) Trial 1 and (right) Trial 2. Each column represents an individual bird.

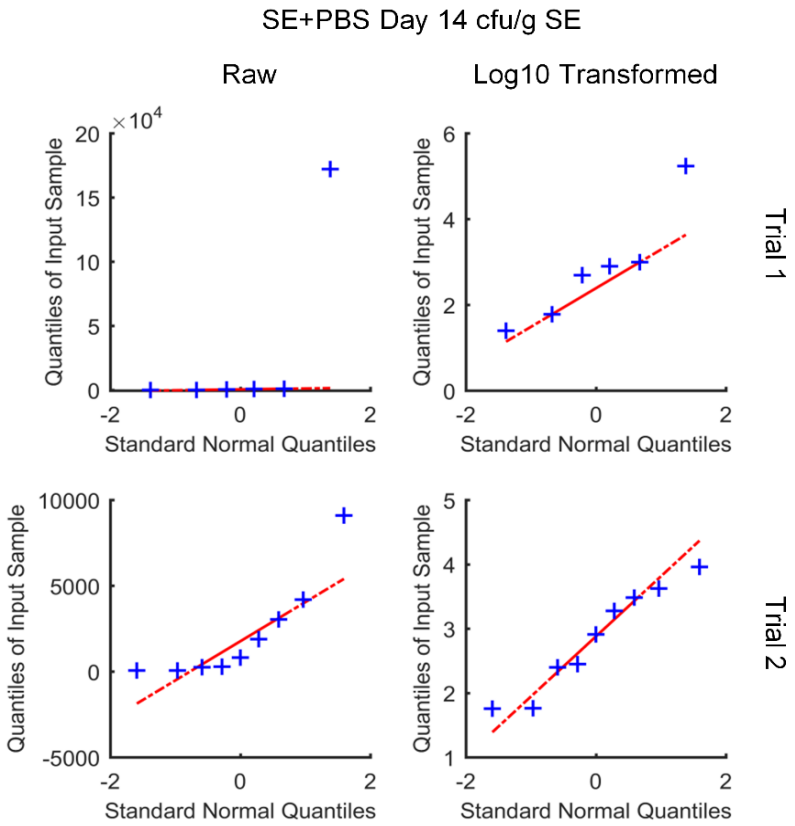

Figure 8-12. *Q-Q plot for comparing raw and log10 transformed data for normality.* A Q-Q plot enables the determination of whether a distribution assumption is valid. The SE counts from day 14 in both Trial 1 (top) and 2 (bottom) were tested for normality using the raw (left) and transformed (right) values. The transformed data appears to yield a better approximation.

Table 8-4. *Sequences of promoters, Pmcja, Pcvi, and Pmcc.* The uppercase regions represent the homology regions used for the HIFI assembly reaction

Promoter	Sequence
Pmcja MccJ25 Upstream of *mcja*	TGAGTGAAGGCCGTCAAGGCCGCATTCTAGAttttttcttaattgatggctaaatattctgaaataattagaaaaa tgtataaaaatccaaaatattgtactaaatttgaccacttttgcagattgattagtttatggatgtttgtatctaaatgattttattg ataaattactaaagcgtaatgattattgatctcaattgtattttgtgctaataaaattctaacagaaggacgtgaggttcctctgt aaaaatcatcatactatttccatcaaataGAATTCAAGGAGGAAACAGCTATGAGTAAAG
Pcvi MccV Upstream of *cvi*	TGAGTGAAGGCCGTCAAGGCCGCATTCTAGActtataggggttgagggcctcctacccttcactcttgactatgt taacgataatcattatcgttagtgtttgtgtggtaatgggatagaaagtaatgggatGAATTCAAGGAGGAAACAGCT ATGAGTAAAG
Pmcc Mcc7 Upstream of *mcca*	TGAGTGAAGGCCGTCAAGGCCGCATTCTAGAatgtataaccgcaaataatatgattgtgctgttctttttttgtgaaat gaatctatgtttgtatattttcatgaggaatattgtttttatagtgataaaaacacttgtgaattaatcacagtaatGAATTCAAG GAGGAAACAGCTATGAGTAAAG

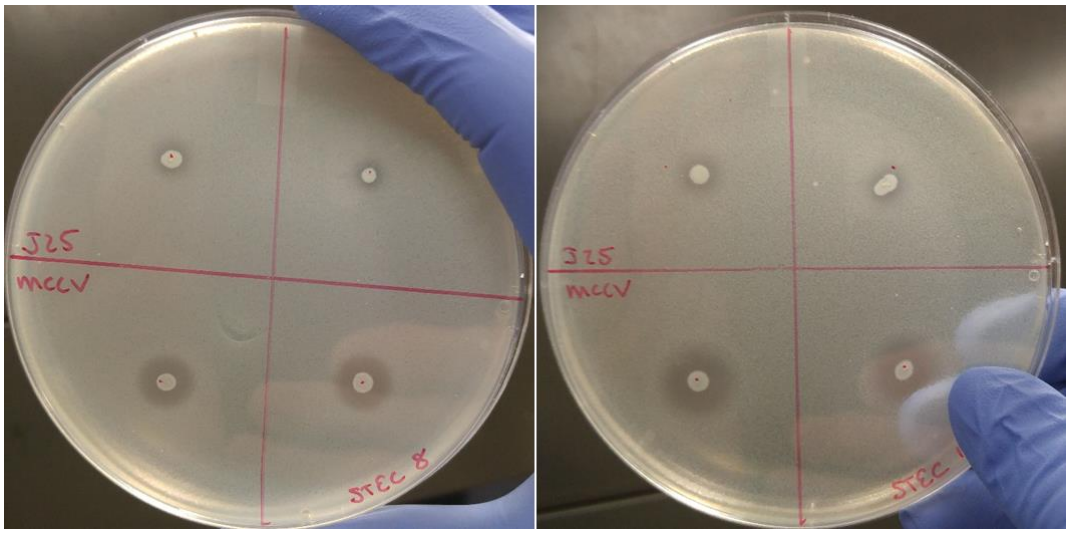

Figure 8-13. *Zone-of-Inhibition screens of MccV and MccJ25 against JJ1901 and MVAST020.* MC1061 cells producing pBF25 and pMPES3 were screened against JJ1901(left) and MVAST020(right) in duplicate.